Energy & Buildings 297 (2023) 113462

Contents lists available at ScienceDirect

Energy & Buildings

journal homepage: www.elsevier.com/locate/enb

Integrating embodied greenhouse gas emissions assessment into the structural design of tall buildings: A framework and software tool for design decision-making

James Helal [a,*,1], André Stephan [b], Robert H. Crawford [a]

[a] Faculty of Architecture, Building and Planning, The University of Melbourne, Victoria 3010, Australia
[b] Louvain Research Institute for Landscape, Architecture, Built Environment, Université catholique de Louvain, B-1348 Louvain-la-Neuve, Belgium

ARTICLE INFO

Keywords:
Embodied carbon
Structural design
Life cycle assessment
Premium for height
Structural systems
Tall buildings

ABSTRACT

Urgent changes are needed in the construction industry to address the adverse effects of material production on the environment. The construction of tall buildings results in a high temporal and spatial concentration of greenhouse gas (GHG) emissions. This is largely due to the compounding influence of wind and earthquake loads on structural material requirements. Thus, to meet short-term climate change mitigation goals, the structural design of tall buildings must consider and minimise the embodied GHG emissions of structural systems.

This study aimed to develop a framework to inform the design of tall building structural systems in order to minimise their embodied GHG emissions. A software tool was developed to implement the framework and automate the design, analysis, and embodied GHG emissions assessment of structural systems for tall buildings. Approximately 1,000 building models were iteratively designed, analysed, and assessed using the software tool. Through regression analyses, the resulting dataset was used to construct predictive models for the embodied GHG emissions of 12 unique combinations of structural system typologies and materials. By applying the framework and software tool to a 52-storey case study building, it is estimated that optimising structural material choices and geometric design strategies could reduce the embodied GHG emissions of tall building structural systems by up to 20% compared to current practices.

The developed framework and software tool allow designers to use environmental assessment as a design decision-making tool, rather than an appraisal method for evaluating completed buildings, helping to reduce the environmental effects associated with tall building construction.

1. Introduction

The influence of human activity on climate change is evident. Recent anthropogenic emissions of greenhouse gases (GHG) are the highest they have been in recorded history [1]. These emissions, which are largely driven by economic and population growth, alter the radiative balance of the Earth and warm its atmosphere. In its Sixth Assessment Report, the Intergovernmental Panel on Climate Change (IPCC) [1] stated that urgent and fundamental changes are required to stabilise global mean surface temperature increase to well below 2 degrees Celsius relative to pre-industrial levels [1].

Buildings account for 37% of global energy use and GHG emissions [2]. This figure is likely to increase in response to expected trends in global population growth and urbanisation. Nevertheless, reductions in the GHG emissions associated with buildings represent the most significant short term abatement opportunities while using existing technology and established practices [1].

Materials, waste and emissions flow throughout the life cycle of buildings and can be classified as either embodied environmental flows, operational environmental flows or end-of-life environmental flows. Embodied environmental flows are associated with the extraction of raw materials, the manufacturing of building materials and the construction of buildings, and the repair and replacement of building components. Operational environmental flows relate to the ongoing uses of buildings such as lighting, ventilation, heating, cooling and other operational demands. End-of-life environmental flows are associated with the

* Corresponding author.
E-mail address: james.helal@unimelb.edu.au (J. Helal).
1 ORCID: 0000-0002-8211-1454.

https://doi.org/10.1016/j.enbuild.2023.113462
Received 13 April 2023; Received in revised form 10 August 2023; Accepted 13 August 2023
Available online 14 August 2023

decommissioning and deconstruction of buildings as well as the transportation of their waste materials. Traditionally, operational environmental flows have been the primary focus of regulations and attempts to improve the environmental performance of buildings [3–5]. However, existing studies have revealed that embodied energy can represent up to 60% of the life cycle energy demand of buildings [6–11]. Additionally, strategies that aim to improve the operational efficiency of buildings often dictate the use of materials and assemblies that have a high intensity of embodied environmental flows [12]. This is most evident in advanced thermal insulation and innovative façade systems. Therefore, as the operational environmental flows of buildings are minimised, the significance of embodied environmental flows in buildings will progressively grow [13,14].

Increasing rates of urbanisation have been met with an exponential growth in the construction of tall buildings. In the period between 2000 and 2021, the total number of buildings taller than 200 m has increased by more than 550%, globally [15]. The construction of tall buildings results in a high temporal and spatial concentration of GHG emissions, which is described by Säynäjoki et al. [14] as a 'carbon spike'. Indeed, existing studies have shown that the embodied environmental flows per gross floor area of tall buildings can be up to 60% higher than that of low-rise buildings [16,17]. This is largely due to the compounding influence of wind loads and earthquake loads on the structural material requirements of tall buildings, a phenomenon described by Khan [18] as the 'premium for height'. Therefore, minimising the embodied environmental flows associated with the structural systems of tall buildings must become a design priority.

In the practice of structural analysis and design, preliminary layouts and initial structural member sizes are first adopted and then iteratively refined until all relevant structural design requirements are fulfilled. However, this iterative approach may not produce a final structural design solution that yields minimal embodied environmental flows. To address this limitation, several studies have applied a comparative life cycle assessment (LCA) approach to evaluate the embodied environmental flows of alternative structural materials and typologies for tall buildings. However, as discussed in Section 2, these studies commonly neglect the influence of a variety of building parameters, use inconsistent structural analysis techniques, and/or adopt incomplete environmental assessment approaches. Consequently, existing studies have failed to yield reliable and trustworthy findings that can meaningfully guide the structural design of tall buildings based on minimising their embodied environmental flows.

In response to the increasing environmental effects of urbanisation and climate change, comprehensive embodied environmental flow assessment approaches must be integrated into advanced structural design frameworks for tall buildings. Doing so can help guide early-stage design decisions that minimise potential effects on the environment. Thus, the aim of this study is to develop a framework and software tool to inform the design of structural systems for tall buildings in order to minimise their embodied GHG emissions.

1.1. Notions and definitions

This work adopts the definition of a tall building as proposed by Stafford Smith and Coull [19], coupled with a minimum height criterion of 35 m, as set by Emporis Standards [20].

Structural systems for tall buildings are generally composed of a lateral load resisting system to predominantly resist wind loads and earthquake loads, and a vertical load resisting system to predominantly resist loads in the direction of gravity [21]. This work classifies structural system typologies for tall buildings based on their lateral load resisting system. For example, if the lateral load resisting system of a tall building is a shear wall, the entire structural system is referred to as a 'shear wall' typology. This classification system is widely adopted throughout the literature on tall buildings, most notably by Moon, Connor, and Fernandez [22].

Life Cycle Assessment (LCA) is a process of evaluating the environmental effects associated with a product or service throughout its life cycle, from raw material extraction through materials processing, manufacture, distribution, use, repair and maintenance, to disposal, reuse or recycling [23]. Inputs to this process include raw materials, energy, and water, while outputs are typically waste and greenhouse gas (GHG) emissions.

The ISO 14040 [24] standard delineates the four stages of an LCA. The first stage, goal and scope definition, sets out the purpose and boundaries of the study. The second stage, life cycle inventory (LCI), involves identifying and quantifying the life cycle inputs and outputs associated with the product or service under investigation. The third stage, life cycle impact assessment, examines the extent and importance of potential environmental effects of these inputs and outputs. Finally, the interpretation stage includes the evaluation and conclusions drawn from the LCA results.

The terminology used in this section, including the definitions of LCA, LCI, and the various stages of LCA, will be used throughout this study, as these terms are crucial for understanding the overall context of the embodied environmental assessment of structural systems for tall buildings.

1.2. Structure

This paper comprises six sections. Section 2 outlines the existing studies that incorporate embodied environmental flows into the structural design of tall buildings. Section 3 presents the methodology used to develop the framework and software tool, which automate and integrate the assessment of embodied greenhouse gas emissions (EGHGE) into the structural design of tall buildings using comprehensive life cycle inventory approaches and advanced structural analysis techniques. Section 4 presents the results of the data simulation, regression analyses, and software validation. Additionally, it includes an analysis of a case study tall building to demonstrate the potential of the framework and software tool in reducing the EGHGE of structural systems for tall buildings. Section 5 interprets these results and discusses the limitations of the framework and software tool. Finally, Section 6 offers conclusions and future research directions for improving tall building design by minimising life cycle environmental flows.

2. Existing studies that integrate the assessment of embodied environmental flows into the structural design of tall buildings

A total of 10 comparative life cycle assessment (LCA) studies of structural systems for tall buildings have been identified in the existing literature. The case study tall buildings analysed in these studies range in height from 15 to 120 storeys and are designed to be built in Australia, South Korea, Italy and China. The identified studies assessed a range of structural systems for tall buildings including rigid frame, braced frame, shear wall, outrigger and belt, and diagrid. A range of alternative structural system typologies (i.e., rigid frame, braced frame, shear wall, outrigger and belt, and diagrid) and alternative structural materials (i.e., reinforced concrete, steel and composite) are considered in these studies. This section presents a detailed review of these studies, which are summarised in Table 1.

Tae et al. [25] compared the life cycle greenhouse gas emissions (LCGHGE) of two alternative shear wall structural systems for a 35-storey building in Korea. The systems comprised varying grades of reinforced concrete (RC) with different concrete mix proportions and minimum strengths achieved after a 28-day curing period. The first system used a range of RC grades, with lower grades used at higher storeys. This study found that by adopting 40 MPa RC instead of 32 MPa RC, the quantities of concrete and steel reinforcement decreased by around 9% and 30%, respectively. This led to a 6% and 20% reduction in overall quantities of concrete and steel reinforcement across the entire structural system, respectively. Using an input–output based life cycle

Table 1
Summary of existing comparative embodied environmental flow assessment studies of structural systems for tall buildings.

Study	LCI Method	Storeys	Structural typologies	Structural materials	Other varied building parameters	Considered lateral loads	Parametric analysis
Tae, Baek, and Shin [25]	Input-output	35	Shear wall	RC	Material strength	Not specified	–
Cho, Kim, Hong, and Kim [26]	Process (SUSB)	30	Braced frame, Outrigger and Belt	Steel	Bracing type	Wind	–
Foraboschi, Mercanzin, and Trabucco [27]	Process (ICE)	20, 30, 40, 50, 60, 70	Shear wall	RC, Composite	Floor type	Wind	–
Zhao and Haojia [28]	Process (ICE)	70	Shear wall, Outrigger and Belt	RC, Composite	Number of outrigger and belts	Not specified	–
Moussavi Nadoushani and Akbarnezhad [29]	Process (ICE)	5, 10, 15	Rigid frame, Braced frame, Shear wall	RC, Steel	–	Earthquake	–
Trabucco, Wood, Vassart, Popa, and Davies [30]	Process (various)	60, 120	Shear wall, Diagrid	RC, Composite, Steel	Material strength, element dimensions	Not specified	–
Mavrokapnidis, Mitropoulou, and Lagaros [31]	Not specified	64	Braced tube, Tube in tube, Diagrid, Outrigger and Belt	RC, Steel	–	Wind	–
Helal, Stephan, and Crawford [32]	Process (ICE and EPiC),Input-output (EPiC) ,Hybrid (EPiC)	10, 20, 30, 40, 50	Shear wall	RC, Steel	–	Wind, earthquake	✓
Helal, Stephan, and Crawford [33]	Hybrid (EPiC)	5, 10, 15, 20, 25, 30, 50	Shear wall	RC	Structural loads	Wind, earthquake	✓
Helal, Mehdipanah, Stephan, Lumantarna, and Crawford [34]	Hybrid (EPiC)	15	Shear wall	RC	Floor plan shape	Wind, earthquake	–
Helal [35]	Hybrid (EPiC)	5, 10, 20, 30, 40, 50, 60, 70, 80	Shear wall, Outrigger and belt, Braced tube	RC, Steel	–	Wind, earthquake	✓

Note: RC = Reinforced Concrete; ICE = Inventory of Carbon and Energy; EPiC = Environmental Performance in Construction.

inventory (LCI) approach, the study demonstrated a 52% reduction in LCGHGE by using higher grade RC. However, the study lacked data transparency regarding tall building structural design, making its findings difficult to verify.

Cho et al. [26] assessed the LCGHGE of three steel structural systems (braced frame, single outrigger and belt, and double outrigger and belt) for a 35-storey residential building in Seoul, South Korea. The study evaluated different bracing configurations (Chevron-braced and X-braced), without varying geometric parameters. To ensure structural performance equivalence, all systems were subject to a lateral displacement limit (1/400th of building height) in response to wind loads. However, the study did not consider earthquake loads. The LCGHGE was quantified using a process-based LCI approach, which may underestimate embodied environmental flows by up to 80% [36]. The braced frame system was found to have 16% less LCGHGE than the outrigger and belt systems, and Chevron braces reduced LCGHGE by 5.28% compared to X braces.

Foraboschi et al. [27] assessed the embodied energy (EE) and greenhouse gas emissions (EGHGE) of two alternative structural systems for six building scenarios in Italy of different heights (20–70 storeys). The alternative structural systems used a reinforced concrete shear wall and a rigid frame made of either reinforced concrete (RC) or steel. Six unique floor systems were also considered, including traditional and composite slabs made of reinforced concrete, and lightweight products. The structural design loads were much larger than those adopted by Cho et al. [26], but earthquake loads were also omitted. The neglect of earthquake loads was justified by Foraboschi et al. [27] by arguing that the dynamic behaviour of tall buildings is generally dictated by the first mode of vibration, which is not particularly susceptible to the frequencies induced by seismic events. As demonstrated by Mendis et al. [37], this claim is questionable and does not hold in even moderately seismically active areas. Structural systems were deemed equivalent by a lateral displacement limit of 1/400th of the building height. The Inventory of Carbon and Energy (ICE) database, which adopts a process-based approach to derive material coefficients, was used to quantify the EE and EGHGE of the alternative structural systems. In addition to its systemic incompleteness, the ICE (Version 2) database averages material coefficients irrespective of their underlying methodological, temporal and geographic differences while providing no information on the assumptions made to compile these coefficients [38]. Foraboschi et al. [27] found that using RC rigid frames resulted in up to 44% less EE per net floor area (NFA) than steel frames. Interestingly, the study showed that the use of lightweight floor systems, which often have higher intensities of embodied environmental flows, typically leads to increases in EE and EGHGE per NFA of the entire structural system.

Zhao and Haojia [28] studied EGHGE of three alternative structural systems for a 69-storey building scenario in China. The structural systems evaluated were a shear wall and frame made of RC, a single outrigger and belt made of steel positioned on the 44th floor, and two outriggers and belts made of steel located on the 44th and 57th floors. The ICE (Version 2) database was used to quantify the EGHGE of the structural systems, and the shear wall system was found to have significantly lower EGHGE per NFA than the two outrigger and belt systems. Despite the systemic incompleteness that is inherent to the adopted LCI approach, Zhao and Haojia [28] found the shear wall structural system to have 45% and 40% less EGHGE per NFA than the single outrigger and belt structural system and the double outrigger and belt structural system, respectively. It must be noted that this study by Zhao and Haojia [28] lacked data and method transparency pertaining to the structural design of tall buildings. Thus, these findings are unverifiable.

Moussavi Nadoushani and Akbarnezhad [29] assessed EGHGE of two structural typologies (rigid frame and braced frame) and materials (RC and steel) for a 15-storey building scenario. To ensure design requirements are met, imposed and superimposed loads were considered and assigned values of 200 kg/m^2 and 370 kg/m^2, respectively. Wind loads were not included in the structural analysis. The overestimation of vertical loads and the underestimation of lateral loads may have a significant influence on the resulting structural material requirements. By also using process-based material coefficients from the ICE (Version 2) database, the steel braced frame was found to be the optimal structural system for the 15-storey building scenario based on EGHGE per NFA, while the EGHGE per NFA of rigid frame systems made of RC and steel were 22% and 10% higher, respectively.

The Council of Tall Buildings and Urban Habitat (CTBUH), in their report titled 'Life Cycle Assessment of Tall Building Structural Systems' evaluated the EE and global warming potential (GWP) of two alternative structural systems (shear wall and diagrid) and three materials (RC, steel, and composite) for a 60- and 120-storey building [30]. Ecoinvent and Worldsteel databases were used for the LCI analysis of steel, and environmental product declarations (EPDs) were used for the LCI analysis of concrete. More building parameters were considered in this study than in similar studies, but method transparency was lacking. Trabucco et al. [30] found that steel structural systems had lower GWP but higher EE than RC systems, highlighting the complexity of building material selection based on different environmental impact categories. Transportation of construction material and construction activities had low to insignificant environmental flows.

Mavrokapnidis et al. [31] conducted a comparative EGHGE assessment of five structural systems for a 64-storey tall building. The structural systems considered were RC braced tube, steel braced tube, RC tube in tube, steel diagrid, and steel outrigger and belt. Similar to Foraboschi et al. [27], the study did not account for earthquake loads in the structural design of the tall buildings, potentially underestimating structural material requirements and associated embodied greenhouse gas emissions (EGHGE). The study lacked transparency in the adopted LCI approach, simply stating that the EGHGE coefficients were extracted from the study by Chau, Leung, and Ng [39]. A closer inspection of the referenced study indicated that Chau et al. [39] also extracted EGHGE coefficients from a series of studies that differ in their adopted LCI approaches as well as their geographical and temporal coverage. Relying on multiple layers of inconsistent secondary sources reduces the reliability and validity of the findings by Mavrokapnidis et al. [31]. Nevertheless, the study found that the steel structural systems consistently resulted in approximately twice the EGHGE as the RC structural systems.

In a series of studies [32,33], investigated the effects of various methodological variations in life cycle assessment and structural design on the EGHGE of structural systems for tall buildings. Their study on the influence of LCI approaches assessed the EGHGE of structural systems for 5 tall building scenarios, ranging in height from 10 to 50 storeys, that were parametrically designed using finite element modelling [32]. For each scenario, two alternative structural systems were proposed and different LCI approaches (process-based, input–output-based and hybrid-based) were used for the comparison of EGHGE. Results showed that the LCI approach can significantly impact EGHGE values of structural systems, by up to 116%, and can influence the choice of structural systems for tall buildings based on minimising EGHGE [32]. Similarly, Helal et al. [33] evaluated the influence of structural design methods and considerations on the EGHGE of 80 structural systems for tall buildings, also parametrically designed using finite element modelling, with their EGHGE quantified using a hybrid LCI approach. The study demonstrated that structural design methods can significantly influence the EGHGE of structural systems for tall buildings, by up to 22% [33]. The findings confirm the need for clarity, consistency, transparency, and comprehensiveness in LCI approaches and structural design methods when conducting comparative LCA studies of structural systems for tall buildings.

Furthermore, a study by Helal, Mehdipanah, Stephan, Lumantarna, and Crawford [34] assessed the influence of plan irregularity on the EGHGE of structural systems in tall buildings. This influence was evaluated using three finite element models of structural systems with varying degrees of plan irregularity in a 15-storey building scenario. All three structural systems consisted of an RC shear wall and moment-resisting frame that included band beams, columns, and one-way slabs. A hybrid LCI analysis method was employed to quantify the EGHGE of the structural systems. The findings offered an initial estimation of the EGHGE premium for plan irregularity and confirmed the need to reduce and eliminate such irregularities in order to minimise the EGHGE of structural systems in tall buildings.

Notable recent contributions, such as the studies by Gauch, Hawkins, Ibell, Allwood, and Dunant [40], Dunant, Drewniok, Orr, and Allwood [41] and Hart, D'Amico, and Pomponi [42], have illuminated the impact of strategic early-stage design decisions on both EGHGE and cost, while extending the comparative analysis across multiple structural frame materials. These studies provide substantial insight into the optimisation of structural frames under vertical loads and demonstrate the influence of various building parameters on the EGHGE of building structures. However, these works primarily apply to low- and medium-rise buildings, where vertical loads govern the design. In the context of tall buildings, the critical influence of lateral loads, such as those induced by wind and earthquakes, cannot be overlooked. These lateral forces introduce additional complexities that significantly affect the design, performance, and, consequently, embodied environmental flows of tall building structures. The consideration of these critical aspects of lateral loads in the structural design of tall buildings, thus marks a novel contribution within the existing body of research, providing a more comprehensive and environmentally responsive framework for the unique design conditions of tall buildings.

In summary, most existing comparative LCA studies that assess the embodied environmental flows of tall building structural systems use process-based LCI approaches, which have been shown to be systematically incomplete and inconsistent. Other LCI approaches, such as environmentally-extended input–output (EEIO) analysis and hybrid analysis, offer alternative approaches to LCI, which are discussed in more detail in Section 3.3. Additionally, the Inventory of Carbon and Energy (ICE), which has also been shown to be systematically incomplete and inconsistent [38,43], was the most commonly used source of embodied environmental flow coefficients. Due to the potential for ill-informed decision-making, efforts to minimise the embodied environmental flows of structural systems for tall buildings can be hampered when such LCI approaches and data sources are adopted.

Moreover, the use of incomplete and inadequate structural analysis approaches and considerations may distort structural material requirements and associated embodied environmental flows, thereby affecting the validity of their findings and conclusions. A widespread absence of transparency in the studies reviewed further exacerbates this issue, complicating comparisons across different studies. This has the potential to misguide structural design strategies leading to adverse consequences on the environmental effects associated with tall buildings. Finally, the reviewed studies unanimously omit the effects of various building parameters (e.g., slenderness, length of column spans, etc.) that have been shown to have a significant influence on the material quantities of tall building structural systems [44–46]. Consequently, the approaches adopted by the reviewed studies do not yield a comprehensive design framework that minimises the embodied environmental flows of tall buildings using different design strategies. Therefore, there is an urgent need to develop such a framework that considers a wide variety of building parameters to minimise embodied environmental flows using comprehensive methods for LCI analysis. Advanced structural analysis is also needed to ensure the validity of the framework, which has the potential to assist structural engineers and other building designers in selecting and designing structural systems while minimising their effect on the environment.

3. Method

To inform the structural design of tall buildings in order to minimise the EGHGE of their structural systems, the following framework (which represents a workflow process) is proposed:

1. Parametrically designing a large set of structural systems for tall buildings of varying structural materials, structural system typologies, and geometries;
2. Quantifying the EGHGE of the structural systems that have been designed;
3. Conducting regression analyses using the generated dataset of structural systems to develop predictive models for their EGHGE as a function of various building parameters; and
4. Developing a dashboard that uses the developed predictive models to facilitate design decision-making by enabling the rapid comparison of alternative structural designs for tall buildings based on minimising the EGHGE of their structural systems.

Thus, this research is largely concerned with establishing causation between various building parameters and the associated EGHGE of structural systems for tall buildings. To establish causation, a large dataset of structural systems is created using an automated and iterative approach of parametric structural modelling, analysis and optimisation. The complexity of structural design, which involves the utilisation of equations with millions of parameters, necessitates finite element modelling and analysis to ensure strength, serviceability and stability requirements for structural systems. The adopted methods and considerations for structural design are presented in Section 3.2.

The structural material quantities that are calculated and derived from the processes of finite element modelling, analysis and optimisation are then converted to EGHGE using the Path Exchange (PXC) method for hybridisation (see Section 3.3). By designing a large range of equivalent structural systems for tall buildings, an ordinary least squares linear regression analysis is then conducted to develop a set of equations that can be used to predict EGHGE as a function of alternative structural materials, structural system typologies and geometric parameters. The regression analysis method is presented in Section 3.4.

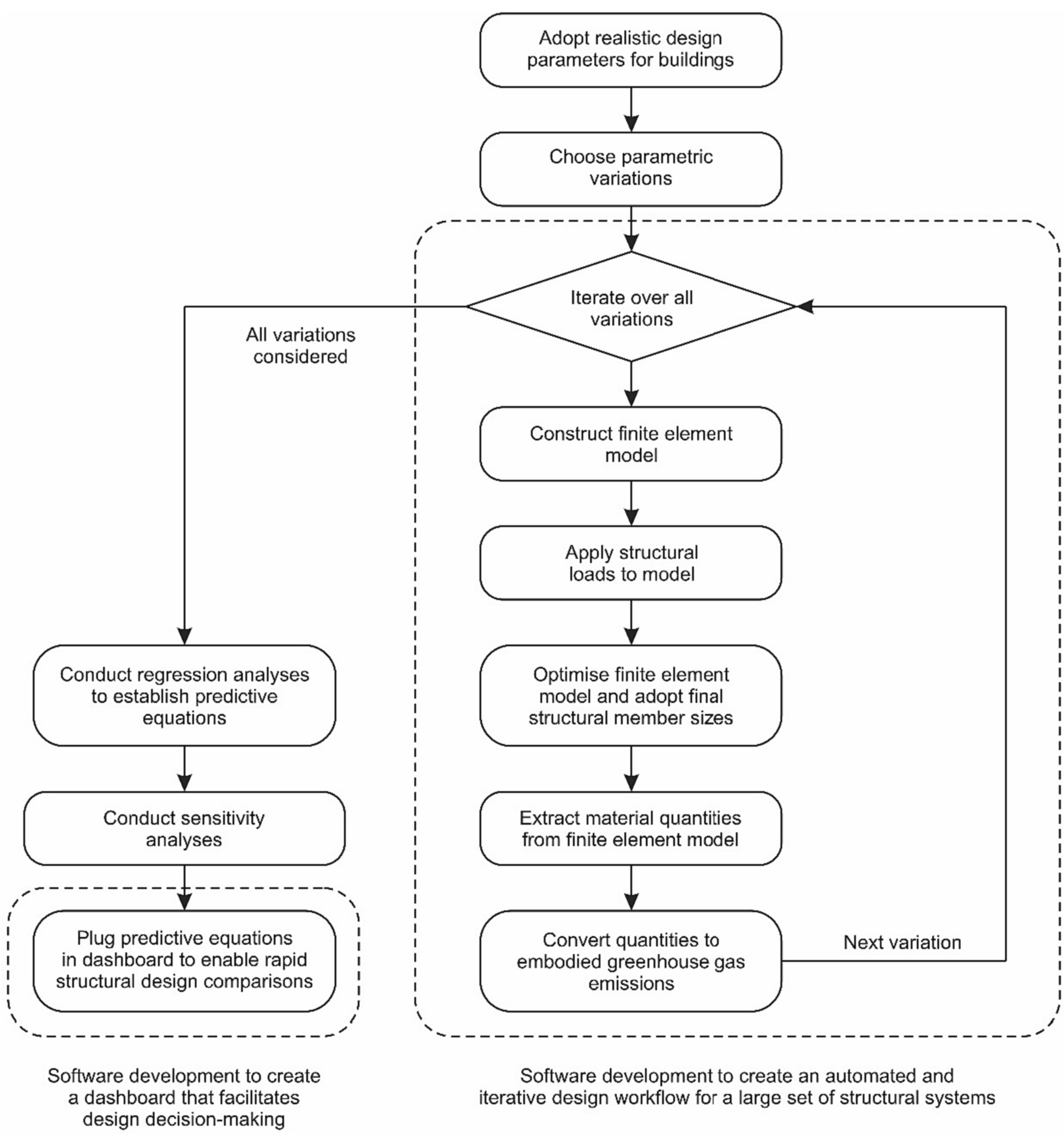

Fig. 1. Overall research method.

This iterative process of structural design and EGHGE assessment, followed by regression analyses, requires the automation of a complex sequence of actions. Thus, a software tool is developed to formalise the proposed framework and automate its structural design and environmental assessment sequence. Section 3.5 outlines the method of developing the software tool.

The overall research method is presented in Fig. 1. Detailed explanations and justifications for each step are outlined in Sections 3.1 to 3.5.

3.1. Goal and scope of framework

The goal of the framework is to provide the necessary information to integrate the assessment of EGHGE into the structural design of tall buildings during early-stage design. This integration will enable structural engineers, architects, researchers and decision makers to tackle EGHGE while assessing structural performance, potentially leading to the reduction of the environmental effects associated with the construction of tall buildings.

Structural systems made of reinforced concrete (RC) and/or steel are incorporated into the framework and accompanying software tool because they remain to be the most commonly used structural materials for tall buildings [47]. Limited by the availability of reliable and comprehensive material coefficients for EGHGE in the database of choice (see Section 3.3), three different grades of RC (i.e., 32 MPa, 40 MPa and 50 MPa) are considered by the framework. To limit the scope of work and ensure its feasiblity, the framework considers residential tall buildings made of three structural system typologies. No robust evidence is currently available on the prevalence of different types of structural system typologies for tall buildings; such information is only available anecdotally. Consequently, the following structural systems are considered due to their high prevalence in tall buildings: shear wall, outrigger and belt, and braced tube. Thus, in considering four alternative structural materials and three alternative structural system typologies, the developed framework and software tool allows users to compare the EGHGE of 12 unique combinations of structural materials and structural system typologies. The complete list of considered structural systems is presented in Table 2 along with the material composition of their structural members.

In designing the structural systems, a select number of building parameters are adopted to reflect common practices. These building parameters, which are listed in Table 3, are used to study the relationships between them and the resulting EGHGE of structural systems for tall buildings. Detailed justifications for the selection of these building parameter values are presented in Table 3.

Moreover, while the present framework focuses on rectangular floor plans, the potential impact of more complex floor plan geometries on the EGHGE of structural systems must be recognised. Plan irregularities, as demonstrated by Helal et al. [34], can notably affect EGHGE, with the study suggesting that an increase in plan irregularity could increase the EGHGE of columns by up to 23% and lead to an overall increase of up to 3% in the EGHGE of the entire structural system. While these percentages may appear minor, they highlight the potential compounding effects of plan irregularities that could become significant in the context of tall buildings. The inclusion of these irregularities and a broader spectrum of floor plan shapes warrants an expansion of the existing framework, recommended as a worthwhile pursuit for future research. Such an enhancement would yield a more comprehensive understanding of the EGHGE in tall buildings and diversify the range of real-world scenarios catered to by this framework, thereby improving its practical applicability.

This framework employs a life cycle greenhouse gas emissions assessment (LCGHGEA) to aid structural design decision-making, taking into account the well-established relationship between GHG emissions and climate change. By using LCGHGEA, the framework avoids the relative complexity of a comprehensive life cycle assessment (LCA) while still providing sufficient accuracy to evaluate resource use and environmental effects [39,50,51].

Although the primary focus of this work is on superstructures, the role of foundations and other building systems in contributing to the total EGHGE of tall buildings should not be overlooked. Foundation design is particularly complex and varies significantly based on site-specific conditions and decisions related to building parameters. For instance, past studies have shown a wide range of EGHGE contributions from foundations, varying from as low as 2% to as high as 26% [52,53]. Moreover, Treloar et al. [17] found that as building height increases, the proportion of embodied energy in the substructure tends to decrease, further illustrating the complex relationship between building height and foundation design. However, the design of foundations and other building systems remains beyond the scope of the current work. Future research should consider incorporating these elements into the framework for a more comprehensive assessment and design optimisation. By doing so, the framework can facilitate more informed decision-making

Table 2
Unique combinations of structural materials and system typologies considered within the scope of the framework.

#	Structural System Name	Frame	Walls	Braces	Slabs
1	32 MPa RC Shear Wall	32 MPa RC	32 MPa RC	–	32 MPa RC
2	32 MPa RC Outrigger Belt	32 MPa RC	32 MPa RC	32 MPa RC	32 MPa RC
3	32 MPa RC Braced Tube	32 MPa RC	32 MPa RC	32 MPa RC	32 MPa RC
4	40 MPa RC Shear Wall	40 MPa RC	40 MPa RC	–	32 MPa RC
5	40 MPa RC Outrigger Belt	40 MPa RC	40 MPa RC	40 MPa RC	32 MPa RC
6	40 MPa RC Braced Tube	40 MPa RC	40 MPa RC	40 MPa RC	32 MPa RC
7	50 MPa RC Shear Wall	50 MPa RC	50 MPa RC	–	32 MPa RC
8	50 MPa RC Outrigger Belt	50 MPa RC	50 MPa RC	50 MPa RC	32 MPa RC
9	50 MPa RC Braced Tube	50 MPa RC	50 MPa RC	50 MPa RC	32 MPa RC
10	Steel Shear Wall	Steel	40 MPa RC	–	32 MPa RC
11	Steel Outrigger Belt	Steel	40 MPa RC	Steel	32 MPa RC
12	Steel Braced Tube	Steel	40 MPa RC	Steel	32 MPa RC

Note: RC = Reinforced Concrete.

Table 3
Building parameters and values considered within the scope of the framework.

Building parameter	Values	Justification of values
Floor plan shape	Rectangular	A 25 m to 50 m square floor plan is the most commonly used floor plan for tall buildings [44].
Width	[37,40] (m)	
Depth	[37,40] (m)	
Column span	{4.8, 7.2} (m)	Column spans for tall buildings are often influenced by the column layout of the parking storeys. Typical spans of 4.8 m and 7.2 m allow 2 cars or 3 cars to be parked within a span, respectively (Standards [48].
Number of storeys	{5, 10, 20, 30, 40, 50, 60, 70, 80}	As of 2021, the average number of storeys of the tallest 100 buildings in Australia is 54 storeys and the standard deviation is 13 storeys [15]. Thus, this selected range of values includes approximately 85% of the tallest 100 buildings in Australia.
Inter-storey height	3.5 (m)	This value represents typical inter-storey heights for tall buildings [49].

in the early stages of structural design, potentially reducing the overall environmental effects associated with the construction of tall buildings.

Structural systems are typically designed to fulfil their intended function with minimal maintenance and repair being required throughout their design working life [44]. As such, this study considers the recurring environmental flows associated with structural systems to be insignificant and thus outside the scope of work. Similarly, the environmental flows associated with the transportation and construction stages (A4 and A5) are considered to be low to insignificant, based on findings by Trabucco et al. [30], and thus are also not included in the scope of this work. Furthermore, the end-of-life environmental flows for structural systems were not considered due to their relative insignificance, representing approximately 1% of the total life cycle environmental flows of buildings [30,54]. End-of-life environmental flows were also not considered due to the uncertain and unpredictable nature of deconstruction and demolition processes decades into the future. According to European standard EN 15643:2021, the life cycle of a building, as seen in Fig. 2, is divided into four stages: product stage (A1-A3), construction stage (A4-A5), use stage (B1-B7) and end-of-life stage (C1-C4) [55]. The scope of this framework, as illustrated and summarised in Fig. 2, encompasses the EGHGE of structural systems for tall buildings associated with the product stage (A1-A3).

The scope of this framework is much larger than that of most studies that use a comparative LCA approach to examine alternative structural systems for tall buildings. In the case of tall buildings, with multiple interacting non-linear effects, it is critical to adopt broad search criteria as to increase the robustness of the findings. The consideration of a vast range of structural system typologies, materials and geometric parameters yields approximately 1,000 unique structural systems, allowing the framework to adopt a parametric analysis approach whereby the effects of various building parameters on the EGHGE of structural systems are better understood and utilised to assist in early-stage structural design.

This approach may result in the consideration of structural design solutions that are traditionally considered to be uncommon or perhaps prohibitively costly. The inclusion of cost analysis and optimisation is discussed in Section 5.1 as a potential improvement to the framework and software tool. However, the focus on minimising the EGHGE of structural systems for tall buildings is in line with the goal of the framework and may lead to findings that have historically been overlooked by industry.

3.2. *Modelling, analysing and designing structural systems for tall buildings*

As discussed in Section 2, existing studies that assess and evaluate alternative structural systems for tall buildings based on minimising embodied environmental flows typically use inconsistent and inadequate structural design approaches. These have been shown to significantly influence the embodied environmental flows of structural systems for tall buildings, by up to 22% [33]. In the aim of ensuring clarity, transparency and comprehensiveness in the structural design process, this section presents the adopted methods of considering structural design loads for tall buildings.

The finite element method is a numerical technique used to approximate the solution of complex engineering and mathematical physics problems by dividing them into smaller, well-understood components or 'elements.' In structural engineering, it is particularly useful for computing the displacements of structures under loading. Since the 1960s, the method has been extensively applied to complex engineering problems, including the structural design of Burj Khalifa, the tallest building in the world as of 2023 [56]. ETABS, a reliable and powerful structural analysis and design software widely used for multi-storey

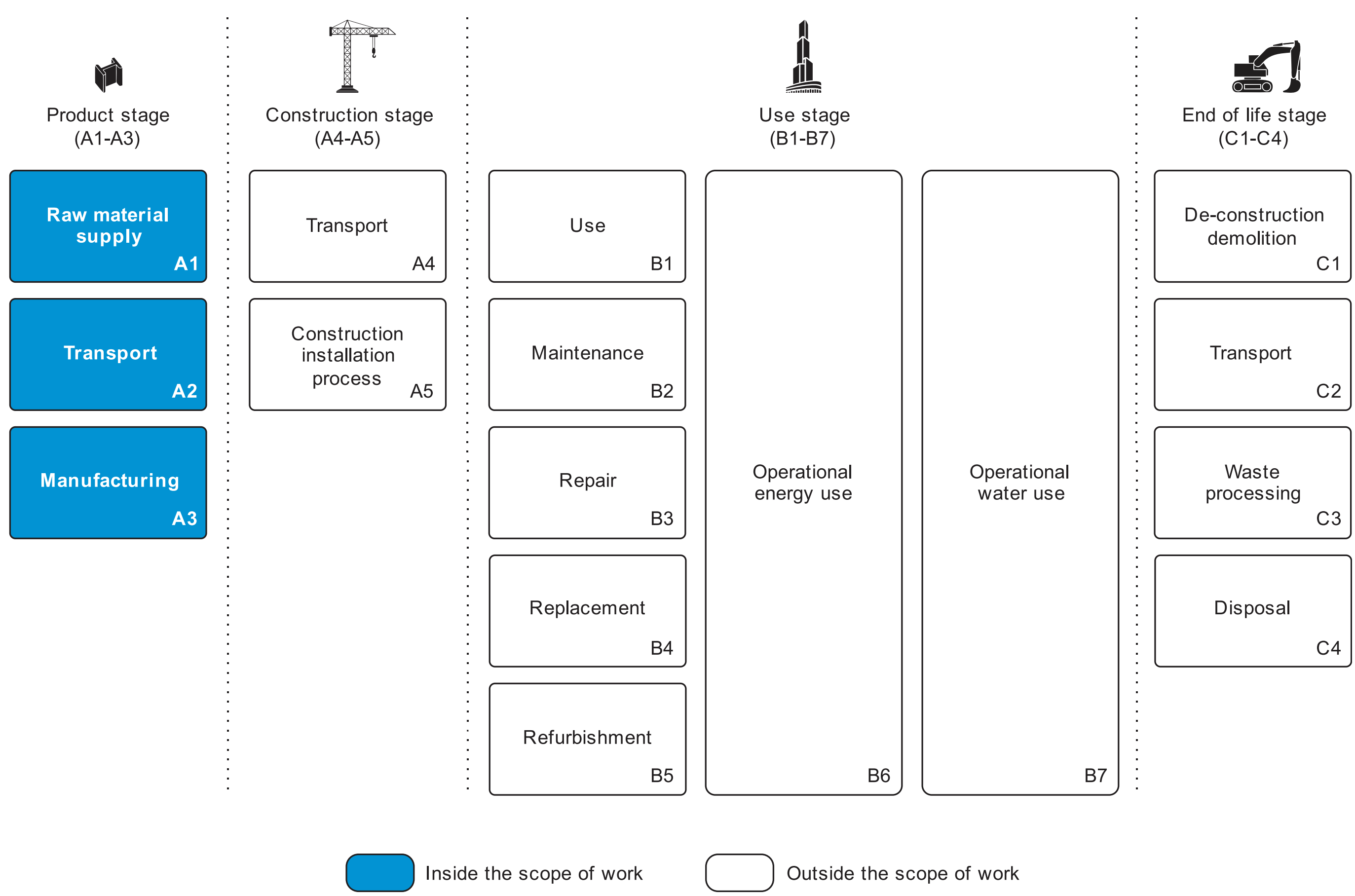

Fig. 2. Scope of the proposed framework based on EN 15643:2021.

buildings, is employed in this study for the finite element modelling and analysis of tall buildings [57].

In accordance with the design requirements for residential structures as prescribed by Australian Standard AS1170.1:2002, Appendix A summaries the adopted permanent and imposed loads in the design of the structural systems considered in this study. Moreover, Appendix A summarises the detailed methods of computing the applied wind loads and earthquake loads as prescribed by Australian Standards AS1170.2:2011 and AS1170.4:2007, respectively.

3.3. Assessing the embodied greenhouse gas emissions of structural systems for tall buildings

As outlined in Section 2, existing studies that integrate embodied environmental flow assessment into the structural design of tall buildings typically adopt inconsistent and incomplete life cycle inventory (LCI) approaches, which have been shown to influence the embodied environmental flows of structural systems by up to 116%. This section describes the selection of the assessment techniques adopted by this framework to calculate the EGHGE of structural systems for tall buildings.

There are three main approaches for compiling an LCI: process analysis, environmentally-extended input–output (EEIO) analysis and hybrid analysis.

A process analysis examines that processes that are specific to the considered product or service in order to list its inputs, outputs and resulting environmental effects throughout its life cycle [58]. Although this approach offers a high degree of accuracy, it can suffer from systemic incompleteness due to the challenge of comprehensively assessing the supply chain of a product or service [59–61]. Indeed, Crawford [59] demonstrated that this incomplete assessment can lead to a truncation error of up to 87% of the embodied energy (EE) of a building material or product, indicating that process analysis may significantly underestimate EE in buildings.

The EEIO analysis assumes that economic flows are indicative of physical flows. Based on this assumption, EEIO analysis merges economic data from input-output tables with environmental data of the correct format, such as GJ or tonnes of CO_2 equivalent emissions per unit currency [60,62]. The EEIO analysis approach minimises and potentially eliminates the truncation errors that are inherent to the process-based LCI approach. Input-output data is typically aggregated at the level of an industry (e.g., residential construction, steel manufacturing, etc.) and at the level of a product group (e.g., concrete, plasterboard, etc.). Thus, an EEIO analysis approach fails to make the distinction between different actors within the same industry. Similarly, this approach also often fails to make the distinction between different products within the same product group [43,61].

Various types of hybrid LCI approaches have been developed to overcome the inherent limitations of process analysis and EEIO analysis. Of all the developed hybrid analysis techniques, the Path Exchange (PXC) method, which was developed by Treloar [63], later formalised by Lenzen and Crawford [43] and automated by Stephan, Crawford, and Bontinck [38] is the most efficient LCI method, globally, while maintaining comprehensive coverage of the system boundary. The PXC method enables the identification of mutually exclusive pathways. These pathways are considered equivalent to known processes and can be replaced with specific process-based data when available [43].

Due to its comprehensiveness, transparency and data quality, this framework uses the Environmental Performance in Construction (EPiC) database of embodied environmental flow coefficients compiled by Crawford, Stephan, and Prideaux [64] using the Path Exchange (PXC) method for hybridisation. Additionally, the EPiC database was chosen because it is the only available database of hybrid embodied environmental flow coefficients for construction materials that are specific to Australia. The EGHGE of structural systems in tall buildings is calculated using the following equation:

$$EGHGE_{SS} = \sum_{m=1}^{M} \left(Q_{m,SS} \times EGHGEC_m \right) \quad (1)$$

Where $EGHGE_{SS}$ = embodied greenhouse gas emissions of structural system SS in $kgCO_2$-e; $Q_{m,SS}$ = quantity of material m in structural system SS (e.g. steel in kg); and $EGHGEC_m$ = embodied greenhouse gas emissions coefficient of material m (e.g. 2.86 $kgCO_2$-e/kg for steel).

It is important to note that the EPiC database uses an input–output-based hybrid approach, reflecting the domestic economic and environmental interdependencies specific to Australia. This approach implies that imported materials are represented based on domestic production conditions. It must be noted that most of these imports are predominantly from China, which relies on an energy mix relatively similar to Australia. Thus, this somewhat mitigates the potential discrepancies between the production conditions of imported and domestic materials. Nevertheless, this approach, while standard in input–output modelling due to the complexities of accurately accounting for international trade, is acknowledged as a potential source of uncertainty. It highlights an area for future refinement as data quality and modelling techniques continue to evolve.

3.4. Establishing relationships between embodied greenhouse gas emissions and building parameter values

The choice of a statistical modelling technique to establish relationships between embodied environmental flows and various building parameters is determined by the model's ease of operation, familiarity, speed, and a satisfactory degree of accuracy (Walpole, 2013). The ordinary least squares linear regression analysis technique has been widely applied across the literature, mainly in the aim of estimating cost and/or material quantities [65]; García de Soto et al., 2014; Idowu & Lam, 2020).

By designing a large set of equivalent structural systems for tall buildings using different structural materials, systems and geometries, an ordinary least squares linear regression analysis can be conducted to develop predictive models for the EGHGE of structural systems. For each combination of structural material and structural system typology (e.g., 40 MPa RC outrigger and belt), a predictive model (in the form of a regression equation) is constructed for the EGHGE/NFA of structural systems. Since this work considered three structural systems (shear wall, braced tube and outrigger and belt) and four structural materials (32 MPa RC, 40 MPa RC, 50 MPa RC and steel), 12 regression equations can be developed for the 12 unique combinations of structural materials and structural system typologies listed in Table 2. The following n-variable equation would result from the regression analysis for each unique combination of structural material and system typology:

$$EGHGEPNFA_{SS,m} = \beta_0 + \beta_1 X_1 + \cdots + \beta_n X_n \quad (2)$$

Where $EGHGEPNFA_{SS,m}$ = the embodied GHG emissions per net floor area for a structural system SS made of material m in $kgCO_2$-e/m^2; β_1 through β_n = regression coefficients for the corresponding predictor; and X_1 through X_n = predictor building parameters (e.g., number of storeys, width, depths, etc.).

To construct the regression equations and determine the most appropriate set of predictors, a forward stepwise selection is adopted starting with an empty model. Building parameters that have an established causal relationship with structural material quantities and that best improve the goodness of fit were iteratively added to yield the lowest squared error in the regression analysis.

These regression equations can then be plugged into the software tool to facilitate structural design decision-making based on the predicted EGHGE of structural systems. The method of developing the software tool is presented in the following section.

3.5. *Developing a software tool for the integration of embodied greenhouse gas emissions assessment into the structural design of tall buildings*

The integration of environmental assessment into the structural design of tall buildings is a complicated task that requires the automation of a complex sequence of actions. A software tool is developed to formalise the design framework presented in Sections 3.2 to 3.4 and automate its structural design and environmental assessment sequence.

The software tool is written in the Python programming language, which is a powerful multiparadigm computer programming language that is optimised for developer productivity, code readability and software. This open-source programming language has been used extensively by the software industry in a wide variety of applications. Python possesses a large collection of prebuilt and portable functionalities, known as the standard library. Third-party extensions such as pandas [66], NumPy [67], SciPy [68], Matplotlib [69] and Plotly [70] are heavily relied on in the development of the software tool to provide the appropriate and necessary data structures, algorithms, functions, numerical methods and data visualisation tools. These essential and well-established Python libraries contribute to the reliability of the software tool.

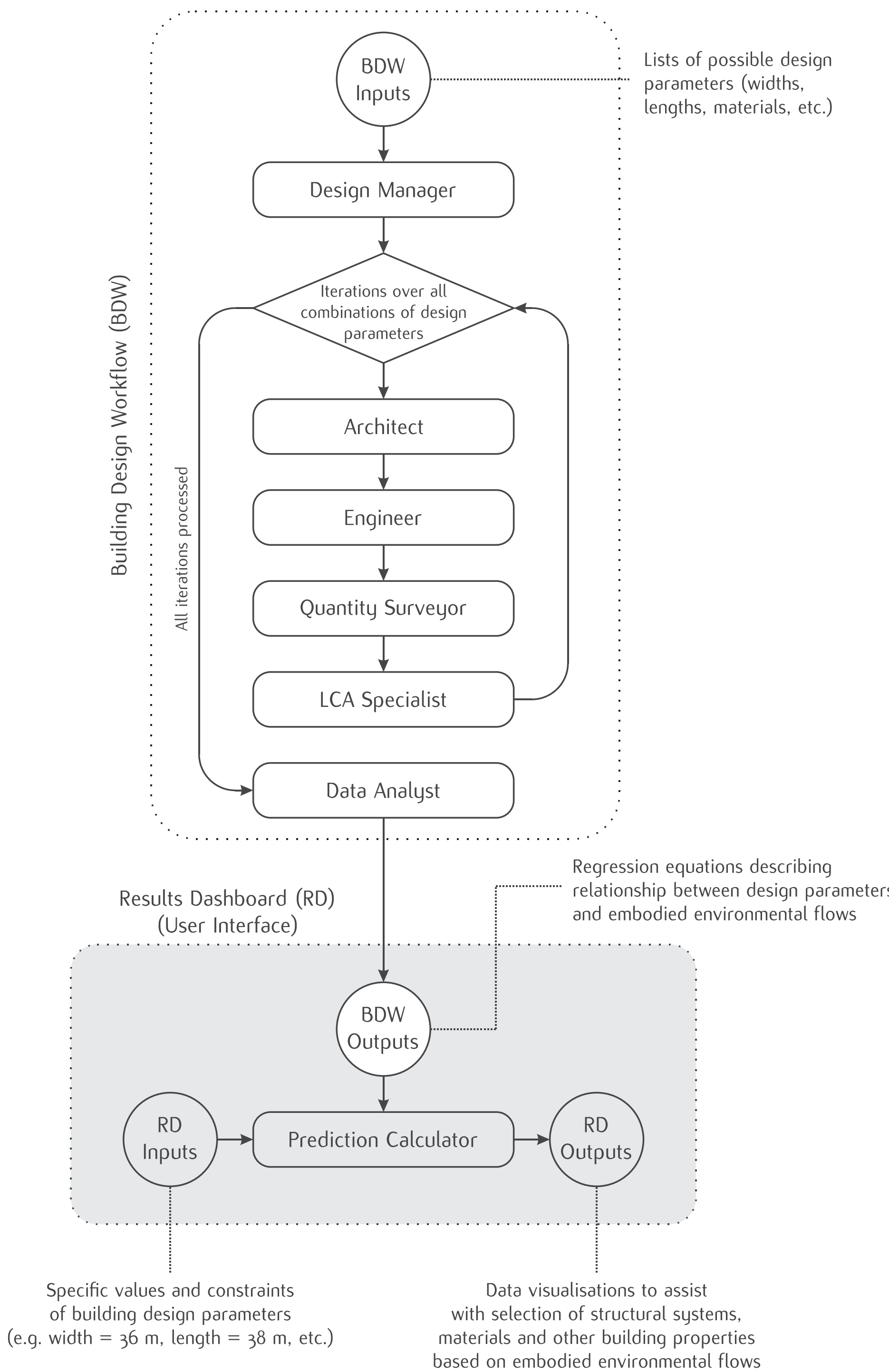

Fig. 3. General architecture of the software tool.

The software tool is composed of two main components: the *Building Design Workflow* and the *Results Dashboard*. The architecture of the software tool is depicted in Fig. 3, where circles denote input or output data, rounded rectangles denote software modules and solid arrows denote data flows. The arrows also depict the iterative process that is characteristic to the *Building Design Workflow*.

The *Building Design Workflow* component is composed of the Architect, Engineer, Quantity Surveyor, Life Cycle Assessment (LCA) Specialist and Data Analyst modules. Together, these modules automate and iterate the process of structural modelling, structural analysis, structural optimisation, quantity surveying and embodied environmental flow assessment for all combinations of inputted building parameters. Once the iterations are complete, the Data Analyst module conducts a regression analysis on the collected data to develop a set of equations that can be used to predict the EGHGE of structural systems in comparing a wide variety of alternative structural materials, systems and geometric parameters. A video demonstration of the *Building Design Workflow* is made available at BDW Demonstration 1 (https://youtu.be/BC9QHX7fhFc) and BDW Demonstration 2 (https://youtu.be/z4gcVnS_–co).

The *Results Dashboard* component represents a simple tool for designers to predict, study and compare the EGHGE of a wide variety of building designs of alternative structural materials, systems and geometric parameters. A video demonstration of the dashboard is made available at RD Demonstration (https://youtu.be/ufi7Fcs3A7E).

The regression equations that are produced by the Data Analyst module of the *Building Design Workflow* component are plugged into the Prediction Calculator module of the *Result Dashboard* component. The Prediction Calculator represents the software engine of the *Results Dashboard* that drives its functionality by predicting the values of EGHGE (dependent variable) using the inputted values of building design parameters (independent variables) such as width, depth, number of storeys, etc.

The design of the user interface is essential to the development of the *Results Dashboard*. The user interface must be designed to ensure a seamless interaction between the user and the dashboard to facilitate effective operation and control of software functions. For the *Results Dashboard* component to maximise its operability and utility, the user interface must be designed in accordance with the digital skills, experience, and expectations of prospective users (Adams, 2015).

3.5.1. *Verification of the software tool*

Following the initial development of the software tool, a verification process is carried out to identify and rectify any errors. The selection of verification tests is guided by the objective of ensuring that the values that most affect the comparison of structural designs based on their EGHGE are calculated correctly. Thus, in line with what is commonly referred to in the literature as correctness testing or functional testing, manual calculations using Microsoft Excel are performed on the calculation of various quantities.

Using stratified random sampling, the building models generated using the software tool are divided into smaller strata based on their unique set of structural materials and system typologies (e.g., 40 MPa RC outrigger and belt). A 10% verification sample size is implemented for each stratum to ensure that the verification sample best represents the total set of generated models.

A maximum relative change of 0.001% is imposed as a verification test between the software output quantity and the quantity obtained manually as the reference value. The calculation of the relative change, which is indicative of software precision, is performed according to the following equation:

$$\varepsilon_{(SQ,MQ)} = \frac{|SQ - MQ|}{SQ} \times 100 \tag{3}$$

Where $\varepsilon_{(SQ,MQ)}$ = relative change between the software output and the manually obtained reference value in %; SQ = software output quantity; and MQ = manually obtained quantity.

By comparing the corresponding ETABs finite element models with the generated Microsoft Excel files, each of the following values for the selected models are verified:

- Total structural material volumes and masses;
- Structural material volumes and masses by element type;
- Total EGHGE; and
- Embodied EGHGE/NFA.

3.5.2. *Validation of the software tool*

The validation of the software tool is performed by comparing the EGHGE/NFA output values of the software tool with that of case study tall buildings. To ensure a high degree of trueness, a maximum relative change of 10% is imposed as a validation test between the software output and the EGHGE of the case study tall buildings. This maximum relative change was selected as it aligns with the early-stage decision-making process, where the software tool is most beneficial.

During these preliminary design stages, broader estimates are typically acceptable, reflecting the flexible nature of early design decisions and the potential for refinement in subsequent design phases. The 10% validation benchmark thus acknowledges the considerable additional structural analysis and detailing procedures typically required to finalise a structural design for construction.

The calculation of the relative change is performed according to the following equation:

$$\varepsilon_{(SQ,CSQ)} = \frac{|SQ - CSQ|}{SQ} \times 100 \tag{4}$$

Where $\varepsilon_{(SQ,CSQ)}$ = relative change between the software output and the case study reference value in %; SQ = software output quantity of EGHGE/NFA in kgCO_2-e/m^2, respectively; and CSQ = case study quantity reference value of EGHGE/NFA in kgCO_2-e/m^2.

As discussed in Section 3.2, in designing structural systems, the software tool considers various combinations of the following structural design loads: permanent, imposed, wind and earthquake loads. However, other primary loads (e.g., loads due to construction activity and eccentricities, rain, snow and floods) and secondary loads (e.g., loads due to temperature changes, material shrinkage and foundation settlement) might govern the design of individual structural members and lead to slightly different material and EGHGE values.

3.5.3. *Description of building models used for software validation*

A study by Sang Kim, Lee, and Scanlon [71] analysed and compared alternative structural systems and materials for representative residential tall buildings in Seoul, South Korea according to their structural material quantities. The software tool is validated by comparing its outputs with the EGHGE/NFA of the representative tall building models developed by Sang Kim et al. [71].

Like Australia, the seismic hazard level in the Korean Peninsula is classified as low seismicity [72,73]. The Korean Peninsula is also similar to Australia in its exposure levels to strong wind loads that typically govern the design of tall buildings [74]. Therefore, due to the similar conditions that yield comparable lateral design loads, case study tall buildings that are designed to be in Seoul, South Korea are deemed to be suitable for the validation of the software tool.

Alternative structural systems were developed by Sang Kim et al. [71] for 40-, 60-, and 80-storey building scenarios. For the 40-storey building scenario, a 40 MPa RC shear wall structural system was proposed and evaluated. In contrast, for the 60- and 80-storey building scenarios, a 50 MPa RC outrigger and belt structural system was designed. These models are referred to as C40, C60, and C80 for the respective storey scenarios. All the building models adopted a square floor plan (35 m × 35 m) with three column spans in each orthogonal direction. Structural material quantities for models C40, C60, and C80 can be found in Appendix B.

To validate the software tool, the structural material quantities of C40, C60 and C80 are manually converted to EGHGE/NFA using the coefficients of the EPiC database. These values of EGHGE/NFA are considered reference values to which the outputs of the software tool are compared. The data inputs used to model C40, C60 and C80 in the software tool are listed in Appendix B.

The validation of the software tool using these building models provides an opportunity to assess the degree of agreement between the framework, software tool and building models that meet design requirements, as well as to test all related assumptions and approximations.

3.5.4. Description of case study tall building used to explore the potential of the framework and software tool

Once the software tool is verified and validated, the 101 Collins Street building is used as a case study to demonstrate the use of the software tool and its potential in guiding early-stage structural design decisions. As seen in Fig. 4, 101 Collins Street is a 52-storey building located in the Central Business District of Melbourne, Australia. It is currently the 11th tallest building in Australia (CTBUH, 2023). Its structure is composed of a reinforced concrete core and frame, which yields a shear wall structural system typology. Using the *Results Dashboard* of the software tool, the base case modelling of 101 Collins Street is conducted to establish the base case EGHGE/NFA value.

Subsequently, variations in structural materials, system typologies and geometries - and their influence on EGHGE/NFA - are compared to the base case results of 101 Collins Street. The data inputs used to model 101 Collins Street in the software tool are listed in Appendix B.

Fig. 4. 101 Collins Street, Melbourne.

4. Results

The aim of this section is to present the results of the regression analyses as well as the verification and validation of the framework and software tool. This section also explores the potential of the framework and software tool for comparing alternative structural materials, system typologies and geometries of tall buildings based on their embodied greenhouse gas emissions (EGHGE). The results of the regression analyses, which are presented in Section 4.1, represent the predictive models used by the developed software tool to quantify the EGHGE of structural systems for tall buildings.

4.1. Predictive modelling using regression analysis

Using the *Building Design Workflow* component of the software tool (see Section 3.5), a total of 960 building models were designed and their EGHGE were assessed. The entire catalogue of building models is provided in Appendix C. To enhance the utilisation of the data accumulated in this work, the constructed finite element models and derived material quantities of all 960 building models created for the purpose of this study have been curated and are readily available online at Rephrame FEM GitHub Repository (https://github.com/jhelal/RephrameFEM.git) and Rephame Excel GitHub Repository (https://github.com/jhelal/RephrameExcel.git), respectively.

As discussed in Section 3.4, an ordinary least squares linear regression analysis was conducted on the dataset of building models to develop predictive models for the EGHGE of the 12 considered unique combinations of structural materials and structural system typologies.

To construct the regression equations, a forward stepwise selection was adopted starting with an empty model. Building parameters that have an established causal relationship with structural material quantities (rooted in the first principles of structural design and analysis) and that best improve the goodness of fit were iteratively added to yield the lowest squared error in the regression analysis. After numerous iterations, the following building parameters were found to maximise the absolute correlation with the EGHGE/NFA of the 12 unique combinations of structural systems and structural materials:

- Storeys;
- Width;
- Number of column spans across building width;
- Depth;
- Number of column spans across building depth;
- Aspect ratio (presented in Eq. (5)); and
- Slenderness ratio (presented in Eq. (6)).

The following equation represents the aspect ratio parameters for a building with a rectangular floorplan:

$$AR_b = \frac{max(w_b, d_b)}{min(w_b, d_b)} \tag{5}$$

Where AR_b = aspect ratio between the width and depth of building b with a rectangular floorplan; w_b = building width in m; and d_b = building depth in m.

The following equation represents the slenderness ratio predictor:

$$SR_b = \frac{h_b}{min(w_b, d_b)} \tag{6}$$

Where SR_b = slenderness ratio between the height of building b and the narrower dimension of its rectangular floorplan; w_b = building width in m; and d_b = building depth in m.

The following regression equation was found to maximise the predictive performance of all 12 predictive models:

$$EGHGEPNFA_{SS,m,b} = \beta_0 + \beta_1 S_b^2 + \beta_2 S_b + \beta_3 W_b + \beta_4 CSW_b$$
$$+ \beta_5 D_b + \beta_6 CSD_b + \beta_7 AR_b + \beta_8 SR_b \quad (7)$$

where $EGHGEPNFA_{SS,M,b}$ = the embodied greenhouse gas emissions per net floor area for a structural system *SS* made of material *m* for building *b* in $kgCO_2$-e/m^2; β_0 through β_8 = regression coefficients for the corresponding predictor; S_b = number of storeys; W_b = building width in m; *CSWb* = number of column spans along building width; D_b = building depth in m; CSD_b = number of column spans along building depth; AR_b = aspect ratio as defined in Eq. (5); and SR_b = slenderness ratio as defined in Eq. (6).

Regression coefficients and basic descriptive statistics for the 12 predictive models are presented in Appendix D. As measured by their coefficient of determination (R^2), the predictive models were able to account for between 84% and 97% of the variance in the observed data of EGHGE/NFA. These high R^2 values, presented in Appendix D for each regression equation, imply that the predictive models highly fit the observed data for the 960 building models, thereby indicating a high level of predictive precision and accuracy.

As discussed in Section 3.5, the predictive models are plugged into the *Results Dashboard* component of the software tool to facilitate structural design decision-making based on the EGHGE of structural systems.

4.2. Verification of the developed software tool

Verification tests were conducted on the software tool to ensure the accurate calculation of values that significantly impact the comparison of structural designs based on their EGHGE. Manual calculations were performed using Microsoft Excel, employing stratified random sampling to select a 10% verification sample (96 models) from the 960 building models generated using the software tool. The results of the verification tests showed that all cases met the stringent acceptance criterion of a maximum relative change of 0.001% between the software output quantity and the manually obtained reference value.

These results highlight the accuracy of the software tool in calculating the values most relevant to the comparison of structural designs based on their EGHGE.

4.3. Validation of the developed software tool

The validation of the software tool was conducted by comparing its output values of EGHGE per NFA with the manually calculated values for building models C40, C60, and C80, as described in Section 3.5.3 and designed by Sang Kim et al. [71]. To ensure a high degree of trueness, a maximum relative change of 10% was set as a validation test between the software output and the EGHGE of the case study tall buildings.

The validation process involved manually calculating the EGHGE of the building models using the same EGHGE coefficients adopted by the software tool, to account for any differences in life cycle inventory analysis approaches. The structural material quantities as well as the data inputs used to model C40, C60 and C80 in the software tool are listed in Appendix B. Using the material coefficients from the Environmental Performance in Construction (EPiC) database, the manually calculated values were 265, 330, and 408 $kgCO_2$-e/m^2 for models C40, C60, and C80, respectively.

As shown in Fig. 5, the software tool predicted EGHGE per NFA values of 288, 334, and 425 $kgCO_2$-e/m^2 for the structural systems of C40, C60, and C80, respectively.

The outputs for all three building models are within the acceptable maximum relative change of 10%, demonstrating the validity of the software tool in estimating EGHGE/NFA of structural systems for tall buildings, as per the justification provided in Section 3.5.2.

4.4. Case study: 101 Collins Street Building, Melbourne, Australia

This section demonstrates the potential of the framework and software tool in comparing alternative structural materials, system typologies, and geometries for the structural system of the 101 Collins Street building. Using the *Results Dashboard* of the software tool, the base case modelling of 101 Collins Street yielded a predicted EGHGE/NFA value of 262 $kgCO_2$-e/m^2. Subsequently, variations in structural materials, system typologies and geometries - and their influence on EGHGE/NFA - are compared to the base case results of 101 Collins Street. The graphical outputs of the *Results Dashboard* are presented throughout this section to demonstrate its use and potential in guiding early-stage structural design decisions.

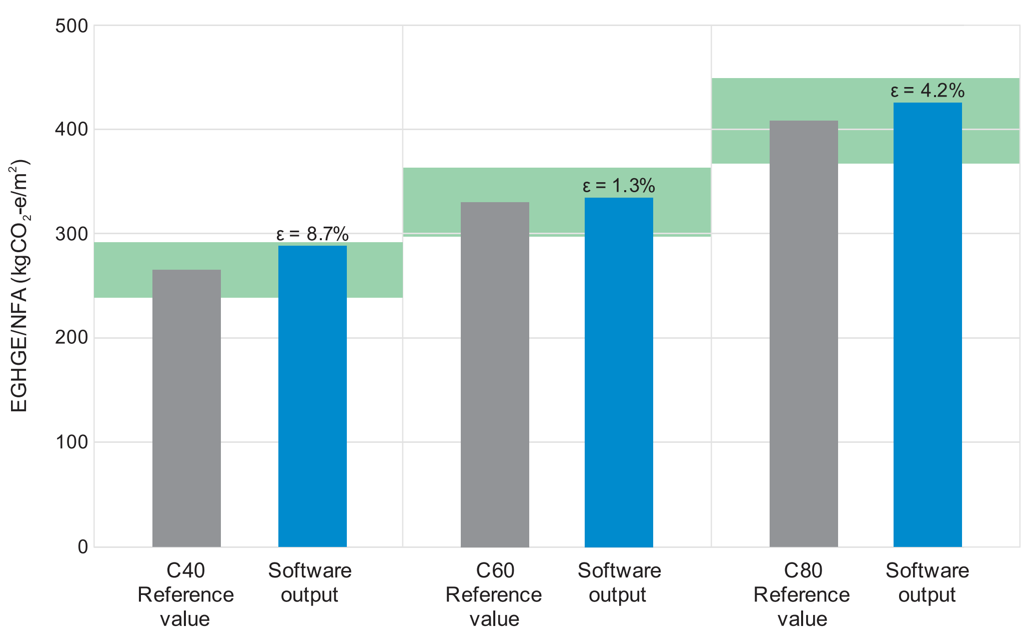

Fig. 5. EGHGE/NFA validation results of C40, C60 and C80 depicting the relative change of the software outputs compared to the reference value. Note: the green area depicts the acceptable relative change of 10% as outlined in Section 3.5.2. (For interpretation of the references to colour in this figure legend, the reader is referred to the web version of this article.)

4.4.1. Variations in structural materials and system typologies

This section explores the potential of the framework and software tool in comparing alternative structural materials and system typologies based on the EGHGE/NFA of structural systems using the case study building of 101 Collins Street. As mentioned in Section 3,1, the structural materials considered are 32 MPa RC, 40 MPa RC, 50 MPa RC, and steel, while the structural system typologies include shear wall, outrigger and belt, and braced tube.

Using the *Results Dashboard* of the software tool, the base case modelling produced an EGHGE/NFA value of 262 kgCO_2-e/m^2. Subsequently, variations in structural materials, system typologies and geometries - and their influence on EGHGE/NFA - are compared to the base case result of 101 Collins Street.

Fig. 6 demonstrates the potential of the *Results Dashboard* for rapidly assessing the EGHGE of various structural systems composed of alternative structural materials and typologies. This figure includes the following comparisons based on EGHGE/NFA:

- Fig. 6(a): Shear wall structural systems composed of different RC grades.
- Fig. 6(b): All considered structural systems as alternatives for the 32 MPa RC material.
- Fig. 6(c): All combinations of structural systems (i.e., shear wall, outrigger and belt, and braced tube) and RC grades (i.e., 32 MPa RC, 40 MPa RC, and 50 MPa RC).

To augment the analytical depth of Fig. 6 and enhance interpretation of the regression model outcomes, uncertainty - specifically standard error - has been quantified and incorporated as shaded plots. This visualization indicates a 95% confidence interval around the prediction, thereby offering a pragmatic tool for interpreting the robustness of the predicted results.

The standard error is determined using the square root of the variance of the coefficients obtained from the regression model. Each regression coefficient (β_i) in Eq. (7) is associated with an uncertainty calculated as the standard error (SE_i) using the following formula:

$$SE_i = \sqrt{Var(\beta_i)} \quad (8)$$

Where SE_i = the standard error associated with the regression coefficient β_i from Eq. (7); and $Var(\beta_i)$ = the variance of the regression coefficient β_i, which is a measure of how much the estimated value of β_i could potentially vary or deviate across different model iterations or subsets of the data.

Through the introduction of the standard error into the analysis and data visualisation, the reliability and validity of the predictive models are enhanced, facilitating more informed structural design choices based on EGHGE of alternative structural systems.

Fig. 6(c) demonstrates that the optimal combination of structural system typologies and materials for 101 Collins Street is the 50 MPa RC outrigger and belt system, which is predicted to reduce the EGHGE/NFA of the base case structural system by 17.6%. Through the selection of optimal structural systems, the demonstrated savings in EGHGE conform with the reduction targets of 10% to 25% aspired to by the Structural Engineers 2050 (SE 2050) Commitment Program to ensure substantive EGHGE reductions in the construction of new buildings.

The results challenge the notion that materials with low embodied environmental flow intensities are consistently favourable in the design and construction of the built environment. Furthermore, the use of a steel frame instead of 32 MPa RC used in the base case of 101 Collins Street leads to a significant increase in EGHGE/NFA (up to +178%), reaffirming the relative inefficiency of steel structural systems compared to RC based on EGHGE/NFA. This was also demonstrated by existing comparative life cycle assessment studies, such as those by Foraboschi et al. [27], Trabucco et al. [30] and Mavrokapnidis et al. [31].

4.4.2. Variations in building geometry

This section investigates the potential of the developed framework and software tool for comparing alternative floor plan geometries based on EGHGE/NFA of structural systems using the case study building of 101 Collins Street. The analysis covers variations in the number of column spans, width, depth, aspect ratio, and slenderness ratio.

Fig. 7 shows the consolidated results of the analyses, depicting the plots generated by the *Results Dashboard* of the software tool when different numbers of column spans (5, 7, and 9 along both building width and depth) and alternative depths are selected for comparison. As in Fig. 6, uncertainty is represented in Fig. 7 through shaded plots, providing a 95% confidence interval around the predictions to enable a more robust interpretation of the results.

As seen in Fig. 7(a), the results indicate that the EGHGE of the structural system of 101 Collins Street is significantly influenced by the number of column spans by up to 20%. When the number of column spans is increased from 5 to 7, there is a decrease of 10.3% in EGHGE/NFA. When the number of column spans is further increased from 5 to 9, the effect is doubled with a 20.6% decrease in EGHGE/NFA. The influence of the number of column spans on the EGHGE/NFA of the structural system of 101 Collins Street is consistent across all possible building heights, as shown in the upward shift of the premium-for-height plots in Fig. 7(a) with each increase in the number of column spans.

In terms of variations in width, depth, aspect ratio, and slenderness ratio, the results depicted in Fig. 7(b) demonstrate that the floor plan geometry of the 101 Collins Street building has a significant influence on the EGHGE of its structural system. As the depth of 101 Collins Street decreases, the EGHGE/NFA of its structural system increases. When the depth of the case study building is reduced from 45 m to 36 m, an increase of 8.4% in EGHGE/NFA is predicted. When the depth is further reduced by another 9 m, a more significant increase of 23.3% in EGHGE/NFA is predicted. This observed non-proportional inverse relationship between floor plan geometric properties and EGHGE/NFA suggests that the efficiency of the structural system of 101 Collins Street is adversely affected by decreasing depths, decreasing aspect ratios, and increasing slenderness ratios.

5. Discussion

Based on the results presented in Section 4, this section discusses various means to reduce the EGHGE of structural systems for tall buildings. The limitations and potential improvements to the developed framework and software tool are also discussed.

The concept of a premium for height for tall buildings is well documented in the scientific literature of structural engineering and LCA (see Section 4.1). Existing studies show that tall buildings can have up to 60% more embodied environmental flows per NFA compared to low rise buildings [17,30,75]. This reported increase in embodied environmental flows conforms with the findings of this work, which demonstrates that among all the considered structural designs, the optimal structural system for a 50-storey building has 65% more EGHGE/NFA than the optimal structural system for a 10-storey building (see Figs. 6 and 7). Thus, reducing the height of tall buildings is a definite means of minimising the EGHGE of structural systems.

This work also demonstrated that tall buildings are characterised by a premium for slenderness. The application of the developed software tool to the 52-storey case study building showed that reducing the width of the building by 40%, thereby increasing its slenderness, resulted in a 23% increase in EGHGE/NFA. None of the comparative LCA studies reviewed in Section 2 assess alternative structural designs with varying slenderness ratios. However, the detrimental influence of slenderness on the structural efficiency of tall buildings is well established in the structural engineering body of knowledge [44,76,77]. Thus, in assessing alternative structural designs for tall buildings, comparative LCA studies must consider the effects of slenderness on the embodied environmental flows of structural systems.

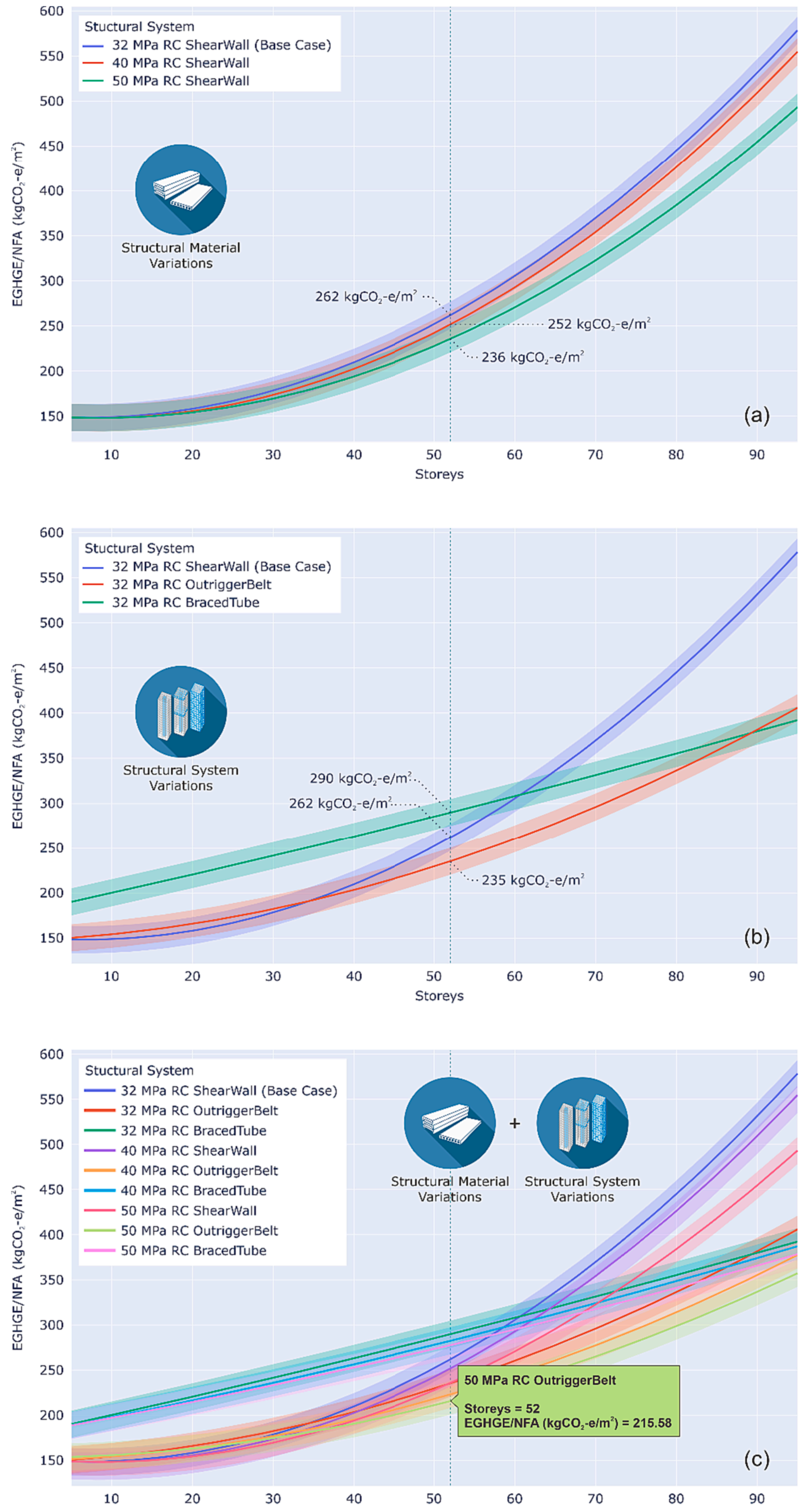

Fig. 6. EGHGE/NFA premium-for-height plots with shaded 95% confidence intervals generated by the Results Dashboard of the software tool to compare variations in structural materials and system typologies for 101 Collins Street.

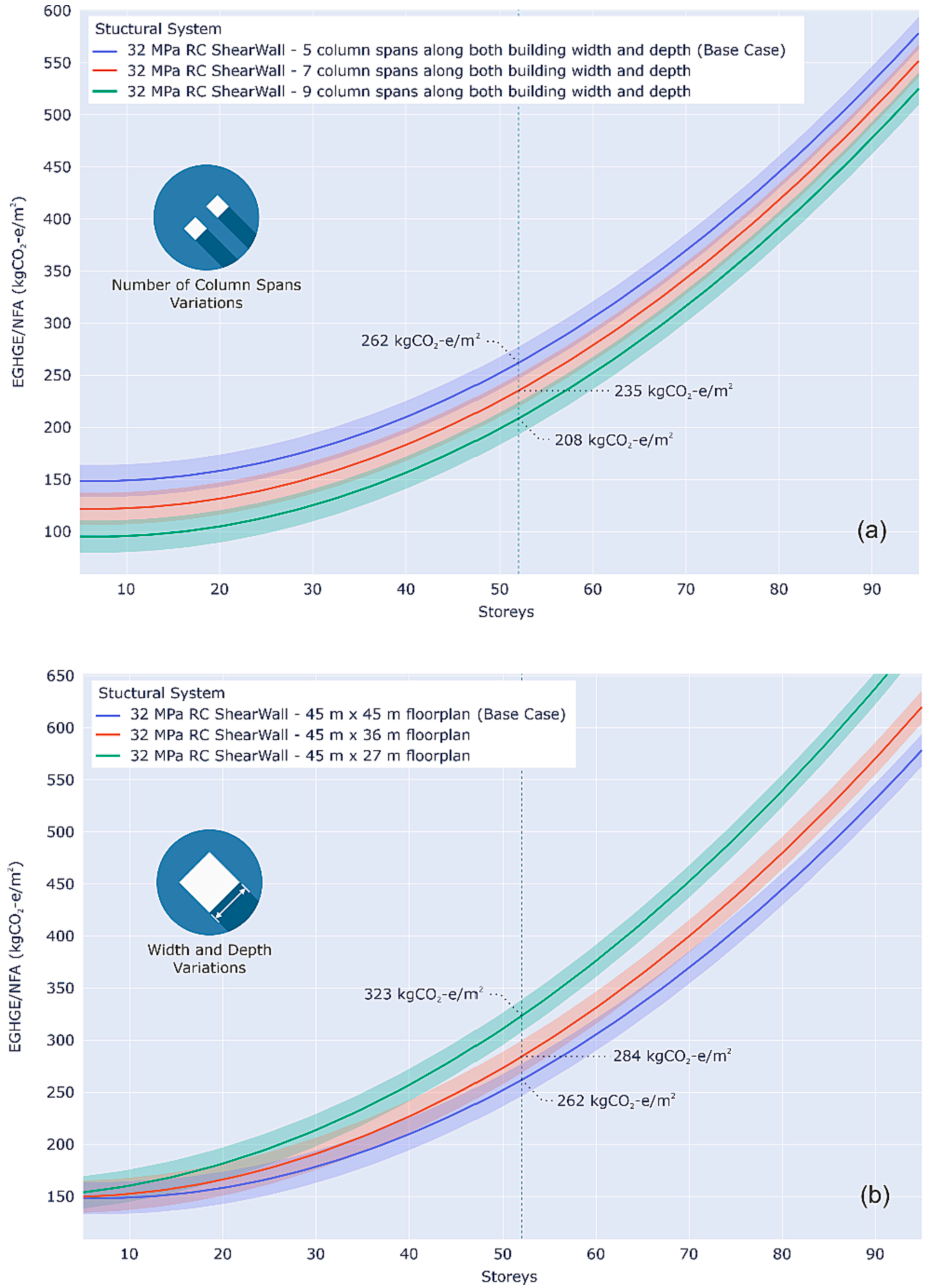

Fig. 7. EGHGE/NFA premium-for-height plots with shaded 95% confidence intervals generated by the Results Dashboard of the software tool to compare column spans, width and depth variations for 101 Collins Street.

Regarding the premium for wide-open spaces, the application of the developed software tool to the case study building demonstrated that decreasing the number of columns by 20%, thereby widening the open spaces within their floor plans, led to a 10% increase in the EGHGE/NFA of their structural systems. In an extensive parametric study of structural material quantities for vertical load resisting systems, the same conclusion was reached by D'Amico and Pomponi [65] despite their exclusion of lateral loads in the adopted structural design and analysis approaches. Like the premium for slenderness, the premium for wide-open spaces is relatively unexplored in existing comparative LCA studies. A loss of architectural quality is often alluded to by these studies to justify their neglect or omission of this effective means of reducing the embodied environmental flows of structural systems [27,78]. However, faced with the immense challenges of climate change, all means of optimisation must be explored to better inform the architectural and structural design decision-making process.

Despite methodological differences, the results of this work generally conform with the findings of the studies by Foraboschi et al. [27], Trabucco et al. [30] and Mavrokapnidis et al. [31], which demonstrated that RC frames can yield significantly less EGHGE/NFA than steel frames for tall buildings. By contrast, the findings of this work differed from that of Zhao and Haojia [28], which involved evaluating the EGHGE of three alternative structural systems (i.e., shear wall and outrigger and belt) for a 69-storey building scenario. As discussed in Section 2, by adopting a process-based LCI approach, Zhao and Haojia [28] found that the shear wall structural system resulted in an EGHGE/NFA that was approximately 40% to 45% lower than that of the outrigger and belt structural systems. Conversely, this study demonstrated the higher efficiency of outrigger and belt structural systems compared to shear wall structural systems based on their EGHGE for a 69-storey tall building. In the absence of transparency within the structural analysis and modelling approaches adopted by Zhao and Haojia [28], a meaningful analysis of the discrepancy is impossible to conduct thoroughly to better understand the factors to which it can be attributed to. Only tentative explanations can be provided. It is possible that the discrepancy is due to the number and placement of outriggers and belts, which differ between this work and the study by Zhao and Haojia [28]. However, this work adopted a design strategy that is consistent with common practice by placing outriggers and belts at intervals of 12 to 15 storeys.

In addition to the differences in design strategies, another aspect that may have contributed to the discrepancy in results could be the variability in the adopted EGHGE coefficients. Studies such as the one conducted by Helal et al. [32] (discussed in Section 2) highlight the significant impact that life cycle inventory (LCI) approaches, including the resulting EGHGE coefficients, can have on the results of comparative LCA studies. The study revealed that different LCI approaches can influence the EGHGE of structural systems for tall buildings by up to 116%, and may even lead to contradictory choices in structural systems for tall buildings based on minimising their EGHGE. The findings of this study confirm the need for clarity, transparency and comprehensiveness in the use of LCI approaches for comparative LCA studies, particularly in the structural design of tall buildings.

5.1. Limitations and future research

As in any scientific inquiry, this study suffers from limitations. Most notably, the findings of the study are restricted to the considered structural materials (i.e., 32/40/50 MPa reinforced concrete and steel), structural typologies (i.e., shear wall, outrigger and belt and braced tube) and rectangular floor plan geometries. The findings are also restricted to the numerous design strategies that were adopted in the creation of the finite element models that were used to generate the predictive models for the embodied greenhouse gas emissions per net floor area of structural systems (e.g., placement of outriggers and belts, equidistant column spans, placement of shear walls, etc.).

This work relies on Australian hybrid data for calculating EGHGE, which are specific to the local economic conditions and energy mix of Australia. Despite the geographic specificity of the results pertaining to EGHGE, the resulting structural material quantities, which were calculated using advanced structural analysis techniques, are still relevant. Given material coefficients for EGHGE that are specific to other regions with similar exposure levels to lateral loads (i.e., wind loads and earthquake loads), future research can convert the existing structural material quantities to more specific and appropriate values of EGHGE for other regions.

Naturally, further research could be conducted outside the scope of this work to enhance the comprehensiveness of the developed framework and software tool. These include, but are not limited to, considering additional structural materials, typologies, and geometries, broadening the system boundary to include more life cycle stages (i.e., operational and end-of-life stages) and other building systems (e.g., façade, vertical transportation, etc.) and incorporating cost analyses due to its major influence on the decision-making process. Research in these areas has the potential to ensure that reductions in environmental flows in one building system and one life cycle stage are not shifted to others.

6. Conclusion

The aim of this research was to develop a framework and software tool that integrates the assessment of embodied greenhouse gas emissions into the structural design of tall buildings. This framework has been developed using comprehensive hybrid methods for life cycle inventory analysis and advanced structural design and finite element modelling techniques. An advanced software tool was implemented to automate the structural design, modelling, analysis, optimisation and embodied greenhouse gas emissions assessment of structural systems for tall buildings. Approximately 1,000 building models were iteratively designed, analysed, optimised and assessed using the software tool. Through regression analyses, the resulting dataset of structural material quantities was used to construct predictive models for the embodied greenhouse gas emissions per net floor area of 12 unique combinations of structural system typologies and structural materials.

These predictive models were integrated into a results dashboard, which enables engineers and tall building designers to compare alternative structural materials (i.e., 32/40/50 MPa reinforced concrete and steel), typologies (i.e., shear wall, outrigger and belt and braced tube) and geometries (i.e. rectangular floor plan geometries) according to the embodied greenhouse gas emissions per net floor area of structural systems. Three case study tall buildings of different heights, structural system typologies and structural materials were used to validate the framework and software tool. Another case study tall building was used to illustrate the potential of the framework and software tool in reducing the embodied greenhouse gas emissions of structural systems for tall buildings of varying heights.

In summary, the developed framework and software tool have been shown to provide the most precise and sophisticated integration of embodied environmental assessment into the parametric structural design of tall buildings as of yet. Through a simple and user-friendly interface, they enable tall building designers to utilise environmental assessment as a design-assisting tool, rather than as an appraisal method to evaluate a completed building. This will potentially lead to reductions in the environmental effects associated with the construction of tall buildings. Furthermore, by enhancing the consistency, transparency and comprehensiveness of the embodied environmental flow assessment of structural systems, this research has the potential to complement multiscale and holistic approaches that aim to identify solutions that reduce the overall life cycle environmental effects associated with buildings, neighbourhoods and cities.

CRediT authorship contribution statement

James Helal: Conceptualization, Methodology, Software, Validation, Formal analysis, Investigation, Resources, Data curation, Writing – original draft, Visualization. **André Stephan:** Supervision, Writing – review & editing. **Robert H. Crawford:** Supervision, Writing – review & editing.

Declaration of Competing Interest

The authors declare that they have no known competing financial interests or personal relationships that could have appeared to influence the work reported in this paper.

Data availability

In the paper, I have provided URLs to my publicly accessible GitHub repository which includes the data that supports the findings of this paper.

Appendix A. Calculating structural design loads

In accordance with the design requirements for residential structures as prescribed by Australian Standard AS1170.1:2002, Table A.1 summarises the considered permanent and imposed loads in the design of the structural systems. Similarly, Tables A.2 and A.3 summarise the coefficients used to generate the considered wind loads and earthquake loads as prescribed by Australian Standards AS1170.2:2011 and AS1170.4:2007, respectively.

Table A1
Structural loads considered in the design of the finite element models.

Considered loads	Values
Permanent loads	Based on building geometry and material densities
Imposed loads	2 kPa
Super-imposed loads	1 kPa
Façade loads	3.5 kN/m

Table A2
Wind coefficients to generate wind loads according to AS/NZA 1170.2:2002.

Wind Load Inputs	Values	Justification of values
Regional wind speed (V_R)	46 m/s	Described in AS/NZS 1170.2:2011 Section 3.2
Wind direction multiplier (M_d)	1	Described in AS/NZS 1170.2:2011 Section 3.3
Terrain category ($M_{z,cat}$)	4	Described in AS/NZS 1170.2:2011 Section 4.2
Shielding multiplier (M_s)	1	Described in AS/NZS 1170.2:2011 Section 4.3
Topographic multiplier (M_t)	1	Described in AS/NZS 1170.2:2011 Section 4.4
Windward coefficient (C_{pw})	0.8	Described in AS/NZS 1170.2:2011 Section 5.2
Leeward coefficient (C_{pl})	0.5	Described in AS/NZS 1170.2:2011 Section 5.2
Area reduction factor (K_a)	1	Described in AS/NZS 1170.2:2011 Section 5.4.2
Combination factor (K_c)	1	Described in AS/NZS 1170.2:2011 Section 5.4.3
Local pressure factor (K_l)	1	Described in AS/NZS 1170.2:2011 Section 5.4.4
Porous cladding factor (K_p)	1	Described in AS/NZS 1170.2:2011 Section 5.4.5
Dynamic response factor (C_{dyn})	*	Described in AS/NZS 1170.2:2011 Section 6.1

*For structures with a first mode fundamental frequency greater than 1 Hz, $C_{dyn} = 1.0$. For structures with a first mode fundamental frequencies between 0.2 Hz and 1 Hz, C_{dyn} was computed in accordance with AS/NZS 1170.2:2002 Section 6.1. None of the modelled buildings had a first mode fundamental frequency less than 0.2 Hz.

Table A3
Earthquake coefficients to generate earthquake loads according to AS1170.4:2007.

Earthquake Load Inputs	Values	Justification of values
Site subsoil class	D	Described in AS/NZS 1170.4:2007 Section 4.2.
Probability factor (k_p)	1.1	Described in AS/NZS 1170.4:2007 Section 3.1.
Hazard factor (Z)	0.08	Described in AS/NZS 1170.4:2007 Section 3.2.
Performance factor (S_p)	0.77	Described in AS/NZS 1170.4:2007 Section 6.5.
Ductility factor (u)	2	Described in AS/NZS 1170.4:2007 Section 6.5.

All tall buildings will experience most, if not all, of the loads listed in Tables A.1, A.2 and A.3. The challenge of structural design is to determine the governing combination of loads and design a tall building accordingly. To ensure safety and consistency, structural design standards recommend load combinations that reflect probable and conservative loading conditions. The load combinations that are adopted by this paper for the structural design of tall buildings, are listed in Section 4 of Australian Standard AS1170.0:2002 and include 1.2 × Permanent Load (G) + 1.5 × Imposed Load (Q), 1.35 × G, 1.2 × G + 0.4 × Q + Wind (W), 1.2 × G + 0.4 × Q + Earthquake (E) and 16 other load combinations.

Figs. A.1 and A.2 demonstrate the detailed methods of computing the applied wind loads and earthquake loads, respectively.

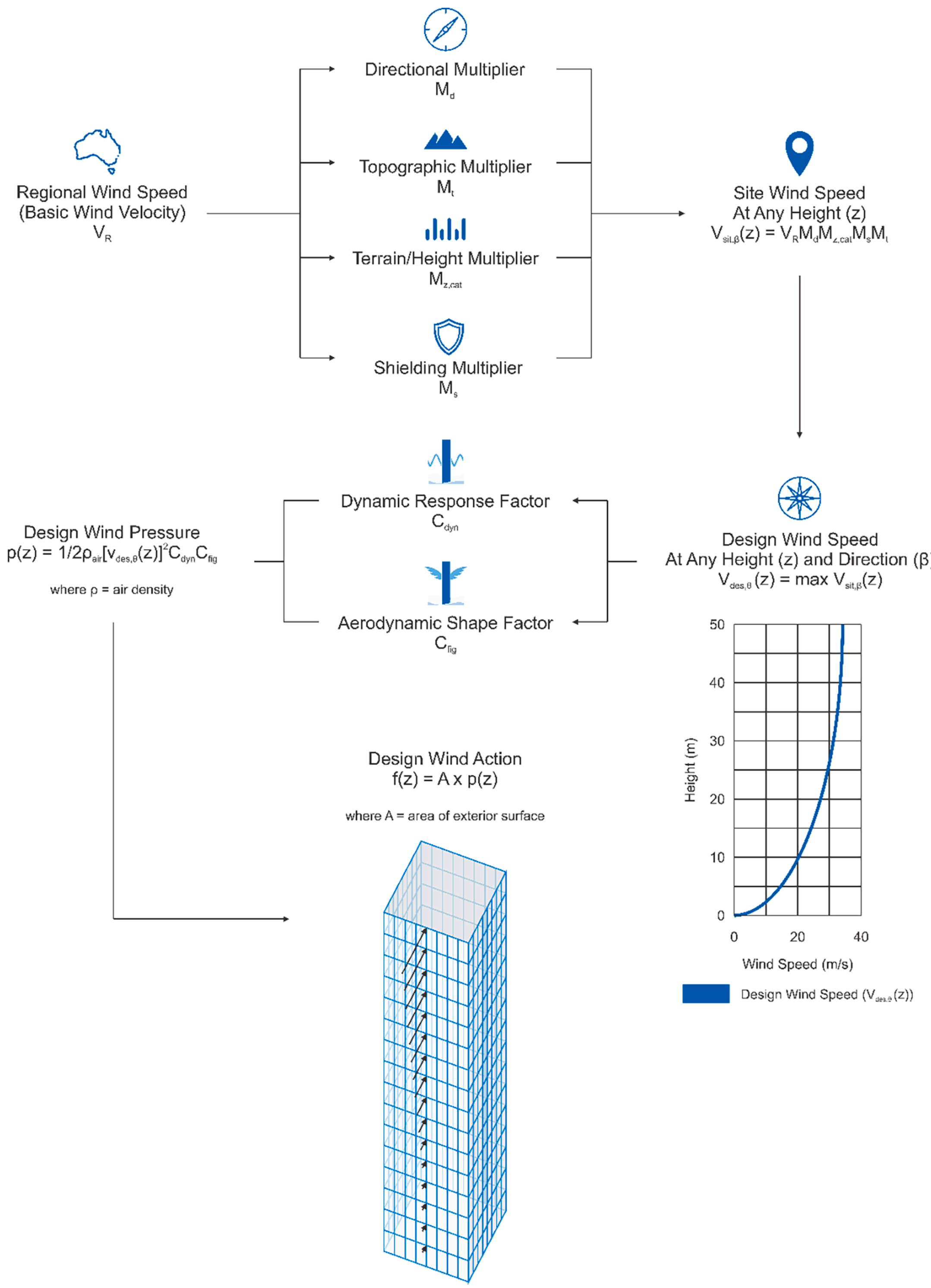

Fig. A1. Process of calculating wind loads as prescribed by Australian Standard AS1170.2:2011.

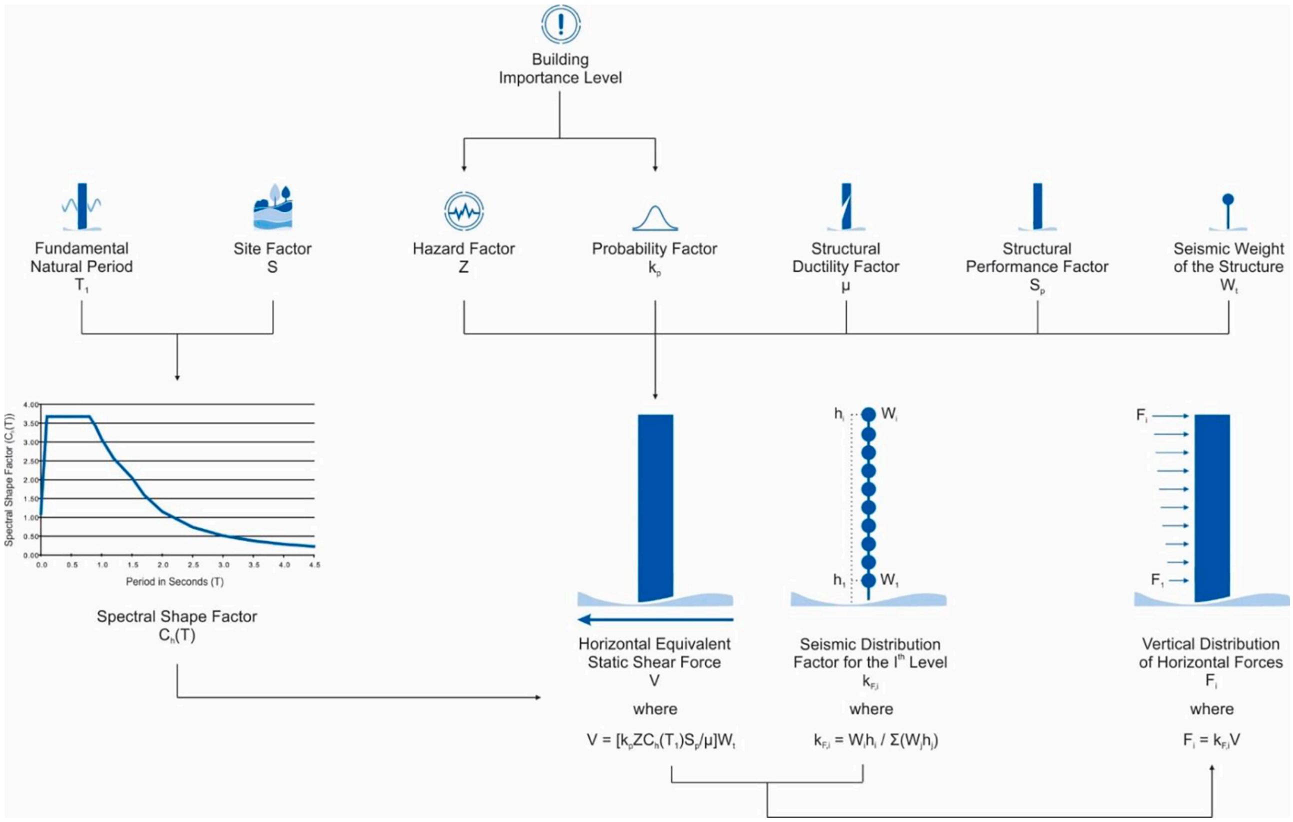

Fig. A2. Process of calculating equivalent static earthquake loads as prescribed by Australian Standard AS1170.4:2007.

Appendix B. Case studies used for software validation and demonstration the potential of the framework and software tool

A study by Sang Kim et al. [71] analysed and compared alternative structural systems and materials for representative residential tall buildings in Seoul, South Korea according to their structural material quantities. The software tool is validated by comparing its outputs with the embodied greenhouse gas emissions (EGHGE) of the representative tall building models developed by Sang Kim et al. [71].

Table B.1 presents the alternative structural systems and materials designed by Sang Kim et al. [71] for the 40, 60 and 80 storey building scenarios. Of these structural systems, models C40, C60 and C80 fall within the current material coverage of the software tool and are therefore suitable for validation purposes. Conversely, models S40, S60 and S80 are not considered in this analysis due to their use of composite structural members in the frame and the outrigger and belt.

Table B1
Structural systems and materials of the building models developed by Sang Kim et al. [71].

#	Storeys	Structural System	Structural Materials	Suitable for Validation
S40	40	Shear Wall	40 MPa RC Shear Wall + Composite Frame	×
C40	40	Shear Wall	40 MPa RC Shear Wall + Frame	✓
S60	60	Outrigger and Belt	50 MPa RC Shear Wall + Composite Frame + Composite Outrigger and Belt	×
C60	60	Outrigger and Belt	50 MPa RC Shear Wall + Frame + Outrigger and Belt	✓
S80	80	Outrigger and Belt	50 MPa RC Shear Wall + Composite Frame + Composite Outrigger and Belt	×
C80	80	Outrigger and Belt	50 MPa RC Shear Wall + Frame + Outrigger and Belt	✓

A square floor plan, as seen in Fig. B.1, is adopted for all the building models listed in Table B.1. Fig. B.1 also shows the dimensions of the floor plan (35 m × 35 m) and the three column spans along each dimension. The lists of structural material quantities for models C40, C60 and C80 are presented in Table B.2

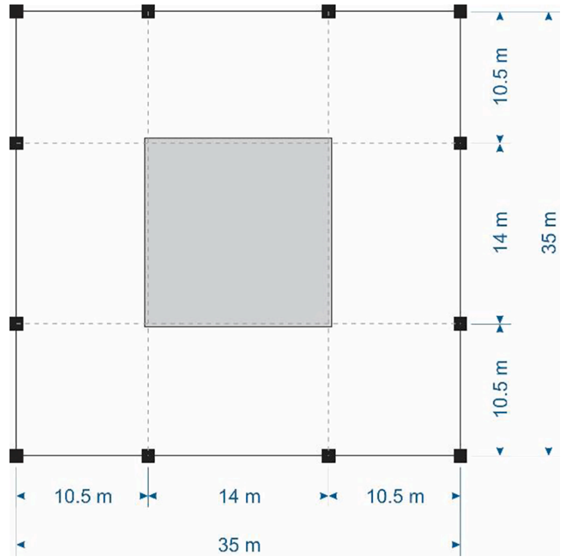

Fig. B1. Floor plan of the representative case study buildings in Seoul, South Korea. Adapted from Sang Kim et al. [71].

Table B2
List of structural material quantities for the suitable building models developed by Sang Kim et al. [71].

Model	NFA (m^2)	Material	Quantity	Unit
C40	55,353	40 MPa concrete	29,454	m^3
		Steel reinforcement	3,587	t
C60	79,113	50 MPa concrete	43,512	m^3
		Steel reinforcement	5,262	t
C80	103,716	50 MPa concrete	70,527	m^3
		Steel reinforcement	8,450	t

.

To validate the software tool, the structural material quantities of C40, C60 and C80 are converted to EGHGE/NFA using the coefficients of the Environmental Performance in Construction (EPiC) database. The data inputs used to model C40, C60 and C80 in the software tool are listed in Table B.3.

Table B3
List of software inputs used to model C40, C60 and C80.

Software inputs	Values		
	C40	C60	C80
Storeys	40	60	80
Floor plan shape	Rectangle	Rectangle	Rectangle
Width	35 m	35 m	35 m
Columns spans along building width	3	3	3
Depth	35 m	35 m	35 m
Columns spans along building depth	3	3	3
Structural material	40 MPa RC	50 MPa RC	50 MPa RC
Structural system	Shear Wall	Outrigger and Belt	Outrigger and Belt

The validation of the software tool using these building models provides an opportunity to assess the degree of agreement between the framework, software tool and building models that meet design requirements, as well as to test all related assumptions and approximations.

Once the software tool is verified and validated, the 101 Collins Street building is used as a case study to demonstrate the use of the software tool and its potential in guiding early-stage structural design decisions. The 101 Collins Street building is located in the Central Business District of Melbourne, Australia. Having 52 storeys, it is currently the 11th tallest building in Australia (CTBUH, 2023). Its structure is composed of a reinforced concrete core and a reinforced concrete frame, which yields a shear wall structural system typology.

Using the *Results Dashboard* of the software tool, the base case modelling of 101 Collins Street is conducted to establish the base case EGHGE/NFA value. The data inputs used to model 101 Collins Street in the software tool are listed in Table B.5

Table B5
List of software inputs used to model 101 Collins Street.

Software inputs	Values
Storeys	52
Floor plan shape	Rectangle
Width	45 m
Number of columns spans along building width	5
Depth	45 m
Number of columns spans along building depth	5
Structural material	32 MPa RC
Structural system	Shear wall

.

Appendix C. Constructed finite element models with adopted structural design methods

Using the *Building Design Workflow* component of the software tool, a total of 960 building models were designed, analysed, optimised and assessed according to their embodied greenhouse gas emissions. The entire catalogue of building models, which lists their parameters and the resulting embodied environmental flows per net floor area (NFA), is presented in Table C.1

Table C1
Catalogue of generated building models

#	Name	Storeys	Frame Material	LLRS	LLRS Material	Grid	Column Span in X Dir (m)	Column Span in Y Dir (m)
1	FEM1	5	32MPa RC	ShearWall	32 MPa RC	[5, 5]	4.8	4.8
2	FEM2	5	40 MPa RC	ShearWall	40 MPa RC	[5, 5]	4.8	4.8
3	FEM3	5	50 MPa RC	ShearWall	50 MPa RC	[5, 5]	4.8	4.8
4	FEM4	5	Steel	ShearWall	40 MPa RC	[5, 5]	4.8	4.8
5	FEM5	5	32 MPa RC	ShearWall	32 MPa RC	[5, 5]	4.8	7.2
6	FEM6	5	40 MPa RC	ShearWall	40 MPa RC	[5, 5]	4.8	7.2
7	FEM7	5	50 MPa RC	ShearWall	50 MPa RC	[5, 5]	4.8	7.2
8	FEM8	5	Steel	ShearWall	40 MPa RC	[5, 5]	4.8	7.2
9	FEM9	5	32 MPa RC	ShearWall	32 MPa RC	[5, 5]	7.2	4.8
10	FEM10	5	40 MPa RC	ShearWall	40 MPa RC	[5, 5]	7.2	4.8
11	FEM11	5	50 MPa RC	ShearWall	50 MPa RC	[5, 5]	7.2	4.8
12	FEM12	5	Steel	ShearWall	40 MPa RC	[5, 5]	7.2	4.8
13	FEM13	5	32 MPa RC	ShearWall	32 MPa RC	[5, 5]	7.2	7.2
14	FEM14	5	40 MPa RC	ShearWall	40 MPa RC	[5, 5]	7.2	7.2
15	FEM15	5	50 MPa RC	ShearWall	50 MPa RC	[5, 5]	7.2	7.2
16	FEM16	5	Steel	ShearWall	40 MPa RC	[5, 5]	7.2	7.2
17	FEM17	5	32 MPa RC	ShearWall	32 MPa RC	[5, 7]	4.8	4.8
18	FEM18	5	40 MPa RC	ShearWall	40 MPa RC	[5, 7]	4.8	4.8
19	FEM19	5	50 MPa RC	ShearWall	50 MPa RC	[5, 7]	4.8	4.8
20	FEM20	5	Steel	ShearWall	40 MPa RC	[5, 7]	4.8	4.8
21	FEM21	5	32 MPa RC	ShearWall	32 MPa RC	[5, 7]	4.8	7.2
22	FEM22	5	40 MPa RC	ShearWall	40 MPa RC	[5, 7]	4.8	7.2
23	FEM23	5	50 MPa RC	ShearWall	50 MPa RC	[5, 7]	4.8	7.2
24	FEM24	5	Steel	ShearWall	40 MPa RC	[5, 7]	4.8	7.2
25	FEM25	5	32 MPa RC	ShearWall	32 MPa RC	[5, 7]	7.2	4.8
26	FEM26	5	40 MPa RC	ShearWall	40 MPa RC	[5, 7]	7.2	4.8
27	FEM27	5	50 MPa RC	ShearWall	50 MPa RC	[5, 7]	7.2	4.8
28	FEM28	5	Steel	ShearWall	40 MPa RC	[5, 7]	7.2	4.8
29	FEM29	5	32 MPa RC	ShearWall	32 MPa RC	[5, 7]	7.2	7.2
30	FEM30	5	40 MPa RC	ShearWall	40 MPa RC	[5, 7]	7.2	7.2
31	FEM31	5	50 MPa RC	ShearWall	50 MPa RC	[5, 7]	7.2	7.2
32	FEM32	5	Steel	ShearWall	40 MPa RC	[5, 7]	7.2	7.2
33	FEM33	5	32 MPa RC	ShearWall	32 MPa RC	[7, 7]	4.8	4.8
34	FEM34	5	40 MPa RC	ShearWall	40 MPa RC	[7, 7]	4.8	4.8
35	FEM35	5	50 MPa RC	ShearWall	50 MPa RC	[7, 7]	4.8	4.8
36	FEM36	5	Steel	ShearWall	40 MPa RC	[7, 7]	4.8	4.8
37	FEM37	5	32 MPa RC	ShearWall	32 MPa RC	[7, 7]	4.8	7.2
38	FEM38	5	40 MPa RC	ShearWall	40 MPa RC	[7, 7]	4.8	7.2
39	FEM39	5	50 MPa RC	ShearWall	50 MPa RC	[7, 7]	4.8	7.2
40	FEM40	5	Steel	ShearWall	40 MPa RC	[7, 7]	4.8	7.2
41	FEM41	5	32 MPa RC	ShearWall	32 MPa RC	[7, 7]	7.2	4.8
42	FEM42	5	40 MPa RC	ShearWall	40 MPa RC	[7, 7]	7.2	4.8
43	FEM43	5	50 MPa RC	ShearWall	50 MPa RC	[7, 7]	7.2	4.8
44	FEM44	5	Steel	ShearWall	40 MPa RC	[7, 7]	7.2	4.8
45	FEM45	5	32 MPa RC	ShearWall	32 MPa RC	[7, 7]	7.2	7.2
46	FEM46	5	40 MPa RC	ShearWall	40 MPa RC	[7, 7]	7.2	7.2
47	FEM47	5	50 MPa RC	ShearWall	50 MPa RC	[7, 7]	7.2	7.2
48	FEM48	5	Steel	ShearWall	40 MPa RC	[7, 7]	7.2	7.2
49	FEM49	10	32 MPa RC	ShearWall	32 MPa RC	[5, 5]	4.8	4.8
50	FEM50	10	40 MPa RC	ShearWall	40 MPa RC	[5, 5]	4.8	4.8

(continued on next page)

Table C1 (*continued*)

#	Name	Storeys	Frame Material	LLRS	LLRS Material	Grid	Column Span in X Dir (m)	Column Span in Y Dir (m)
51	FEM51	10	50 MPa RC	ShearWall	50 MPa RC	[5, 5]	4.8	4.8
52	FEM52	10	Steel	ShearWall	40 MPa RC	[5, 5]	4.8	4.8
53	FEM53	10	32 MPa RC	ShearWall	32 MPa RC	[5, 5]	4.8	7.2
54	FEM54	10	40 MPa RC	ShearWall	40 MPa RC	[5, 5]	4.8	7.2
55	FEM55	10	50 MPa RC	ShearWall	50 MPa RC	[5, 5]	4.8	7.2
56	FEM56	10	Steel	ShearWall	40 MPa RC	[5, 5]	4.8	7.2
57	FEM57	10	32 MPa RC	ShearWall	32 MPa RC	[5, 5]	7.2	4.8
58	FEM58	10	40 MPa RC	ShearWall	40 MPa RC	[5, 5]	7.2	4.8
59	FEM59	10	50 MPa RC	ShearWall	50 MPa RC	[5, 5]	7.2	4.8
60	FEM60	10	Steel	ShearWall	40 MPa RC	[5, 5]	7.2	4.8
61	FEM61	10	32 MPa RC	ShearWall	32 MPa RC	[5, 5]	7.2	7.2
62	FEM62	10	40 MPa RC	ShearWall	40 MPa RC	[5, 5]	7.2	7.2
63	FEM63	10	50 MPa RC	ShearWall	50 MPa RC	[5, 5]	7.2	7.2
64	FEM64	10	Steel	ShearWall	40 MPa RC	[5, 5]	7.2	7.2
65	FEM65	10	32 MPa RC	ShearWall	32 MPa RC	[5, 7]	4.8	4.8
66	FEM66	10	40 MPa RC	ShearWall	40 MPa RC	[5, 7]	4.8	4.8
67	FEM67	10	50 MPa RC	ShearWall	50 MPa RC	[5, 7]	4.8	4.8
68	FEM68	10	Steel	ShearWall	40 MPa RC	[5, 7]	4.8	4.8
69	FEM69	10	32 MPa RC	ShearWall	32 MPa RC	[5, 7]	4.8	7.2
70	FEM70	10	40 MPa RC	ShearWall	40 MPa RC	[5, 7]	4.8	7.2
71	FEM71	10	50 MPa RC	ShearWall	50 MPa RC	[5, 7]	4.8	7.2
72	FEM72	10	Steel	ShearWall	40 MPa RC	[5, 7]	4.8	7.2
73	FEM73	10	32 MPa RC	ShearWall	32 MPa RC	[5, 7]	7.2	4.8
74	FEM74	10	40 MPa RC	ShearWall	40 MPa RC	[5, 7]	7.2	4.8
75	FEM75	10	50 MPa RC	ShearWall	50 MPa RC	[5, 7]	7.2	4.8
76	FEM76	10	Steel	ShearWall	40 MPa RC	[5, 7]	7.2	4.8
77	FEM77	10	32 MPa RC	ShearWall	32 MPa RC	[5, 7]	7.2	7.2
78	FEM78	10	40 MPa RC	ShearWall	40 MPa RC	[5, 7]	7.2	7.2
79	FEM79	10	50 MPa RC	ShearWall	50 MPa RC	[5, 7]	7.2	7.2
80	FEM80	10	Steel	ShearWall	40 MPa RC	[5, 7]	7.2	7.2
81	FEM81	10	32 MPa RC	ShearWall	32 MPa RC	[7, 7]	4.8	4.8
82	FEM82	10	40 MPa RC	ShearWall	40 MPa RC	[7, 7]	4.8	4.8
83	FEM83	10	50 MPa RC	ShearWall	50 MPa RC	[7, 7]	4.8	4.8
84	FEM84	10	Steel	ShearWall	40 MPa RC	[7, 7]	4.8	4.8
85	FEM85	10	32 MPa RC	ShearWall	32 MPa RC	[7, 7]	4.8	7.2
86	FEM86	10	40 MPa RC	ShearWall	40 MPa RC	[7, 7]	4.8	7.2
87	FEM87	10	50 MPa RC	ShearWall	50 MPa RC	[7, 7]	4.8	7.2
88	FEM88	10	Steel	ShearWall	40 MPa RC	[7, 7]	4.8	7.2
89	FEM89	10	32 MPa RC	ShearWall	32 MPa RC	[7, 7]	7.2	4.8
90	FEM90	10	40 MPa RC	ShearWall	40 MPa RC	[7, 7]	7.2	4.8
91	FEM91	10	50 MPa RC	ShearWall	50 MPa RC	[7, 7]	7.2	4.8
92	FEM92	10	Steel	ShearWall	40 MPa RC	[7, 7]	7.2	4.8
93	FEM93	10	32 MPa RC	ShearWall	32 MPa RC	[7, 7]	7.2	7.2
94	FEM94	10	40 MPa RC	ShearWall	40 MPa RC	[7, 7]	7.2	7.2
95	FEM95	10	50 MPa RC	ShearWall	50 MPa RC	[7, 7]	7.2	7.2
96	FEM96	10	Steel	ShearWall	40 MPa RC	[7, 7]	7.2	7.2
97	FEM97	15	32 MPa RC	ShearWall	32 MPa RC	[5, 5]	4.8	4.8
98	FEM98	15	40 MPa RC	ShearWall	40 MPa RC	[5, 5]	4.8	4.8
99	FEM99	15	50 MPa RC	ShearWall	50 MPa RC	[5, 5]	4.8	4.8
100	FEM100	15	Steel	ShearWall	40 MPa RC	[5, 5]	4.8	4.8
101	FEM101	15	32 MPa RC	ShearWall	32 MPa RC	[5, 5]	4.8	7.2
102	FEM102	15	40 MPa RC	ShearWall	40 MPa RC	[5, 5]	4.8	7.2
103	FEM103	15	50 MPa RC	ShearWall	50 MPa RC	[5, 5]	4.8	7.2
104	FEM104	15	Steel	ShearWall	40 MPa RC	[5, 5]	4.8	7.2
105	FEM105	15	32 MPa RC	ShearWall	32 MPa RC	[5, 5]	7.2	4.8
106	FEM106	15	40 MPa RC	ShearWall	40 MPa RC	[5, 5]	7.2	4.8
107	FEM107	15	50 MPa RC	ShearWall	50 MPa RC	[5, 5]	7.2	4.8
108	FEM108	15	Steel	ShearWall	40 MPa RC	[5, 5]	7.2	4.8
109	FEM109	15	32 MPa RC	ShearWall	32 MPa RC	[5, 5]	7.2	7.2
110	FEM110	15	40 MPa RC	ShearWall	40 MPa RC	[5, 5]	7.2	7.2
111	FEM111	15	50 MPa RC	ShearWall	50 MPa RC	[5, 5]	7.2	7.2
112	FEM112	15	Steel	ShearWall	40 MPa RC	[5, 5]	7.2	7.2
113	FEM113	15	32 MPa RC	ShearWall	32 MPa RC	[5, 7]	4.8	4.8
114	FEM114	15	40 MPa RC	ShearWall	40 MPa RC	[5, 7]	4.8	4.8
115	FEM115	15	50 MPa RC	ShearWall	50 MPa RC	[5, 7]	4.8	4.8
116	FEM116	15	Steel	ShearWall	40 MPa RC	[5, 7]	4.8	4.8
117	FEM117	15	32 MPa RC	ShearWall	32 MPa RC	[5, 7]	4.8	7.2
118	FEM118	15	40 MPa RC	ShearWall	40 MPa RC	[5, 7]	4.8	7.2
119	FEM119	15	50 MPa RC	ShearWall	50 MPa RC	[5, 7]	4.8	7.2
120	FEM120	15	Steel	ShearWall	40 MPa RC	[5, 7]	4.8	7.2
121	FEM121	15	32 MPa RC	ShearWall	32 MPa RC	[5, 7]	7.2	4.8
122	FEM122	15	40 MPa RC	ShearWall	40 MPa RC	[5, 7]	7.2	4.8
123	FEM123	15	50 MPa RC	ShearWall	50 MPa RC	[5, 7]	7.2	4.8
124	FEM124	15	Steel	ShearWall	40 MPa RC	[5, 7]	7.2	4.8
125	FEM125	15	32 MPa RC	ShearWall	32 MPa RC	[5, 7]	7.2	7.2
126	FEM126	15	40 MPa RC	ShearWall	40 MPa RC	[5, 7]	7.2	7.2

(*continued on next page*)

Table C1 (*continued*)

#	Name	Storeys	Frame Material	LLRS	LLRS Material	Grid	Column Span in X Dir (m)	Column Span in Y Dir (m)
127	FEM127	15	50 MPa RC	ShearWall	50 MPa RC	[5, 7]	7.2	7.2
128	FEM128	15	Steel	ShearWall	40 MPa RC	[5, 7]	7.2	7.2
129	FEM129	15	32 MPa RC	ShearWall	32 MPa RC	[7, 7]	4.8	4.8
130	FEM130	15	40 MPa RC	ShearWall	40 MPa RC	[7, 7]	4.8	4.8
131	FEM131	15	50 MPa RC	ShearWall	50 MPa RC	[7, 7]	4.8	4.8
132	FEM132	15	Steel	ShearWall	40 MPa RC	[7, 7]	4.8	4.8
133	FEM133	15	32 MPa RC	ShearWall	32 MPa RC	[7, 7]	4.8	7.2
134	FEM134	15	40 MPa RC	ShearWall	40 MPa RC	[7, 7]	4.8	7.2
135	FEM135	15	50 MPa RC	ShearWall	50 MPa RC	[7, 7]	4.8	7.2
136	FEM136	15	Steel	ShearWall	40 MPa RC	[7, 7]	4.8	7.2
137	FEM137	15	32 MPa RC	ShearWall	32 MPa RC	[7, 7]	7.2	4.8
138	FEM138	15	40 MPa RC	ShearWall	40 MPa RC	[7, 7]	7.2	4.8
139	FEM139	15	50 MPa RC	ShearWall	50 MPa RC	[7, 7]	7.2	4.8
140	FEM140	15	Steel	ShearWall	40 MPa RC	[7, 7]	7.2	4.8
141	FEM141	15	32 MPa RC	ShearWall	32 MPa RC	[7, 7]	7.2	7.2
142	FEM142	15	40 MPa RC	ShearWall	40 MPa RC	[7, 7]	7.2	7.2
143	FEM143	15	50 MPa RC	ShearWall	50 MPa RC	[7, 7]	7.2	7.2
144	FEM144	15	Steel	ShearWall	40 MPa RC	[7, 7]	7.2	7.2
145	FEM145	20	32 MPa RC	ShearWall	32 MPa RC	[5, 5]	4.8	4.8
146	FEM146	20	40 MPa RC	ShearWall	40 MPa RC	[5, 5]	4.8	4.8
147	FEM147	20	50 MPa RC	ShearWall	50 MPa RC	[5, 5]	4.8	4.8
148	FEM148	20	Steel	ShearWall	40 MPa RC	[5, 5]	4.8	4.8
149	FEM149	20	32 MPa RC	ShearWall	32 MPa RC	[5, 5]	4.8	7.2
150	FEM150	20	40 MPa RC	ShearWall	40 MPa RC	[5, 5]	4.8	7.2
151	FEM151	20	50 MPa RC	ShearWall	50 MPa RC	[5, 5]	4.8	7.2
152	FEM152	20	Steel	ShearWall	40 MPa RC	[5, 5]	4.8	7.2
153	FEM153	20	32 MPa RC	ShearWall	32 MPa RC	[5, 5]	7.2	4.8
154	FEM154	20	40 MPa RC	ShearWall	40 MPa RC	[5, 5]	7.2	4.8
155	FEM155	20	50 MPa RC	ShearWall	50 MPa RC	[5, 5]	7.2	4.8
156	FEM156	20	Steel	ShearWall	40 MPa RC	[5, 5]	7.2	4.8
157	FEM157	20	32 MPa RC	ShearWall	32 MPa RC	[5, 5]	7.2	7.2
158	FEM158	20	40 MPa RC	ShearWall	40 MPa RC	[5, 5]	7.2	7.2
159	FEM159	20	50 MPa RC	ShearWall	50 MPa RC	[5, 5]	7.2	7.2
160	FEM160	20	Steel	ShearWall	40 MPa RC	[5, 5]	7.2	7.2
161	FEM161	20	32 MPa RC	ShearWall	32 MPa RC	[5, 7]	4.8	4.8
162	FEM162	20	40 MPa RC	ShearWall	40 MPa RC	[5, 7]	4.8	4.8
163	FEM163	20	50 MPa RC	ShearWall	50 MPa RC	[5, 7]	4.8	4.8
164	FEM164	20	Steel	ShearWall	40 MPa RC	[5, 7]	4.8	4.8
165	FEM165	20	32 MPa RC	ShearWall	32 MPa RC	[5, 7]	4.8	7.2
166	FEM166	20	40 MPa RC	ShearWall	40 MPa RC	[5, 7]	4.8	7.2
167	FEM167	20	50 MPa RC	ShearWall	50 MPa RC	[5, 7]	4.8	7.2
168	FEM168	20	Steel	ShearWall	40 MPa RC	[5, 7]	4.8	7.2
169	FEM169	20	32 MPa RC	ShearWall	32 MPa RC	[5, 7]	7.2	4.8
170	FEM170	20	40 MPa RC	ShearWall	40 MPa RC	[5, 7]	7.2	4.8
171	FEM171	20	50 MPa RC	ShearWall	50 MPa RC	[5, 7]	7.2	4.8
172	FEM172	20	Steel	ShearWall	40 MPa RC	[5, 7]	7.2	4.8
173	FEM173	20	32 MPa RC	ShearWall	32 MPa RC	[5, 7]	7.2	7.2
174	FEM174	20	40 MPa RC	ShearWall	40 MPa RC	[5, 7]	7.2	7.2
175	FEM175	20	50 MPa RC	ShearWall	50 MPa RC	[5, 7]	7.2	7.2
176	FEM176	20	Steel	ShearWall	40 MPa RC	[5, 7]	7.2	7.2
177	FEM177	20	32 MPa RC	ShearWall	32 MPa RC	[7, 7]	4.8	4.8
178	FEM178	20	40 MPa RC	ShearWall	40 MPa RC	[7, 7]	4.8	4.8
179	FEM179	20	50 MPa RC	ShearWall	50 MPa RC	[7, 7]	4.8	4.8
180	FEM180	20	Steel	ShearWall	40 MPa RC	[7, 7]	4.8	4.8
181	FEM181	20	32 MPa RC	ShearWall	32 MPa RC	[7, 7]	4.8	7.2
182	FEM182	20	40 MPa RC	ShearWall	40 MPa RC	[7, 7]	4.8	7.2
183	FEM183	20	50 MPa RC	ShearWall	50 MPa RC	[7, 7]	4.8	7.2
184	FEM184	20	Steel	ShearWall	40 MPa RC	[7, 7]	4.8	7.2
185	FEM185	20	32 MPa RC	ShearWall	32 MPa RC	[7, 7]	7.2	4.8
186	FEM186	20	40 MPa RC	ShearWall	40 MPa RC	[7, 7]	7.2	4.8
187	FEM187	20	50 MPa RC	ShearWall	50 MPa RC	[7, 7]	7.2	4.8
188	FEM188	20	Steel	ShearWall	40 MPa RC	[7, 7]	7.2	4.8
189	FEM189	20	32 MPa RC	ShearWall	32 MPa RC	[7, 7]	7.2	7.2
190	FEM190	20	40 MPa RC	ShearWall	40 MPa RC	[7, 7]	7.2	7.2
191	FEM191	20	50 MPa RC	ShearWall	50 MPa RC	[7, 7]	7.2	7.2
192	FEM192	20	Steel	ShearWall	40 MPa RC	[7, 7]	7.2	7.2
193	FEM193	25	32 MPa RC	ShearWall	32 MPa RC	[5, 5]	4.8	4.8
194	FEM194	25	40 MPa RC	ShearWall	40 MPa RC	[5, 5]	4.8	4.8
195	FEM195	25	50 MPa RC	ShearWall	50 MPa RC	[5, 5]	4.8	4.8
196	FEM196	25	Steel	ShearWall	40 MPa RC	[5, 5]	4.8	4.8
197	FEM197	25	32 MPa RC	ShearWall	32 MPa RC	[5, 5]	4.8	7.2
198	FEM198	25	40 MPa RC	ShearWall	40 MPa RC	[5, 5]	4.8	7.2
199	FEM199	25	50 MPa RC	ShearWall	50 MPa RC	[5, 5]	4.8	7.2
200	FEM200	25	Steel	ShearWall	40 MPa RC	[5, 5]	4.8	7.2
201	FEM201	25	32 MPa RC	ShearWall	32 MPa RC	[5, 5]	7.2	4.8
202	FEM202	25	40 MPa RC	ShearWall	40 MPa RC	[5, 5]	7.2	4.8

(*continued on next page*)

Table C1 (*continued*)

#	Name	Storeys	Frame Material	LLRS	LLRS Material	Grid	Column Span in X Dir (m)	Column Span in Y Dir (m)
203	FEM203	25	50 MPa RC	ShearWall	50 MPa RC	[5, 5]	7.2	4.8
204	FEM204	25	Steel	ShearWall	40 MPa RC	[5, 5]	7.2	4.8
205	FEM205	25	32 MPa RC	ShearWall	32 MPa RC	[5, 5]	7.2	7.2
206	FEM206	25	40 MPa RC	ShearWall	40 MPa RC	[5, 5]	7.2	7.2
207	FEM207	25	50 MPa RC	ShearWall	50 MPa RC	[5, 5]	7.2	7.2
208	FEM208	25	Steel	ShearWall	40 MPa RC	[5, 5]	7.2	7.2
209	FEM209	25	32 MPa RC	ShearWall	32 MPa RC	[5, 7]	4.8	4.8
210	FEM210	25	40 MPa RC	ShearWall	40 MPa RC	[5, 7]	4.8	4.8
211	FEM211	25	50 MPa RC	ShearWall	50 MPa RC	[5, 7]	4.8	4.8
212	FEM212	25	Steel	ShearWall	40 MPa RC	[5, 7]	4.8	4.8
213	FEM213	25	32 MPa RC	ShearWall	32 MPa RC	[5, 7]	4.8	7.2
214	FEM214	25	40 MPa RC	ShearWall	40 MPa RC	[5, 7]	4.8	7.2
215	FEM215	25	50 MPa RC	ShearWall	50 MPa RC	[5, 7]	4.8	7.2
216	FEM216	25	Steel	ShearWall	40 MPa RC	[5, 7]	4.8	7.2
217	FEM217	25	32 MPa RC	ShearWall	32 MPa RC	[5, 7]	7.2	4.8
218	FEM218	25	40 MPa RC	ShearWall	40 MPa RC	[5, 7]	7.2	4.8
219	FEM219	25	50 MPa RC	ShearWall	50 MPa RC	[5, 7]	7.2	4.8
220	FEM220	25	Steel	ShearWall	40 MPa RC	[5, 7]	7.2	4.8
221	FEM221	25	32 MPa RC	ShearWall	32 MPa RC	[5, 7]	7.2	7.2
222	FEM222	25	40 MPa RC	ShearWall	40 MPa RC	[5, 7]	7.2	7.2
223	FEM223	25	50 MPa RC	ShearWall	50 MPa RC	[5, 7]	7.2	7.2
224	FEM224	25	Steel	ShearWall	40 MPa RC	[5, 7]	7.2	7.2
225	FEM225	25	32 MPa RC	ShearWall	32 MPa RC	[7, 7]	4.8	4.8
226	FEM226	25	40 MPa RC	ShearWall	40 MPa RC	[7, 7]	4.8	4.8
227	FEM227	25	50 MPa RC	ShearWall	50 MPa RC	[7, 7]	4.8	4.8
228	FEM228	25	Steel	ShearWall	40 MPa RC	[7, 7]	4.8	4.8
229	FEM229	25	32 MPa RC	ShearWall	32 MPa RC	[7, 7]	4.8	7.2
230	FEM230	25	40 MPa RC	ShearWall	40 MPa RC	[7, 7]	4.8	7.2
231	FEM231	25	50 MPa RC	ShearWall	50 MPa RC	[7, 7]	4.8	7.2
232	FEM232	25	Steel	ShearWall	40 MPa RC	[7, 7]	4.8	7.2
233	FEM233	25	32 MPa RC	ShearWall	32 MPa RC	[7, 7]	7.2	4.8
234	FEM234	25	40 MPa RC	ShearWall	40 MPa RC	[7, 7]	7.2	4.8
235	FEM235	25	50 MPa RC	ShearWall	50 MPa RC	[7, 7]	7.2	4.8
236	FEM236	25	Steel	ShearWall	40 MPa RC	[7, 7]	7.2	4.8
237	FEM237	25	32 MPa RC	ShearWall	32 MPa RC	[7, 7]	7.2	7.2
238	FEM238	25	40 MPa RC	ShearWall	40 MPa RC	[7, 7]	7.2	7.2
239	FEM239	25	50 MPa RC	ShearWall	50 MPa RC	[7, 7]	7.2	7.2
240	FEM240	25	Steel	ShearWall	40 MPa RC	[7, 7]	7.2	7.2
241	FEM241	30	32 MPa RC	ShearWall	32 MPa RC	[5, 5]	4.8	4.8
242	FEM242	30	40 MPa RC	ShearWall	40 MPa RC	[5, 5]	4.8	4.8
243	FEM243	30	50 MPa RC	ShearWall	50 MPa RC	[5, 5]	4.8	4.8
244	FEM244	30	Steel	ShearWall	40 MPa RC	[5, 5]	4.8	4.8
245	FEM245	30	32 MPa RC	ShearWall	32 MPa RC	[5, 5]	4.8	7.2
246	FEM246	30	40 MPa RC	ShearWall	40 MPa RC	[5, 5]	4.8	7.2
247	FEM247	30	50 MPa RC	ShearWall	50 MPa RC	[5, 5]	4.8	7.2
248	FEM248	30	Steel	ShearWall	40 MPa RC	[5, 5]	4.8	7.2
249	FEM249	30	32 MPa RC	ShearWall	32 MPa RC	[5, 5]	7.2	4.8
250	FEM250	30	40 MPa RC	ShearWall	40 MPa RC	[5, 5]	7.2	4.8
251	FEM251	30	50 MPa RC	ShearWall	50 MPa RC	[5, 5]	7.2	4.8
252	FEM252	30	Steel	ShearWall	40 MPa RC	[5, 5]	7.2	4.8
253	FEM253	30	Steel	ShearWall	32 MPa RC	[5, 7]	4.8	7.2
254	FEM254	30	32 MPa RC	ShearWall	40 MPa RC	[5, 7]	7.2	4.8
255	FEM255	30	40 MPa RC	ShearWall	50 MPa RC	[5, 7]	7.2	4.8
256	FEM256	30	50 MPa RC	ShearWall	40 MPa RC	[5, 7]	7.2	4.8
257	FEM257	30	Steel	ShearWall	32 MPa RC	[5, 7]	7.2	4.8
258	FEM258	30	32 MPa RC	ShearWall	40 MPa RC	[5, 7]	7.2	7.2
259	FEM259	30	40 MPa RC	ShearWall	50 MPa RC	[5, 7]	7.2	7.2
260	FEM260	30	50 MPa RC	ShearWall	40 MPa RC	[5, 7]	7.2	7.2
261	FEM261	30	Steel	ShearWall	32 MPa RC	[5, 7]	7.2	7.2
262	FEM262	40	32 MPa RC	ShearWall	40 MPa RC	[5, 5]	7.2	7.2
263	FEM263	40	40 MPa RC	ShearWall	50 MPa RC	[5, 5]	7.2	7.2
264	FEM264	40	50 MPa RC	ShearWall	40 MPa RC	[5, 5]	7.2	7.2
265	FEM265	40	32 MPa RC	ShearWall	32 MPa RC	[7, 7]	7.2	7.2
266	FEM266	40	40 MPa RC	ShearWall	40 MPa RC	[7, 7]	7.2	7.2
267	FEM267	40	50 MPa RC	ShearWall	50 MPa RC	[7, 7]	7.2	7.2
268	FEM268	5	32 MPa RC	OutriggerBelt	32 MPa RC	[5, 5]	4.8	4.8
269	FEM269	5	40 MPa RC	OutriggerBelt	40 MPa RC	[5, 5]	4.8	4.8
270	FEM270	5	50 MPa RC	OutriggerBelt	50 MPa RC	[5, 5]	4.8	4.8
271	FEM271	5	Steel	OutriggerBelt	Steel	[5, 5]	4.8	4.8
272	FEM272	5	32 MPa RC	OutriggerBelt	32 MPa RC	[5, 5]	4.8	7.2
273	FEM273	5	40 MPa RC	OutriggerBelt	40 MPa RC	[5, 5]	4.8	7.2
274	FEM274	5	50 MPa RC	OutriggerBelt	50 MPa RC	[5, 5]	4.8	7.2
275	FEM275	5	Steel	OutriggerBelt	Steel	[5, 5]	4.8	7.2
276	FEM276	5	32 MPa RC	OutriggerBelt	32 MPa RC	[5, 5]	7.2	4.8
277	FEM277	5	40 MPa RC	OutriggerBelt	40 MPa RC	[5, 5]	7.2	4.8
278	FEM278	5	50 MPa RC	OutriggerBelt	50 MPa RC	[5, 5]	7.2	4.8

(*continued on next page*)

Table C1 (*continued*)

#	Name	Storeys	Frame Material	LLRS	LLRS Material	Grid	Column Span in X Dir (m)	Column Span in Y Dir (m)
279	FEM279	5	Steel	OutriggerBelt	Steel	[5, 5]	7.2	4.8
280	FEM280	5	32 MPa RC	OutriggerBelt	32 MPa RC	[5, 5]	7.2	7.2
281	FEM281	5	40 MPa RC	OutriggerBelt	40 MPa RC	[5, 5]	7.2	7.2
282	FEM282	5	50 MPa RC	OutriggerBelt	50 MPa RC	[5, 5]	7.2	7.2
283	FEM283	5	Steel	OutriggerBelt	Steel	[5, 5]	7.2	7.2
284	FEM284	5	32 MPa RC	OutriggerBelt	32 MPa RC	[5, 7]	4.8	4.8
285	FEM285	5	40 MPa RC	OutriggerBelt	40 MPa RC	[5, 7]	4.8	4.8
286	FEM286	5	50 MPa RC	OutriggerBelt	50 MPa RC	[5, 7]	4.8	4.8
287	FEM287	5	Steel	OutriggerBelt	Steel	[5, 7]	4.8	4.8
288	FEM288	5	32 MPa RC	OutriggerBelt	32 MPa RC	[5, 7]	4.8	7.2
289	FEM289	5	40 MPa RC	OutriggerBelt	40 MPa RC	[5, 7]	4.8	7.2
290	FEM290	5	50 MPa RC	OutriggerBelt	50 MPa RC	[5, 7]	4.8	7.2
291	FEM291	5	Steel	OutriggerBelt	Steel	[5, 7]	4.8	7.2
292	FEM292	5	32 MPa RC	OutriggerBelt	32 MPa RC	[5, 7]	7.2	4.8
293	FEM293	5	40 MPa RC	OutriggerBelt	40 MPa RC	[5, 7]	7.2	4.8
294	FEM294	5	50 MPa RC	OutriggerBelt	50 MPa RC	[5, 7]	7.2	4.8
295	FEM295	5	Steel	OutriggerBelt	Steel	[5, 7]	7.2	4.8
296	FEM296	5	32 MPa RC	OutriggerBelt	32 MPa RC	[5, 7]	7.2	7.2
297	FEM297	5	40 MPa RC	OutriggerBelt	40 MPa RC	[5, 7]	7.2	7.2
298	FEM298	5	50 MPa RC	OutriggerBelt	50 MPa RC	[5, 7]	7.2	7.2
299	FEM299	5	Steel	OutriggerBelt	Steel	[5, 7]	7.2	7.2
300	FEM300	5	32 MPa RC	OutriggerBelt	32 MPa RC	[7, 7]	4.8	4.8
301	FEM301	5	40 MPa RC	OutriggerBelt	40 MPa RC	[7, 7]	4.8	4.8
302	FEM302	5	50 MPa RC	OutriggerBelt	50 MPa RC	[7, 7]	4.8	4.8
303	FEM303	5	Steel	OutriggerBelt	Steel	[7, 7]	4.8	4.8
304	FEM304	5	32 MPa RC	OutriggerBelt	32 MPa RC	[7, 7]	4.8	7.2
305	FEM305	5	40 MPa RC	OutriggerBelt	40 MPa RC	[7, 7]	4.8	7.2
306	FEM306	5	50 MPa RC	OutriggerBelt	50 MPa RC	[7, 7]	4.8	7.2
307	FEM307	5	Steel	OutriggerBelt	Steel	[7, 7]	4.8	7.2
308	FEM308	5	32 MPa RC	OutriggerBelt	32 MPa RC	[7, 7]	7.2	4.8
309	FEM309	5	40 MPa RC	OutriggerBelt	40 MPa RC	[7, 7]	7.2	4.8
310	FEM310	5	50 MPa RC	OutriggerBelt	50 MPa RC	[7, 7]	7.2	4.8
311	FEM311	5	Steel	OutriggerBelt	Steel	[7, 7]	7.2	4.8
312	FEM312	5	32 MPa RC	OutriggerBelt	32 MPa RC	[7, 7]	7.2	7.2
313	FEM313	5	40 MPa RC	OutriggerBelt	40 MPa RC	[7, 7]	7.2	7.2
314	FEM314	5	50 MPa RC	OutriggerBelt	50 MPa RC	[7, 7]	7.2	7.2
315	FEM315	5	Steel	OutriggerBelt	Steel	[7, 7]	7.2	7.2
316	FEM316	10	32 MPa RC	OutriggerBelt	32 MPa RC	[5, 5]	4.8	4.8
317	FEM317	10	40 MPa RC	OutriggerBelt	40 MPa RC	[5, 5]	4.8	4.8
318	FEM318	10	50 MPa RC	OutriggerBelt	50 MPa RC	[5, 5]	4.8	4.8
319	FEM319	10	Steel	OutriggerBelt	Steel	[5, 5]	4.8	4.8
320	FEM320	10	32 MPa RC	OutriggerBelt	32 MPa RC	[5, 5]	4.8	7.2
321	FEM321	10	40 MPa RC	OutriggerBelt	40 MPa RC	[5, 5]	4.8	7.2
322	FEM322	10	50 MPa RC	OutriggerBelt	50 MPa RC	[5, 5]	4.8	7.2
323	FEM323	10	Steel	OutriggerBelt	Steel	[5, 5]	4.8	7.2
324	FEM324	10	32 MPa RC	OutriggerBelt	32 MPa RC	[5, 5]	7.2	4.8
325	FEM325	10	40 MPa RC	OutriggerBelt	40 MPa RC	[5, 5]	7.2	4.8
326	FEM326	10	50 MPa RC	OutriggerBelt	50 MPa RC	[5, 5]	7.2	4.8
327	FEM327	10	Steel	OutriggerBelt	Steel	[5, 5]	7.2	4.8
328	FEM328	10	32 MPa RC	OutriggerBelt	32 MPa RC	[5, 5]	7.2	7.2
329	FEM329	10	40 MPa RC	OutriggerBelt	40 MPa RC	[5, 5]	7.2	7.2
330	FEM330	10	50 MPa RC	OutriggerBelt	50 MPa RC	[5, 5]	7.2	7.2
331	FEM331	10	Steel	OutriggerBelt	Steel	[5, 5]	7.2	7.2
332	FEM332	10	32 MPa RC	OutriggerBelt	32 MPa RC	[5, 7]	4.8	4.8
333	FEM333	10	40 MPa RC	OutriggerBelt	40 MPa RC	[5, 7]	4.8	4.8
334	FEM334	10	50 MPa RC	OutriggerBelt	50 MPa RC	[5, 7]	4.8	4.8
335	FEM335	10	Steel	OutriggerBelt	Steel	[5, 7]	4.8	4.8
336	FEM336	10	32 MPa RC	OutriggerBelt	32 MPa RC	[5, 7]	4.8	7.2
337	FEM337	10	40 MPa RC	OutriggerBelt	40 MPa RC	[5, 7]	4.8	7.2
338	FEM338	10	50 MPa RC	OutriggerBelt	50 MPa RC	[5, 7]	4.8	7.2
339	FEM339	10	Steel	OutriggerBelt	Steel	[5, 7]	4.8	7.2
340	FEM340	10	32 MPa RC	OutriggerBelt	32 MPa RC	[5, 7]	7.2	4.8
341	FEM341	10	40 MPa RC	OutriggerBelt	40 MPa RC	[5, 7]	7.2	4.8
342	FEM342	10	50 MPa RC	OutriggerBelt	50 MPa RC	[5, 7]	7.2	4.8
343	FEM343	10	Steel	OutriggerBelt	Steel	[5, 7]	7.2	4.8
344	FEM344	10	32 MPa RC	OutriggerBelt	32 MPa RC	[5, 7]	7.2	7.2
345	FEM345	10	40 MPa RC	OutriggerBelt	40 MPa RC	[5, 7]	7.2	7.2
346	FEM346	10	50 MPa RC	OutriggerBelt	50 MPa RC	[5, 7]	7.2	7.2
347	FEM347	10	Steel	OutriggerBelt	Steel	[5, 7]	7.2	7.2
348	FEM348	10	32 MPa RC	OutriggerBelt	32 MPa RC	[7, 7]	4.8	4.8
349	FEM349	10	40 MPa RC	OutriggerBelt	40 MPa RC	[7, 7]	4.8	4.8
350	FEM350	10	50 MPa RC	OutriggerBelt	50 MPa RC	[7, 7]	4.8	4.8
351	FEM351	10	Steel	OutriggerBelt	Steel	[7, 7]	4.8	4.8
352	FEM352	10	32 MPa RC	OutriggerBelt	32 MPa RC	[7, 7]	4.8	7.2
353	FEM353	10	40 MPa RC	OutriggerBelt	40 MPa RC	[7, 7]	4.8	7.2
354	FEM354	10	50 MPa RC	OutriggerBelt	50 MPa RC	[7, 7]	4.8	7.2

(*continued on next page*)

Table C1 (*continued*)

#	Name	Storeys	Frame Material	LLRS	LLRS Material	Grid	Column Span in X Dir (m)	Column Span in Y Dir (m)
355	FEM355	10	Steel	OutriggerBelt	Steel	[7, 7]	4.8	7.2
356	FEM356	10	32 MPa RC	OutriggerBelt	32 MPa RC	[7, 7]	7.2	4.8
357	FEM357	10	40 MPa RC	OutriggerBelt	40 MPa RC	[7, 7]	7.2	4.8
358	FEM358	10	50 MPa RC	OutriggerBelt	50 MPa RC	[7, 7]	7.2	4.8
359	FEM359	10	Steel	OutriggerBelt	Steel	[7, 7]	7.2	4.8
360	FEM360	10	32 MPa RC	OutriggerBelt	32 MPa RC	[7, 7]	7.2	7.2
361	FEM361	10	40 MPa RC	OutriggerBelt	40 MPa RC	[7, 7]	7.2	7.2
362	FEM362	10	50 MPa RC	OutriggerBelt	50 MPa RC	[7, 7]	7.2	7.2
363	FEM363	10	Steel	OutriggerBelt	Steel	[7, 7]	7.2	7.2
364	FEM364	15	32 MPa RC	OutriggerBelt	32 MPa RC	[5, 5]	4.8	4.8
365	FEM365	15	40 MPa RC	OutriggerBelt	40 MPa RC	[5, 5]	4.8	4.8
366	FEM366	15	50 MPa RC	OutriggerBelt	50 MPa RC	[5, 5]	4.8	4.8
367	FEM367	15	Steel	OutriggerBelt	Steel	[5, 5]	4.8	4.8
368	FEM368	15	32 MPa RC	OutriggerBelt	32 MPa RC	[5, 5]	4.8	7.2
369	FEM369	15	40 MPa RC	OutriggerBelt	40 MPa RC	[5, 5]	4.8	7.2
370	FEM370	15	50 MPa RC	OutriggerBelt	50 MPa RC	[5, 5]	4.8	7.2
371	FEM371	15	Steel	OutriggerBelt	Steel	[5, 5]	4.8	7.2
372	FEM372	15	32 MPa RC	OutriggerBelt	32 MPa RC	[5, 5]	7.2	4.8
373	FEM373	15	40 MPa RC	OutriggerBelt	40 MPa RC	[5, 5]	7.2	4.8
374	FEM374	15	50 MPa RC	OutriggerBelt	50 MPa RC	[5, 5]	7.2	4.8
375	FEM375	15	Steel	OutriggerBelt	Steel	[5, 5]	7.2	4.8
376	FEM376	15	32 MPa RC	OutriggerBelt	32 MPa RC	[5, 5]	7.2	7.2
377	FEM377	15	40 MPa RC	OutriggerBelt	40 MPa RC	[5, 5]	7.2	7.2
378	FEM378	15	50 MPa RC	OutriggerBelt	50 MPa RC	[5, 5]	7.2	7.2
379	FEM379	15	Steel	OutriggerBelt	Steel	[5, 5]	7.2	7.2
380	FEM380	15	32 MPa RC	OutriggerBelt	32 MPa RC	[5, 7]	4.8	4.8
381	FEM381	15	40 MPa RC	OutriggerBelt	40 MPa RC	[5, 7]	4.8	4.8
382	FEM382	15	50 MPa RC	OutriggerBelt	50 MPa RC	[5, 7]	4.8	4.8
383	FEM383	15	Steel	OutriggerBelt	Steel	[5, 7]	4.8	4.8
384	FEM384	15	32 MPa RC	OutriggerBelt	32 MPa RC	[5, 7]	4.8	7.2
385	FEM385	15	40 MPa RC	OutriggerBelt	40 MPa RC	[5, 7]	4.8	7.2
386	FEM386	15	50 MPa RC	OutriggerBelt	50 MPa RC	[5, 7]	4.8	7.2
387	FEM387	15	Steel	OutriggerBelt	Steel	[5, 7]	4.8	7.2
388	FEM388	15	32 MPa RC	OutriggerBelt	32 MPa RC	[5, 7]	7.2	4.8
389	FEM389	15	40 MPa RC	OutriggerBelt	40 MPa RC	[5, 7]	7.2	4.8
390	FEM390	15	50 MPa RC	OutriggerBelt	50 MPa RC	[5, 7]	7.2	4.8
391	FEM391	15	Steel	OutriggerBelt	Steel	[5, 7]	7.2	4.8
392	FEM392	15	32 MPa RC	OutriggerBelt	32 MPa RC	[5, 7]	7.2	7.2
393	FEM393	15	40 MPa RC	OutriggerBelt	40 MPa RC	[5, 7]	7.2	7.2
394	FEM394	15	50 MPa RC	OutriggerBelt	50 MPa RC	[5, 7]	7.2	7.2
395	FEM395	15	Steel	OutriggerBelt	Steel	[5, 7]	7.2	7.2
396	FEM396	15	32 MPa RC	OutriggerBelt	32 MPa RC	[7, 7]	4.8	4.8
397	FEM397	15	40 MPa RC	OutriggerBelt	40 MPa RC	[7, 7]	4.8	4.8
398	FEM398	15	50 MPa RC	OutriggerBelt	50 MPa RC	[7, 7]	4.8	4.8
399	FEM399	15	Steel	OutriggerBelt	Steel	[7, 7]	4.8	4.8
400	FEM400	15	32 MPa RC	OutriggerBelt	32 MPa RC	[7, 7]	4.8	7.2
401	FEM401	15	40 MPa RC	OutriggerBelt	40 MPa RC	[7, 7]	4.8	7.2
402	FEM402	15	50 MPa RC	OutriggerBelt	50 MPa RC	[7, 7]	4.8	7.2
403	FEM403	15	Steel	OutriggerBelt	Steel	[7, 7]	4.8	7.2
404	FEM404	15	32 MPa RC	OutriggerBelt	32 MPa RC	[7, 7]	7.2	4.8
405	FEM405	15	40 MPa RC	OutriggerBelt	40 MPa RC	[7, 7]	7.2	4.8
406	FEM406	15	50 MPa RC	OutriggerBelt	50 MPa RC	[7, 7]	7.2	4.8
407	FEM407	15	Steel	OutriggerBelt	Steel	[7, 7]	7.2	4.8
408	FEM408	15	32 MPa RC	OutriggerBelt	32 MPa RC	[7, 7]	7.2	7.2
409	FEM409	15	40 MPa RC	OutriggerBelt	40 MPa RC	[7, 7]	7.2	7.2
410	FEM410	15	50 MPa RC	OutriggerBelt	50 MPa RC	[7, 7]	7.2	7.2
411	FEM411	15	Steel	OutriggerBelt	Steel	[7, 7]	7.2	7.2
412	FEM412	20	32 MPa RC	OutriggerBelt	32 MPa RC	[5, 5]	4.8	4.8
413	FEM413	20	40 MPa RC	OutriggerBelt	40 MPa RC	[5, 5]	4.8	4.8
414	FEM414	20	50 MPa RC	OutriggerBelt	50 MPa RC	[5, 5]	4.8	4.8
415	FEM415	20	Steel	OutriggerBelt	Steel	[5, 5]	4.8	4.8
416	FEM416	20	32 MPa RC	OutriggerBelt	32 MPa RC	[5, 5]	4.8	7.2
417	FEM417	20	40 MPa RC	OutriggerBelt	40 MPa RC	[5, 5]	4.8	7.2
418	FEM418	20	50 MPa RC	OutriggerBelt	50 MPa RC	[5, 5]	4.8	7.2
419	FEM419	20	Steel	OutriggerBelt	Steel	[5, 5]	4.8	7.2
420	FEM420	20	32 MPa RC	OutriggerBelt	32 MPa RC	[5, 5]	7.2	4.8
421	FEM421	20	40 MPa RC	OutriggerBelt	40 MPa RC	[5, 5]	7.2	4.8
422	FEM422	20	50 MPa RC	OutriggerBelt	50 MPa RC	[5, 5]	7.2	4.8
423	FEM423	20	Steel	OutriggerBelt	Steel	[5, 5]	7.2	4.8
424	FEM424	20	32 MPa RC	OutriggerBelt	32 MPa RC	[5, 5]	7.2	7.2
425	FEM425	20	40 MPa RC	OutriggerBelt	40 MPa RC	[5, 5]	7.2	7.2
426	FEM426	20	50 MPa RC	OutriggerBelt	50 MPa RC	[5, 5]	7.2	7.2
427	FEM427	20	Steel	OutriggerBelt	Steel	[5, 5]	7.2	7.2
428	FEM428	20	32 MPa RC	OutriggerBelt	32 MPa RC	[5, 7]	4.8	4.8
429	FEM429	20	40 MPa RC	OutriggerBelt	40 MPa RC	[5, 7]	4.8	4.8
430	FEM430	20	50 MPa RC	OutriggerBelt	50 MPa RC	[5, 7]	4.8	4.8

(*continued on next page*)

Table C1 (*continued*)

#	Name	Storeys	Frame Material	LLRS	LLRS Material	Grid	Column Span in X Dir (m)	Column Span in Y Dir (m)
431	FEM431	20	Steel	OutriggerBelt	Steel	[5, 7]	4.8	4.8
432	FEM432	20	32 MPa RC	OutriggerBelt	32 MPa RC	[5, 7]	4.8	7.2
433	FEM433	20	40 MPa RC	OutriggerBelt	40 MPa RC	[5, 7]	4.8	7.2
434	FEM434	20	50 MPa RC	OutriggerBelt	50 MPa RC	[5, 7]	4.8	7.2
435	FEM435	20	Steel	OutriggerBelt	Steel	[5, 7]	4.8	7.2
436	FEM436	20	32 MPa RC	OutriggerBelt	32 MPa RC	[5, 7]	7.2	4.8
437	FEM437	20	40 MPa RC	OutriggerBelt	40 MPa RC	[5, 7]	7.2	4.8
438	FEM438	20	50 MPa RC	OutriggerBelt	50 MPa RC	[5, 7]	7.2	4.8
439	FEM439	20	Steel	OutriggerBelt	Steel	[5, 7]	7.2	4.8
440	FEM440	20	32 MPa RC	OutriggerBelt	32 MPa RC	[5, 7]	7.2	7.2
441	FEM441	20	40 MPa RC	OutriggerBelt	40 MPa RC	[5, 7]	7.2	7.2
442	FEM442	20	50 MPa RC	OutriggerBelt	50 MPa RC	[5, 7]	7.2	7.2
443	FEM443	20	Steel	OutriggerBelt	Steel	[5, 7]	7.2	7.2
444	FEM444	20	32 MPa RC	OutriggerBelt	32 MPa RC	[7, 7]	4.8	4.8
445	FEM445	20	40 MPa RC	OutriggerBelt	40 MPa RC	[7, 7]	4.8	4.8
446	FEM446	20	50 MPa RC	OutriggerBelt	50 MPa RC	[7, 7]	4.8	4.8
447	FEM447	20	Steel	OutriggerBelt	Steel	[7, 7]	4.8	4.8
448	FEM448	20	32 MPa RC	OutriggerBelt	32 MPa RC	[7, 7]	4.8	7.2
449	FEM449	20	40 MPa RC	OutriggerBelt	40 MPa RC	[7, 7]	4.8	7.2
450	FEM450	20	50 MPa RC	OutriggerBelt	50 MPa RC	[7, 7]	4.8	7.2
451	FEM451	20	Steel	OutriggerBelt	Steel	[7, 7]	4.8	7.2
452	FEM452	20	32 MPa RC	OutriggerBelt	32 MPa RC	[7, 7]	7.2	4.8
453	FEM453	20	40 MPa RC	OutriggerBelt	40 MPa RC	[7, 7]	7.2	4.8
454	FEM454	20	50 MPa RC	OutriggerBelt	50 MPa RC	[7, 7]	7.2	4.8
455	FEM455	20	Steel	OutriggerBelt	Steel	[7, 7]	7.2	4.8
456	FEM456	20	32 MPa RC	OutriggerBelt	32 MPa RC	[7, 7]	7.2	7.2
457	FEM457	20	40 MPa RC	OutriggerBelt	40 MPa RC	[7, 7]	7.2	7.2
458	FEM458	20	50 MPa RC	OutriggerBelt	50 MPa RC	[7, 7]	7.2	7.2
459	FEM459	20	Steel	OutriggerBelt	Steel	[7, 7]	7.2	7.2
460	FEM460	25	32 MPa RC	OutriggerBelt	32 MPa RC	[5, 5]	4.8	4.8
461	FEM461	25	40 MPa RC	OutriggerBelt	40 MPa RC	[5, 5]	4.8	4.8
462	FEM462	25	50 MPa RC	OutriggerBelt	50 MPa RC	[5, 5]	4.8	4.8
463	FEM463	25	Steel	OutriggerBelt	Steel	[5, 5]	4.8	4.8
464	FEM464	25	32 MPa RC	OutriggerBelt	32 MPa RC	[5, 5]	4.8	7.2
465	FEM465	25	40 MPa RC	OutriggerBelt	40 MPa RC	[5, 5]	4.8	7.2
466	FEM466	25	50 MPa RC	OutriggerBelt	50 MPa RC	[5, 5]	4.8	7.2
467	FEM467	25	Steel	OutriggerBelt	Steel	[5, 5]	4.8	7.2
468	FEM468	25	32 MPa RC	OutriggerBelt	32 MPa RC	[5, 5]	7.2	4.8
469	FEM469	25	40 MPa RC	OutriggerBelt	40 MPa RC	[5, 5]	7.2	4.8
470	FEM470	25	50 MPa RC	OutriggerBelt	50 MPa RC	[5, 5]	7.2	4.8
471	FEM471	25	Steel	OutriggerBelt	Steel	[5, 5]	7.2	4.8
472	FEM472	25	32 MPa RC	OutriggerBelt	32 MPa RC	[5, 5]	7.2	7.2
473	FEM473	25	40 MPa RC	OutriggerBelt	40 MPa RC	[5, 5]	7.2	7.2
474	FEM474	25	50 MPa RC	OutriggerBelt	50 MPa RC	[5, 5]	7.2	7.2
475	FEM475	25	Steel	OutriggerBelt	Steel	[5, 5]	7.2	7.2
476	FEM476	25	32 MPa RC	OutriggerBelt	32 MPa RC	[5, 7]	4.8	4.8
477	FEM477	25	40 MPa RC	OutriggerBelt	40 MPa RC	[5, 7]	4.8	4.8
478	FEM478	25	50 MPa RC	OutriggerBelt	50 MPa RC	[5, 7]	4.8	4.8
479	FEM479	25	Steel	OutriggerBelt	Steel	[5, 7]	4.8	4.8
480	FEM480	25	32 MPa RC	OutriggerBelt	32 MPa RC	[5, 7]	4.8	7.2
481	FEM481	25	40 MPa RC	OutriggerBelt	40 MPa RC	[5, 7]	4.8	7.2
482	FEM482	25	50 MPa RC	OutriggerBelt	50 MPa RC	[5, 7]	4.8	7.2
483	FEM483	25	Steel	OutriggerBelt	Steel	[5, 7]	4.8	7.2
484	FEM484	25	32 MPa RC	OutriggerBelt	32 MPa RC	[5, 7]	7.2	4.8
485	FEM485	25	40 MPa RC	OutriggerBelt	40 MPa RC	[5, 7]	7.2	4.8
486	FEM486	25	50 MPa RC	OutriggerBelt	50 MPa RC	[5, 7]	7.2	4.8
487	FEM487	25	Steel	OutriggerBelt	Steel	[5, 7]	7.2	4.8
488	FEM488	25	32 MPa RC	OutriggerBelt	32 MPa RC	[5, 7]	7.2	7.2
489	FEM489	25	40 MPa RC	OutriggerBelt	40 MPa RC	[5, 7]	7.2	7.2
490	FEM490	25	50 MPa RC	OutriggerBelt	50 MPa RC	[5, 7]	7.2	7.2
491	FEM491	25	Steel	OutriggerBelt	Steel	[5, 7]	7.2	7.2
492	FEM492	25	32 MPa RC	OutriggerBelt	32 MPa RC	[7, 7]	4.8	4.8
493	FEM493	25	40 MPa RC	OutriggerBelt	40 MPa RC	[7, 7]	4.8	4.8
494	FEM494	25	50 MPa RC	OutriggerBelt	50 MPa RC	[7, 7]	4.8	4.8
495	FEM495	25	Steel	OutriggerBelt	Steel	[7, 7]	4.8	4.8
496	FEM496	25	32 MPa RC	OutriggerBelt	32 MPa RC	[7, 7]	4.8	7.2
497	FEM497	25	40 MPa RC	OutriggerBelt	40 MPa RC	[7, 7]	4.8	7.2
498	FEM498	25	50 MPa RC	OutriggerBelt	50 MPa RC	[7, 7]	4.8	7.2
499	FEM499	25	Steel	OutriggerBelt	Steel	[7, 7]	4.8	7.2
500	FEM500	25	32 MPa RC	OutriggerBelt	32 MPa RC	[7, 7]	7.2	4.8
501	FEM501	25	40 MPa RC	OutriggerBelt	40 MPa RC	[7, 7]	7.2	4.8
502	FEM502	25	50 MPa RC	OutriggerBelt	50 MPa RC	[7, 7]	7.2	4.8
503	FEM503	25	Steel	OutriggerBelt	Steel	[7, 7]	7.2	4.8
504	FEM504	25	32 MPa RC	OutriggerBelt	32 MPa RC	[7, 7]	7.2	7.2
505	FEM505	25	40 MPa RC	OutriggerBelt	40 MPa RC	[7, 7]	7.2	7.2
506	FEM506	25	50 MPa RC	OutriggerBelt	50 MPa RC	[7, 7]	7.2	7.2

(*continued on next page*)

Table C1 (*continued*)

#	Name	Storeys	Frame Material	LLRS	LLRS Material	Grid	Column Span in X Dir (m)	Column Span in Y Dir (m)
507	FEM507	25	Steel	OutriggerBelt	Steel	[7, 7]	7.2	7.2
508	FEM508	30	32 MPa RC	OutriggerBelt	32 MPa RC	[5, 5]	4.8	4.8
509	FEM509	30	40 MPa RC	OutriggerBelt	40 MPa RC	[5, 5]	4.8	4.8
510	FEM510	30	50 MPa RC	OutriggerBelt	50 MPa RC	[5, 5]	4.8	4.8
511	FEM511	30	Steel	OutriggerBelt	Steel	[5, 5]	4.8	4.8
512	FEM512	30	32 MPa RC	OutriggerBelt	32 MPa RC	[5, 5]	4.8	7.2
513	FEM513	30	40 MPa RC	OutriggerBelt	40 MPa RC	[5, 5]	4.8	7.2
514	FEM514	30	50 MPa RC	OutriggerBelt	50 MPa RC	[5, 5]	4.8	7.2
515	FEM515	30	Steel	OutriggerBelt	Steel	[5, 5]	4.8	7.2
516	FEM516	30	32 MPa RC	OutriggerBelt	32 MPa RC	[5, 5]	7.2	4.8
517	FEM517	30	40 MPa RC	OutriggerBelt	40 MPa RC	[5, 5]	7.2	4.8
518	FEM518	30	50 MPa RC	OutriggerBelt	50 MPa RC	[5, 5]	7.2	4.8
519	FEM519	30	Steel	OutriggerBelt	Steel	[5, 5]	7.2	4.8
520	FEM520	30	32 MPa RC	OutriggerBelt	32 MPa RC	[5, 5]	7.2	7.2
521	FEM521	30	40 MPa RC	OutriggerBelt	40 MPa RC	[5, 5]	7.2	7.2
522	FEM522	30	50 MPa RC	OutriggerBelt	50 MPa RC	[5, 5]	7.2	7.2
523	FEM523	30	Steel	OutriggerBelt	Steel	[5, 5]	7.2	7.2
524	FEM524	30	32 MPa RC	OutriggerBelt	32 MPa RC	[5, 7]	4.8	4.8
525	FEM525	30	40 MPa RC	OutriggerBelt	40 MPa RC	[5, 7]	4.8	4.8
526	FEM526	30	50 MPa RC	OutriggerBelt	50 MPa RC	[5, 7]	4.8	4.8
527	FEM527	30	Steel	OutriggerBelt	Steel	[5, 7]	4.8	4.8
528	FEM528	30	32 MPa RC	OutriggerBelt	32 MPa RC	[5, 7]	4.8	7.2
529	FEM529	30	40 MPa RC	OutriggerBelt	40 MPa RC	[5, 7]	4.8	7.2
530	FEM530	30	50 MPa RC	OutriggerBelt	50 MPa RC	[5, 7]	4.8	7.2
531	FEM531	30	Steel	OutriggerBelt	Steel	[5, 7]	4.8	7.2
532	FEM532	30	32 MPa RC	OutriggerBelt	32 MPa RC	[5, 7]	7.2	4.8
533	FEM533	30	40 MPa RC	OutriggerBelt	40 MPa RC	[5, 7]	7.2	4.8
534	FEM534	30	50 MPa RC	OutriggerBelt	50 MPa RC	[5, 7]	7.2	4.8
535	FEM535	30	Steel	OutriggerBelt	Steel	[5, 7]	7.2	4.8
536	FEM536	30	32 MPa RC	OutriggerBelt	32 MPa RC	[5, 7]	7.2	7.2
537	FEM537	30	40 MPa RC	OutriggerBelt	40 MPa RC	[5, 7]	7.2	7.2
538	FEM538	30	50 MPa RC	OutriggerBelt	50 MPa RC	[5, 7]	7.2	7.2
539	FEM539	30	Steel	OutriggerBelt	Steel	[5, 7]	7.2	7.2
540	FEM540	30	32 MPa RC	OutriggerBelt	32 MPa RC	[7, 7]	4.8	4.8
541	FEM541	30	40 MPa RC	OutriggerBelt	40 MPa RC	[7, 7]	4.8	4.8
542	FEM542	30	50 MPa RC	OutriggerBelt	50 MPa RC	[7, 7]	4.8	4.8
543	FEM543	30	Steel	OutriggerBelt	Steel	[7, 7]	4.8	4.8
544	FEM544	30	32 MPa RC	OutriggerBelt	32 MPa RC	[7, 7]	4.8	7.2
545	FEM545	30	40 MPa RC	OutriggerBelt	40 MPa RC	[7, 7]	4.8	7.2
546	FEM546	30	50 MPa RC	OutriggerBelt	50 MPa RC	[7, 7]	4.8	7.2
547	FEM547	30	Steel	OutriggerBelt	Steel	[7, 7]	4.8	7.2
548	FEM548	30	32 MPa RC	OutriggerBelt	32 MPa RC	[7, 7]	7.2	4.8
549	FEM549	30	40 MPa RC	OutriggerBelt	40 MPa RC	[7, 7]	7.2	4.8
550	FEM550	30	50 MPa RC	OutriggerBelt	50 MPa RC	[7, 7]	7.2	4.8
551	FEM551	30	Steel	OutriggerBelt	Steel	[7, 7]	7.2	4.8
552	FEM552	30	32 MPa RC	OutriggerBelt	32 MPa RC	[7, 7]	7.2	7.2
553	FEM553	30	40 MPa RC	OutriggerBelt	40 MPa RC	[7, 7]	7.2	7.2
554	FEM554	30	50 MPa RC	OutriggerBelt	50 MPa RC	[7, 7]	7.2	7.2
555	FEM555	30	Steel	OutriggerBelt	Steel	[7, 7]	7.2	7.2
556	FEM556	40	32 MPa RC	OutriggerBelt	32 MPa RC	[5, 5]	4.8	4.8
557	FEM557	40	40 MPa RC	OutriggerBelt	40 MPa RC	[5, 5]	4.8	4.8
558	FEM558	40	50 MPa RC	OutriggerBelt	50 MPa RC	[5, 5]	4.8	4.8
559	FEM559	40	Steel	OutriggerBelt	Steel	[5, 5]	4.8	4.8
560	FEM560	40	32 MPa RC	OutriggerBelt	32 MPa RC	[5, 5]	4.8	7.2
561	FEM561	40	40 MPa RC	OutriggerBelt	40 MPa RC	[5, 5]	4.8	7.2
562	FEM562	40	50 MPa RC	OutriggerBelt	50 MPa RC	[5, 5]	4.8	7.2
563	FEM563	40	Steel	OutriggerBelt	Steel	[5, 5]	4.8	7.2
564	FEM564	40	32 MPa RC	OutriggerBelt	32 MPa RC	[5, 5]	7.2	4.8
565	FEM565	40	40 MPa RC	OutriggerBelt	40 MPa RC	[5, 5]	7.2	4.8
566	FEM566	40	50 MPa RC	OutriggerBelt	50 MPa RC	[5, 5]	7.2	4.8
567	FEM567	40	Steel	OutriggerBelt	Steel	[5, 5]	7.2	4.8
568	FEM568	40	32 MPa RC	OutriggerBelt	32 MPa RC	[5, 5]	7.2	7.2
569	FEM569	40	40 MPa RC	OutriggerBelt	40 MPa RC	[5, 5]	7.2	7.2
570	FEM570	40	50 MPa RC	OutriggerBelt	50 MPa RC	[5, 5]	7.2	7.2
571	FEM571	40	Steel	OutriggerBelt	Steel	[5, 5]	7.2	7.2
572	FEM572	40	32 MPa RC	OutriggerBelt	32 MPa RC	[5, 7]	4.8	4.8
573	FEM573	40	40 MPa RC	OutriggerBelt	40 MPa RC	[5, 7]	4.8	4.8
574	FEM574	40	50 MPa RC	OutriggerBelt	50 MPa RC	[5, 7]	4.8	4.8
575	FEM575	40	Steel	OutriggerBelt	Steel	[5, 7]	4.8	4.8
576	FEM576	40	32 MPa RC	OutriggerBelt	32 MPa RC	[5, 7]	4.8	7.2
577	FEM577	40	40 MPa RC	OutriggerBelt	40 MPa RC	[5, 7]	4.8	7.2
578	FEM578	40	50 MPa RC	OutriggerBelt	50 MPa RC	[5, 7]	4.8	7.2
579	FEM579	40	Steel	OutriggerBelt	Steel	[5, 7]	4.8	7.2
580	FEM580	40	32 MPa RC	OutriggerBelt	32 MPa RC	[5, 7]	7.2	4.8
581	FEM581	40	40 MPa RC	OutriggerBelt	40 MPa RC	[5, 7]	7.2	4.8
582	FEM582	40	50 MPa RC	OutriggerBelt	50 MPa RC	[5, 7]	7.2	4.8

(*continued on next page*)

Table C1 (*continued*)

#	Name	Storeys	Frame Material	LLRS	LLRS Material	Grid	Column Span in X Dir (m)	Column Span in Y Dir (m)
583	FEM583	40	Steel	OutriggerBelt	Steel	[5, 7]	7.2	4.8
584	FEM584	40	32 MPa RC	OutriggerBelt	32 MPa RC	[5, 7]	7.2	7.2
585	FEM585	40	40 MPa RC	OutriggerBelt	40 MPa RC	[5, 7]	7.2	7.2
586	FEM586	40	50 MPa RC	OutriggerBelt	50 MPa RC	[5, 7]	7.2	7.2
587	FEM587	40	Steel	OutriggerBelt	Steel	[5, 7]	7.2	7.2
588	FEM588	40	32 MPa RC	OutriggerBelt	32 MPa RC	[7, 7]	4.8	4.8
589	FEM589	40	40 MPa RC	OutriggerBelt	40 MPa RC	[7, 7]	4.8	4.8
590	FEM590	40	50 MPa RC	OutriggerBelt	50 MPa RC	[7, 7]	4.8	4.8
591	FEM591	40	Steel	OutriggerBelt	Steel	[7, 7]	4.8	4.8
592	FEM592	40	32 MPa RC	OutriggerBelt	32 MPa RC	[7, 7]	4.8	7.2
593	FEM593	40	40 MPa RC	OutriggerBelt	40 MPa RC	[7, 7]	4.8	7.2
594	FEM594	40	50 MPa RC	OutriggerBelt	50 MPa RC	[7, 7]	4.8	7.2
595	FEM595	40	Steel	OutriggerBelt	Steel	[7, 7]	4.8	7.2
596	FEM596	40	32 MPa RC	OutriggerBelt	32 MPa RC	[7, 7]	7.2	4.8
597	FEM597	40	40 MPa RC	OutriggerBelt	40 MPa RC	[7, 7]	7.2	4.8
598	FEM598	40	50 MPa RC	OutriggerBelt	50 MPa RC	[7, 7]	7.2	4.8
599	FEM599	40	Steel	OutriggerBelt	Steel	[7, 7]	7.2	4.8
600	FEM600	40	32 MPa RC	OutriggerBelt	32 MPa RC	[7, 7]	7.2	7.2
601	FEM601	40	40 MPa RC	OutriggerBelt	40 MPa RC	[7, 7]	7.2	7.2
602	FEM602	40	50 MPa RC	OutriggerBelt	50 MPa RC	[7, 7]	7.2	7.2
603	FEM603	40	Steel	OutriggerBelt	Steel	[7, 7]	7.2	7.2
604	FEM604	50	32 MPa RC	OutriggerBelt	32 MPa RC	[5, 5]	4.8	4.8
605	FEM605	50	40 MPa RC	OutriggerBelt	40 MPa RC	[5, 5]	4.8	4.8
606	FEM606	50	50 MPa RC	OutriggerBelt	50 MPa RC	[5, 5]	4.8	4.8
607	FEM607	50	Steel	OutriggerBelt	Steel	[5, 5]	4.8	4.8
608	FEM608	50	32 MPa RC	OutriggerBelt	32 MPa RC	[5, 5]	4.8	7.2
609	FEM609	50	40 MPa RC	OutriggerBelt	40 MPa RC	[5, 5]	4.8	7.2
610	FEM610	50	50 MPa RC	OutriggerBelt	50 MPa RC	[5, 5]	4.8	7.2
611	FEM611	50	Steel	OutriggerBelt	Steel	[5, 5]	4.8	7.2
612	FEM612	50	32 MPa RC	OutriggerBelt	32 MPa RC	[5, 5]	7.2	4.8
613	FEM613	50	40 MPa RC	OutriggerBelt	40 MPa RC	[5, 5]	7.2	4.8
614	FEM614	50	50 MPa RC	OutriggerBelt	50 MPa RC	[5, 5]	7.2	4.8
615	FEM615	50	Steel	OutriggerBelt	Steel	[5, 5]	7.2	4.8
616	FEM616	50	32 MPa RC	OutriggerBelt	32 MPa RC	[5, 5]	7.2	7.2
617	FEM617	50	40 MPa RC	OutriggerBelt	40 MPa RC	[5, 5]	7.2	7.2
618	FEM618	50	50 MPa RC	OutriggerBelt	50 MPa RC	[5, 5]	7.2	7.2
619	FEM619	50	Steel	OutriggerBelt	Steel	[5, 5]	7.2	7.2
620	FEM620	50	32 MPa RC	OutriggerBelt	32 MPa RC	[5, 7]	4.8	4.8
621	FEM621	50	40 MPa RC	OutriggerBelt	40 MPa RC	[5, 7]	4.8	4.8
622	FEM622	50	50 MPa RC	OutriggerBelt	50 MPa RC	[5, 7]	4.8	4.8
623	FEM623	50	Steel	OutriggerBelt	Steel	[5, 7]	4.8	4.8
624	FEM624	50	32 MPa RC	OutriggerBelt	32 MPa RC	[5, 7]	4.8	7.2
625	FEM625	50	40 MPa RC	OutriggerBelt	40 MPa RC	[5, 7]	4.8	7.2
626	FEM626	50	50 MPa RC	OutriggerBelt	50 MPa RC	[5, 7]	4.8	7.2
627	FEM627	50	Steel	OutriggerBelt	Steel	[5, 7]	4.8	7.2
628	FEM628	50	32 MPa RC	OutriggerBelt	32 MPa RC	[5, 7]	7.2	4.8
629	FEM629	50	40 MPa RC	OutriggerBelt	40 MPa RC	[5, 7]	7.2	4.8
630	FEM630	50	50 MPa RC	OutriggerBelt	50 MPa RC	[5, 7]	7.2	4.8
631	FEM631	50	Steel	OutriggerBelt	Steel	[5, 7]	7.2	4.8
632	FEM632	50	32 MPa RC	OutriggerBelt	32 MPa RC	[5, 7]	7.2	7.2
633	FEM633	50	40 MPa RC	OutriggerBelt	40 MPa RC	[5, 7]	7.2	7.2
634	FEM634	50	50 MPa RC	OutriggerBelt	50 MPa RC	[5, 7]	7.2	7.2
635	FEM635	50	Steel	OutriggerBelt	Steel	[5, 7]	7.2	7.2
636	FEM636	50	32 MPa RC	OutriggerBelt	32 MPa RC	[7, 7]	4.8	4.8
637	FEM637	50	40 MPa RC	OutriggerBelt	40 MPa RC	[7, 7]	4.8	4.8
638	FEM638	50	50 MPa RC	OutriggerBelt	50 MPa RC	[7, 7]	4.8	4.8
639	FEM639	50	Steel	OutriggerBelt	Steel	[7, 7]	4.8	4.8
640	FEM640	50	32 MPa RC	OutriggerBelt	32 MPa RC	[7, 7]	4.8	7.2
641	FEM641	50	40 MPa RC	OutriggerBelt	40 MPa RC	[7, 7]	4.8	7.2
642	FEM642	50	50 MPa RC	OutriggerBelt	50 MPa RC	[7, 7]	4.8	7.2
643	FEM643	50	Steel	OutriggerBelt	Steel	[7, 7]	4.8	7.2
644	FEM644	50	32 MPa RC	OutriggerBelt	32 MPa RC	[7, 7]	7.2	4.8
645	FEM645	50	40 MPa RC	OutriggerBelt	40 MPa RC	[7, 7]	7.2	4.8
646	FEM646	50	50 MPa RC	OutriggerBelt	50 MPa RC	[7, 7]	7.2	4.8
647	FEM647	50	Steel	OutriggerBelt	Steel	[7, 7]	7.2	4.8
648	FEM648	50	32 MPa RC	OutriggerBelt	32 MPa RC	[7, 7]	7.2	7.2
649	FEM649	50	40 MPa RC	OutriggerBelt	40 MPa RC	[7, 7]	7.2	7.2
650	FEM650	50	50 MPa RC	OutriggerBelt	50 MPa RC	[7, 7]	7.2	7.2
651	FEM651	50	Steel	OutriggerBelt	Steel	[7, 7]	7.2	7.2
652	FEM652	5	32 MPa RC	BracedTube	32 MPa RC	[5, 5]	4.8	4.8
653	FEM653	5	40 MPa RC	BracedTube	40 MPa RC	[5, 5]	4.8	4.8
654	FEM654	5	50 MPa RC	BracedTube	50 MPa RC	[5, 5]	4.8	4.8
655	FEM655	5	Steel	BracedTube	Steel	[5, 5]	4.8	4.8
656	FEM656	5	32 MPa RC	BracedTube	32 MPa RC	[5, 5]	4.8	7.2
657	FEM657	5	40 MPa RC	BracedTube	40 MPa RC	[5, 5]	4.8	7.2
658	FEM658	5	50 MPa RC	BracedTube	50 MPa RC	[5, 5]	4.8	7.2

(*continued on next page*)

Table C1 (*continued*)

#	Name	Storeys	Frame Material	LLRS	LLRS Material	Grid	Column Span in X Dir (m)	Column Span in Y Dir (m)
659	FEM659	5	Steel	BracedTube	Steel	[5, 5]	4.8	7.2
660	FEM660	5	32 MPa RC	BracedTube	32 MPa RC	[5, 5]	7.2	4.8
661	FEM661	5	40 MPa RC	BracedTube	40 MPa RC	[5, 5]	7.2	4.8
662	FEM662	5	50 MPa RC	BracedTube	50 MPa RC	[5, 5]	7.2	4.8
663	FEM663	5	Steel	BracedTube	Steel	[5, 5]	7.2	4.8
664	FEM664	5	32 MPa RC	BracedTube	32 MPa RC	[5, 5]	7.2	7.2
665	FEM665	5	40 MPa RC	BracedTube	40 MPa RC	[5, 5]	7.2	7.2
666	FEM666	5	50 MPa RC	BracedTube	50 MPa RC	[5, 5]	7.2	7.2
667	FEM667	5	Steel	BracedTube	Steel	[5, 5]	7.2	7.2
668	FEM668	5	32 MPa RC	BracedTube	32 MPa RC	[5, 7]	4.8	4.8
669	FEM669	5	40 MPa RC	BracedTube	40 MPa RC	[5, 7]	4.8	4.8
670	FEM670	5	50 MPa RC	BracedTube	50 MPa RC	[5, 7]	4.8	4.8
671	FEM671	5	Steel	BracedTube	Steel	[5, 7]	4.8	4.8
672	FEM672	5	32 MPa RC	BracedTube	32 MPa RC	[5, 7]	4.8	7.2
673	FEM673	5	40 MPa RC	BracedTube	40 MPa RC	[5, 7]	4.8	7.2
674	FEM674	5	50 MPa RC	BracedTube	50 MPa RC	[5, 7]	4.8	7.2
675	FEM675	5	Steel	BracedTube	Steel	[5, 7]	4.8	7.2
676	FEM676	5	32 MPa RC	BracedTube	32 MPa RC	[5, 7]	7.2	4.8
677	FEM677	5	40 MPa RC	BracedTube	40 MPa RC	[5, 7]	7.2	4.8
678	FEM678	5	50 MPa RC	BracedTube	50 MPa RC	[5, 7]	7.2	4.8
679	FEM679	5	Steel	BracedTube	Steel	[5, 7]	7.2	4.8
680	FEM680	5	32 MPa RC	BracedTube	32 MPa RC	[5, 7]	7.2	7.2
681	FEM681	5	40 MPa RC	BracedTube	40 MPa RC	[5, 7]	7.2	7.2
682	FEM682	5	50 MPa RC	BracedTube	50 MPa RC	[5, 7]	7.2	7.2
683	FEM683	5	Steel	BracedTube	Steel	[5, 7]	7.2	7.2
684	FEM684	5	32 MPa RC	BracedTube	32 MPa RC	[7, 7]	4.8	4.8
685	FEM685	5	40 MPa RC	BracedTube	40 MPa RC	[7, 7]	4.8	4.8
686	FEM686	5	50 MPa RC	BracedTube	50 MPa RC	[7, 7]	4.8	4.8
687	FEM687	5	Steel	BracedTube	Steel	[7, 7]	4.8	4.8
688	FEM688	5	32 MPa RC	BracedTube	32 MPa RC	[7, 7]	4.8	7.2
689	FEM689	5	40 MPa RC	BracedTube	40 MPa RC	[7, 7]	4.8	7.2
690	FEM690	5	50 MPa RC	BracedTube	50 MPa RC	[7, 7]	4.8	7.2
691	FEM691	5	Steel	BracedTube	Steel	[7, 7]	4.8	7.2
692	FEM692	5	32 MPa RC	BracedTube	32 MPa RC	[7, 7]	7.2	4.8
693	FEM693	5	40 MPa RC	BracedTube	40 MPa RC	[7, 7]	7.2	4.8
694	FEM694	5	50 MPa RC	BracedTube	50 MPa RC	[7, 7]	7.2	4.8
695	FEM695	5	Steel	BracedTube	Steel	[7, 7]	7.2	4.8
696	FEM696	5	32 MPa RC	BracedTube	32 MPa RC	[7, 7]	7.2	7.2
697	FEM697	5	40 MPa RC	BracedTube	40 MPa RC	[7, 7]	7.2	7.2
698	FEM698	5	50 MPa RC	BracedTube	50 MPa RC	[7, 7]	7.2	7.2
699	FEM699	5	Steel	BracedTube	Steel	[7, 7]	7.2	7.2
700	FEM700	10	32 MPa RC	BracedTube	32 MPa RC	[5, 5]	4.8	4.8
701	FEM701	10	40 MPa RC	BracedTube	40 MPa RC	[5, 5]	4.8	4.8
702	FEM702	10	50 MPa RC	BracedTube	50 MPa RC	[5, 5]	4.8	4.8
703	FEM703	10	Steel	BracedTube	Steel	[5, 5]	4.8	4.8
704	FEM704	10	32 MPa RC	BracedTube	32 MPa RC	[5, 5]	4.8	7.2
705	FEM705	10	40 MPa RC	BracedTube	40 MPa RC	[5, 5]	4.8	7.2
706	FEM706	10	50 MPa RC	BracedTube	50 MPa RC	[5, 5]	4.8	7.2
707	FEM707	10	Steel	BracedTube	Steel	[5, 5]	4.8	7.2
708	FEM708	10	32 MPa RC	BracedTube	32 MPa RC	[5, 5]	7.2	4.8
709	FEM709	10	40 MPa RC	BracedTube	40 MPa RC	[5, 5]	7.2	4.8
710	FEM710	10	50 MPa RC	BracedTube	50 MPa RC	[5, 5]	7.2	4.8
711	FEM711	10	Steel	BracedTube	Steel	[5, 5]	7.2	4.8
712	FEM712	10	32 MPa RC	BracedTube	32 MPa RC	[5, 5]	7.2	7.2
713	FEM713	10	40 MPa RC	BracedTube	40 MPa RC	[5, 5]	7.2	7.2
714	FEM714	10	50 MPa RC	BracedTube	50 MPa RC	[5, 5]	7.2	7.2
715	FEM715	10	Steel	BracedTube	Steel	[5, 5]	7.2	7.2
716	FEM716	10	32 MPa RC	BracedTube	32 MPa RC	[5, 7]	4.8	4.8
717	FEM717	10	40 MPa RC	BracedTube	40 MPa RC	[5, 7]	4.8	4.8
718	FEM718	10	50 MPa RC	BracedTube	50 MPa RC	[5, 7]	4.8	4.8
719	FEM719	10	Steel	BracedTube	Steel	[5, 7]	4.8	4.8
720	FEM720	10	32 MPa RC	BracedTube	32 MPa RC	[5, 7]	4.8	7.2
721	FEM721	10	40 MPa RC	BracedTube	40 MPa RC	[5, 7]	4.8	7.2
722	FEM722	10	50 MPa RC	BracedTube	50 MPa RC	[5, 7]	4.8	7.2
723	FEM723	10	Steel	BracedTube	Steel	[5, 7]	4.8	7.2
724	FEM724	10	32 MPa RC	BracedTube	32 MPa RC	[5, 7]	7.2	4.8
725	FEM725	10	40 MPa RC	BracedTube	40 MPa RC	[5, 7]	7.2	4.8
726	FEM726	10	50 MPa RC	BracedTube	50 MPa RC	[5, 7]	7.2	4.8
727	FEM727	10	Steel	BracedTube	Steel	[5, 7]	7.2	4.8
728	FEM728	10	32 MPa RC	BracedTube	32 MPa RC	[5, 7]	7.2	7.2
729	FEM729	10	40 MPa RC	BracedTube	40 MPa RC	[5, 7]	7.2	7.2
730	FEM730	10	50 MPa RC	BracedTube	50 MPa RC	[5, 7]	7.2	7.2
731	FEM731	10	Steel	BracedTube	Steel	[5, 7]	7.2	7.2
732	FEM732	10	32 MPa RC	BracedTube	32 MPa RC	[7, 7]	4.8	4.8
733	FEM733	10	40 MPa RC	BracedTube	40 MPa RC	[7, 7]	4.8	4.8
734	FEM734	10	50 MPa RC	BracedTube	50 MPa RC	[7, 7]	4.8	4.8

(*continued on next page*)

Table C1 (*continued*)

#	Name	Storeys	Frame Material	LLRS	LLRS Material	Grid	Column Span in X Dir (m)	Column Span in Y Dir (m)
735	FEM735	10	Steel	BracedTube	Steel	[7, 7]	4.8	4.8
736	FEM736	10	32 MPa RC	BracedTube	32 MPa RC	[7, 7]	4.8	7.2
737	FEM737	10	40 MPa RC	BracedTube	40 MPa RC	[7, 7]	4.8	7.2
738	FEM738	10	50 MPa RC	BracedTube	50 MPa RC	[7, 7]	4.8	7.2
739	FEM739	10	Steel	BracedTube	Steel	[7, 7]	4.8	7.2
740	FEM740	10	32 MPa RC	BracedTube	32 MPa RC	[7, 7]	7.2	4.8
741	FEM741	10	40 MPa RC	BracedTube	40 MPa RC	[7, 7]	7.2	4.8
742	FEM742	10	50 MPa RC	BracedTube	50 MPa RC	[7, 7]	7.2	4.8
743	FEM743	10	Steel	BracedTube	Steel	[7, 7]	7.2	4.8
744	FEM744	10	32 MPa RC	BracedTube	32 MPa RC	[7, 7]	7.2	7.2
745	FEM745	10	40 MPa RC	BracedTube	40 MPa RC	[7, 7]	7.2	7.2
746	FEM746	10	50 MPa RC	BracedTube	50 MPa RC	[7, 7]	7.2	7.2
747	FEM747	10	Steel	BracedTube	Steel	[7, 7]	7.2	7.2
748	FEM748	15	32 MPa RC	BracedTube	32 MPa RC	[5, 5]	4.8	4.8
749	FEM749	15	40 MPa RC	BracedTube	40 MPa RC	[5, 5]	4.8	4.8
750	FEM750	15	50 MPa RC	BracedTube	50 MPa RC	[5, 5]	4.8	4.8
751	FEM751	15	Steel	BracedTube	Steel	[5, 5]	4.8	4.8
752	FEM752	15	32 MPa RC	BracedTube	32 MPa RC	[5, 5]	4.8	7.2
753	FEM753	15	40 MPa RC	BracedTube	40 MPa RC	[5, 5]	4.8	7.2
754	FEM754	15	50 MPa RC	BracedTube	50 MPa RC	[5, 5]	4.8	7.2
755	FEM755	15	Steel	BracedTube	Steel	[5, 5]	4.8	7.2
756	FEM756	15	32 MPa RC	BracedTube	32 MPa RC	[5, 5]	7.2	4.8
757	FEM757	15	40 MPa RC	BracedTube	40 MPa RC	[5, 5]	7.2	4.8
758	FEM758	15	50 MPa RC	BracedTube	50 MPa RC	[5, 5]	7.2	4.8
759	FEM759	15	Steel	BracedTube	Steel	[5, 5]	7.2	4.8
760	FEM760	15	32 MPa RC	BracedTube	32 MPa RC	[5, 5]	7.2	7.2
761	FEM761	15	40 MPa RC	BracedTube	40 MPa RC	[5, 5]	7.2	7.2
762	FEM762	15	50 MPa RC	BracedTube	50 MPa RC	[5, 5]	7.2	7.2
763	FEM763	15	Steel	BracedTube	Steel	[5, 5]	7.2	7.2
764	FEM764	15	32 MPa RC	BracedTube	32 MPa RC	[5, 7]	4.8	4.8
765	FEM765	15	40 MPa RC	BracedTube	40 MPa RC	[5, 7]	4.8	4.8
766	FEM766	15	50 MPa RC	BracedTube	50 MPa RC	[5, 7]	4.8	4.8
767	FEM767	15	Steel	BracedTube	Steel	[5, 7]	4.8	4.8
768	FEM768	15	32 MPa RC	BracedTube	32 MPa RC	[5, 7]	4.8	7.2
769	FEM769	15	40 MPa RC	BracedTube	40 MPa RC	[5, 7]	4.8	7.2
770	FEM770	15	50 MPa RC	BracedTube	50 MPa RC	[5, 7]	4.8	7.2
771	FEM771	15	Steel	BracedTube	Steel	[5, 7]	4.8	7.2
772	FEM772	15	32 MPa RC	BracedTube	32 MPa RC	[5, 7]	7.2	4.8
773	FEM773	15	40 MPa RC	BracedTube	40 MPa RC	[5, 7]	7.2	4.8
774	FEM774	15	50 MPa RC	BracedTube	50 MPa RC	[5, 7]	7.2	4.8
775	FEM775	15	Steel	BracedTube	Steel	[5, 7]	7.2	4.8
776	FEM776	15	32 MPa RC	BracedTube	32 MPa RC	[5, 7]	7.2	7.2
777	FEM777	15	40 MPa RC	BracedTube	40 MPa RC	[5, 7]	7.2	7.2
778	FEM778	15	50 MPa RC	BracedTube	50 MPa RC	[5, 7]	7.2	7.2
779	FEM779	15	Steel	BracedTube	Steel	[5, 7]	7.2	7.2
780	FEM780	15	32 MPa RC	BracedTube	32 MPa RC	[7, 7]	4.8	4.8
781	FEM781	15	40 MPa RC	BracedTube	40 MPa RC	[7, 7]	4.8	4.8
782	FEM782	15	50 MPa RC	BracedTube	50 MPa RC	[7, 7]	4.8	4.8
783	FEM783	15	Steel	BracedTube	Steel	[7, 7]	4.8	4.8
784	FEM784	15	32 MPa RC	BracedTube	32 MPa RC	[7, 7]	4.8	7.2
785	FEM785	15	40 MPa RC	BracedTube	40 MPa RC	[7, 7]	4.8	7.2
786	FEM786	15	50 MPa RC	BracedTube	50 MPa RC	[7, 7]	4.8	7.2
787	FEM787	15	Steel	BracedTube	Steel	[7, 7]	4.8	7.2
788	FEM788	15	32 MPa RC	BracedTube	32 MPa RC	[7, 7]	7.2	4.8
789	FEM789	15	40 MPa RC	BracedTube	40 MPa RC	[7, 7]	7.2	4.8
790	FEM790	15	50 MPa RC	BracedTube	50 MPa RC	[7, 7]	7.2	4.8
791	FEM791	15	Steel	BracedTube	Steel	[7, 7]	7.2	4.8
792	FEM792	15	32 MPa RC	BracedTube	32 MPa RC	[7, 7]	7.2	7.2
793	FEM793	15	40 MPa RC	BracedTube	40 MPa RC	[7, 7]	7.2	7.2
794	FEM794	15	50 MPa RC	BracedTube	50 MPa RC	[7, 7]	7.2	7.2
795	FEM795	15	Steel	BracedTube	Steel	[7, 7]	7.2	7.2
796	FEM796	20	32 MPa RC	BracedTube	32 MPa RC	[5, 5]	4.8	4.8
797	FEM797	20	40 MPa RC	BracedTube	40 MPa RC	[5, 5]	4.8	4.8
798	FEM798	20	50 MPa RC	BracedTube	50 MPa RC	[5, 5]	4.8	4.8
799	FEM799	20	Steel	BracedTube	Steel	[5, 5]	4.8	4.8
800	FEM800	20	32 MPa RC	BracedTube	32 MPa RC	[5, 5]	4.8	7.2
801	FEM801	20	40 MPa RC	BracedTube	40 MPa RC	[5, 5]	4.8	7.2
802	FEM802	20	50 MPa RC	BracedTube	50 MPa RC	[5, 5]	4.8	7.2
803	FEM803	20	Steel	BracedTube	Steel	[5, 5]	4.8	7.2
804	FEM804	20	32 MPa RC	BracedTube	32 MPa RC	[5, 5]	7.2	4.8
805	FEM805	20	40 MPa RC	BracedTube	40 MPa RC	[5, 5]	7.2	4.8
806	FEM806	20	50 MPa RC	BracedTube	50 MPa RC	[5, 5]	7.2	4.8
807	FEM807	20	Steel	BracedTube	Steel	[5, 5]	7.2	4.8
808	FEM808	20	32 MPa RC	BracedTube	32 MPa RC	[5, 5]	7.2	7.2
809	FEM809	20	40 MPa RC	BracedTube	40 MPa RC	[5, 5]	7.2	7.2
810	FEM810	20	50 MPa RC	BracedTube	50 MPa RC	[5, 5]	7.2	7.2

(*continued on next page*)

Table C1 (*continued*)

#	Name	Storeys	Frame Material	LLRS	LLRS Material	Grid	Column Span in X Dir (m)	Column Span in Y Dir (m)
811	FEM811	20	Steel	BracedTube	Steel	[5, 5]	7.2	7.2
812	FEM812	20	32 MPa RC	BracedTube	32 MPa RC	[5, 7]	4.8	4.8
813	FEM813	20	40 MPa RC	BracedTube	40 MPa RC	[5, 7]	4.8	4.8
814	FEM814	20	50 MPa RC	BracedTube	50 MPa RC	[5, 7]	4.8	4.8
815	FEM815	20	Steel	BracedTube	Steel	[5, 7]	4.8	4.8
816	FEM816	20	32 MPa RC	BracedTube	32 MPa RC	[5, 7]	4.8	7.2
817	FEM817	20	40 MPa RC	BracedTube	40 MPa RC	[5, 7]	4.8	7.2
818	FEM818	20	50 MPa RC	BracedTube	50 MPa RC	[5, 7]	4.8	7.2
819	FEM819	20	Steel	BracedTube	Steel	[5, 7]	4.8	7.2
820	FEM820	20	32 MPa RC	BracedTube	32 MPa RC	[5, 7]	7.2	4.8
821	FEM821	20	40 MPa RC	BracedTube	40 MPa RC	[5, 7]	7.2	4.8
822	FEM822	20	50 MPa RC	BracedTube	50 MPa RC	[5, 7]	7.2	4.8
823	FEM823	20	Steel	BracedTube	Steel	[5, 7]	7.2	4.8
824	FEM824	20	32 MPa RC	BracedTube	32 MPa RC	[5, 7]	7.2	7.2
825	FEM825	20	40 MPa RC	BracedTube	40 MPa RC	[5, 7]	7.2	7.2
826	FEM826	20	50 MPa RC	BracedTube	50 MPa RC	[5, 7]	7.2	7.2
827	FEM827	20	Steel	BracedTube	Steel	[5, 7]	7.2	7.2
828	FEM828	20	32 MPa RC	BracedTube	32 MPa RC	[7, 7]	4.8	4.8
829	FEM829	20	40 MPa RC	BracedTube	40 MPa RC	[7, 7]	4.8	4.8
830	FEM830	20	50 MPa RC	BracedTube	50 MPa RC	[7, 7]	4.8	4.8
831	FEM831	20	Steel	BracedTube	Steel	[7, 7]	4.8	4.8
832	FEM832	20	32 MPa RC	BracedTube	32 MPa RC	[7, 7]	4.8	7.2
833	FEM833	20	40 MPa RC	BracedTube	40 MPa RC	[7, 7]	4.8	7.2
834	FEM834	20	50 MPa RC	BracedTube	50 MPa RC	[7, 7]	4.8	7.2
835	FEM835	20	Steel	BracedTube	Steel	[7, 7]	4.8	7.2
836	FEM836	20	32 MPa RC	BracedTube	32 MPa RC	[7, 7]	7.2	4.8
837	FEM837	20	40 MPa RC	BracedTube	40 MPa RC	[7, 7]	7.2	4.8
838	FEM838	20	50 MPa RC	BracedTube	50 MPa RC	[7, 7]	7.2	4.8
839	FEM839	20	Steel	BracedTube	Steel	[7, 7]	7.2	4.8
840	FEM840	20	32 MPa RC	BracedTube	32 MPa RC	[7, 7]	7.2	7.2
841	FEM841	20	40 MPa RC	BracedTube	40 MPa RC	[7, 7]	7.2	7.2
842	FEM842	20	50 MPa RC	BracedTube	50 MPa RC	[7, 7]	7.2	7.2
843	FEM843	20	Steel	BracedTube	Steel	[7, 7]	7.2	7.2
844	FEM844	25	32 MPa RC	BracedTube	32 MPa RC	[5, 5]	4.8	4.8
845	FEM845	25	40 MPa RC	BracedTube	40 MPa RC	[5, 5]	4.8	4.8
846	FEM846	25	50 MPa RC	BracedTube	50 MPa RC	[5, 5]	4.8	4.8
847	FEM847	25	Steel	BracedTube	Steel	[5, 5]	4.8	4.8
848	FEM848	25	32 MPa RC	BracedTube	32 MPa RC	[5, 5]	4.8	7.2
849	FEM849	25	40 MPa RC	BracedTube	40 MPa RC	[5, 5]	4.8	7.2
850	FEM850	25	50 MPa RC	BracedTube	50 MPa RC	[5, 5]	4.8	7.2
851	FEM851	25	Steel	BracedTube	Steel	[5, 5]	4.8	7.2
852	FEM852	25	32 MPa RC	BracedTube	32 MPa RC	[5, 5]	7.2	4.8
853	FEM853	25	40 MPa RC	BracedTube	40 MPa RC	[5, 5]	7.2	4.8
854	FEM854	25	50 MPa RC	BracedTube	50 MPa RC	[5, 5]	7.2	4.8
855	FEM855	25	Steel	BracedTube	Steel	[5, 5]	7.2	4.8
856	FEM856	25	32 MPa RC	BracedTube	32 MPa RC	[5, 5]	7.2	7.2
857	FEM857	25	40 MPa RC	BracedTube	40 MPa RC	[5, 5]	7.2	7.2
858	FEM858	25	50 MPa RC	BracedTube	50 MPa RC	[5, 5]	7.2	7.2
859	FEM859	25	Steel	BracedTube	Steel	[5, 5]	7.2	7.2
860	FEM860	25	32 MPa RC	BracedTube	32 MPa RC	[5, 7]	4.8	4.8
861	FEM861	25	40 MPa RC	BracedTube	40 MPa RC	[5, 7]	4.8	4.8
862	FEM862	25	50 MPa RC	BracedTube	50 MPa RC	[5, 7]	4.8	4.8
863	FEM863	25	Steel	BracedTube	Steel	[5, 7]	4.8	4.8
864	FEM864	25	32 MPa RC	BracedTube	32 MPa RC	[5, 7]	4.8	7.2
865	FEM865	25	40 MPa RC	BracedTube	40 MPa RC	[5, 7]	4.8	7.2
866	FEM866	25	50 MPa RC	BracedTube	50 MPa RC	[5, 7]	4.8	7.2
867	FEM867	25	Steel	BracedTube	Steel	[5, 7]	4.8	7.2
868	FEM868	25	32 MPa RC	BracedTube	32 MPa RC	[5, 7]	7.2	4.8
869	FEM869	25	40 MPa RC	BracedTube	40 MPa RC	[5, 7]	7.2	4.8
870	FEM870	25	50 MPa RC	BracedTube	50 MPa RC	[5, 7]	7.2	4.8
871	FEM871	25	Steel	BracedTube	Steel	[5, 7]	7.2	4.8
872	FEM872	25	32 MPa RC	BracedTube	32 MPa RC	[5, 7]	7.2	7.2
873	FEM873	25	40 MPa RC	BracedTube	40 MPa RC	[5, 7]	7.2	7.2
874	FEM874	25	50 MPa RC	BracedTube	50 MPa RC	[5, 7]	7.2	7.2
875	FEM875	25	Steel	BracedTube	Steel	[5, 7]	7.2	7.2
876	FEM876	25	32 MPa RC	BracedTube	32 MPa RC	[7, 7]	4.8	4.8
877	FEM877	25	40 MPa RC	BracedTube	40 MPa RC	[7, 7]	4.8	4.8
878	FEM878	25	50 MPa RC	BracedTube	50 MPa RC	[7, 7]	4.8	4.8
879	FEM879	25	Steel	BracedTube	Steel	[7, 7]	4.8	4.8
880	FEM880	25	32 MPa RC	BracedTube	32 MPa RC	[7, 7]	4.8	7.2
881	FEM881	25	40 MPa RC	BracedTube	40 MPa RC	[7, 7]	4.8	7.2
882	FEM882	25	50 MPa RC	BracedTube	50 MPa RC	[7, 7]	4.8	7.2
883	FEM883	25	Steel	BracedTube	Steel	[7, 7]	4.8	7.2
884	FEM884	25	32 MPa RC	BracedTube	32 MPa RC	[7, 7]	7.2	4.8
885	FEM885	25	40 MPa RC	BracedTube	40 MPa RC	[7, 7]	7.2	4.8
886	FEM886	25	50 MPa RC	BracedTube	50 MPa RC	[7, 7]	7.2	4.8

(*continued on next page*)

Table C1 (*continued*)

#	Name	Storeys	Frame Material	LLRS	LLRS Material	Grid	Column Span in X Dir (m)	Column Span in Y Dir (m)
887	FEM887	25	Steel	BracedTube	Steel	[7, 7]	7.2	4.8
888	FEM888	25	32 MPa RC	BracedTube	32 MPa RC	[7, 7]	7.2	7.2
889	FEM889	25	40 MPa RC	BracedTube	40 MPa RC	[7, 7]	7.2	7.2
890	FEM890	25	50 MPa RC	BracedTube	50 MPa RC	[7, 7]	7.2	7.2
891	FEM891	25	Steel	BracedTube	Steel	[7, 7]	7.2	7.2
892	FEM892	50	32 MPa RC	BracedTube	32 MPa RC	[5, 5]	4.8	4.8
893	FEM893	50	40 MPa RC	BracedTube	40 MPa RC	[5, 5]	4.8	4.8
894	FEM894	50	50 MPa RC	BracedTube	50 MPa RC	[5, 5]	4.8	4.8
895	FEM895	50	32 MPa RC	BracedTube	32 MPa RC	[5, 5]	4.8	7.2
896	FEM896	50	40 MPa RC	BracedTube	40 MPa RC	[5, 5]	4.8	7.2
897	FEM897	50	50 MPa RC	BracedTube	50 MPa RC	[5, 5]	4.8	7.2
898	FEM898	50	32 MPa RC	BracedTube	32 MPa RC	[5, 5]	7.2	4.8
899	FEM899	50	40 MPa RC	BracedTube	40 MPa RC	[5, 5]	7.2	4.8
900	FEM900	50	50 MPa RC	BracedTube	50 MPa RC	[5, 5]	7.2	4.8
901	FEM901	50	32 MPa RC	BracedTube	32 MPa RC	[5, 5]	7.2	7.2
902	FEM902	50	40 MPa RC	BracedTube	40 MPa RC	[5, 5]	7.2	7.2
903	FEM903	50	50 MPa RC	BracedTube	50 MPa RC	[5, 5]	7.2	7.2
904	FEM904	50	32 MPa RC	BracedTube	32 MPa RC	[5, 7]	4.8	4.8
905	FEM905	50	40 MPa RC	BracedTube	40 MPa RC	[5, 7]	4.8	4.8
906	FEM906	50	50 MPa RC	BracedTube	50 MPa RC	[5, 7]	4.8	4.8
907	FEM907	50	32 MPa RC	BracedTube	32 MPa RC	[5, 7]	4.8	7.2
908	FEM908	50	40 MPa RC	BracedTube	40 MPa RC	[5, 7]	4.8	7.2
909	FEM909	50	50 MPa RC	BracedTube	50 MPa RC	[5, 7]	4.8	7.2
910	FEM910	50	32 MPa RC	BracedTube	32 MPa RC	[5, 7]	7.2	4.8
911	FEM911	50	40 MPa RC	BracedTube	40 MPa RC	[5, 7]	7.2	4.8
912	FEM912	50	50 MPa RC	BracedTube	50 MPa RC	[5, 7]	7.2	4.8
913	FEM913	50	32 MPa RC	BracedTube	32 MPa RC	[5, 7]	7.2	7.2
914	FEM914	50	40 MPa RC	BracedTube	40 MPa RC	[5, 7]	7.2	7.2
915	FEM915	50	50 MPa RC	BracedTube	50 MPa RC	[5, 7]	7.2	7.2
916	FEM916	50	32 MPa RC	BracedTube	32 MPa RC	[7, 7]	4.8	4.8
917	FEM917	50	40 MPa RC	BracedTube	40 MPa RC	[7, 7]	4.8	4.8
918	FEM918	50	50 MPa RC	BracedTube	50 MPa RC	[7, 7]	4.8	4.8
919	FEM919	50	32 MPa RC	BracedTube	32 MPa RC	[7, 7]	4.8	7.2
920	FEM920	50	40 MPa RC	BracedTube	40 MPa RC	[7, 7]	4.8	7.2
921	FEM921	50	50 MPa RC	BracedTube	50 MPa RC	[7, 7]	4.8	7.2
922	FEM922	50	32 MPa RC	BracedTube	32 MPa RC	[7, 7]	7.2	4.8
923	FEM923	50	40 MPa RC	BracedTube	40 MPa RC	[7, 7]	7.2	4.8
924	FEM924	50	50 MPa RC	BracedTube	50 MPa RC	[7, 7]	7.2	4.8
925	FEM925	50	32 MPa RC	BracedTube	32 MPa RC	[7, 7]	7.2	7.2
926	FEM926	50	40 MPa RC	BracedTube	40 MPa RC	[7, 7]	7.2	7.2
927	FEM927	50	50 MPa RC	BracedTube	50 MPa RC	[7, 7]	7.2	7.2
928	FEM928	70	32 MPa RC	BracedTube	32 MPa RC	[5, 7]	4.8	4.8
929	FEM929	70	40 MPa RC	BracedTube	40 MPa RC	[5, 7]	4.8	4.8
930	FEM930	70	50 MPa RC	BracedTube	50 MPa RC	[5, 7]	4.8	4.8
931	FEM931	70	32 MPa RC	BracedTube	32 MPa RC	[5, 7]	4.8	7.2
932	FEM932	70	40 MPa RC	BracedTube	40 MPa RC	[5, 7]	4.8	7.2
933	FEM933	70	50 MPa RC	BracedTube	50 MPa RC	[5, 7]	4.8	7.2
934	FEM934	70	32 MPa RC	BracedTube	32 MPa RC	[5, 7]	7.2	4.8
935	FEM935	70	40 MPa RC	BracedTube	40 MPa RC	[5, 7]	7.2	4.8
936	FEM936	70	50 MPa RC	BracedTube	50 MPa RC	[5, 7]	7.2	4.8
937	FEM937	70	32 MPa RC	BracedTube	32 MPa RC	[5, 7]	7.2	7.2
938	FEM938	70	40 MPa RC	BracedTube	40 MPa RC	[5, 7]	7.2	7.2
939	FEM939	70	50 MPa RC	BracedTube	50 MPa RC	[5, 7]	7.2	7.2
940	FEM940	70	32 MPa RC	BracedTube	32 MPa RC	[5, 5]	4.8	4.8
941	FEM941	70	40 MPa RC	BracedTube	40 MPa RC	[5, 5]	4.8	4.8
942	FEM942	70	50 MPa RC	BracedTube	50 MPa RC	[5, 5]	4.8	4.8
943	FEM943	70	32 MPa RC	BracedTube	32 MPa RC	[5, 5]	4.8	7.2
944	FEM944	70	40 MPa RC	BracedTube	40 MPa RC	[5, 5]	4.8	7.2
945	FEM945	70	50 MPa RC	BracedTube	50 MPa RC	[5, 5]	4.8	7.2
946	FEM946	70	32 MPa RC	BracedTube	32 MPa RC	[5, 5]	7.2	4.8
947	FEM947	70	40 MPa RC	BracedTube	40 MPa RC	[5, 5]	7.2	4.8
948	FEM948	70	50 MPa RC	BracedTube	50 MPa RC	[5, 5]	7.2	4.8
949	FEM949	70	32 MPa RC	BracedTube	32 MPa RC	[5, 5]	7.2	7.2
950	FEM950	70	40 MPa RC	BracedTube	40 MPa RC	[5, 5]	7.2	7.2
951	FEM951	70	50 MPa RC	BracedTube	50 MPa RC	[5, 5]	7.2	7.2
952	FEM952	70	32 MPa RC	BracedTube	32 MPa RC	[7, 7]	4.8	4.8
953	FEM953	70	40 MPa RC	BracedTube	40 MPa RC	[7, 7]	4.8	4.8
954	FEM954	70	50 MPa RC	BracedTube	50 MPa RC	[7, 7]	4.8	4.8
955	FEM955	70	32 MPa RC	BracedTube	32 MPa RC	[7, 7]	4.8	7.2
956	FEM956	70	40 MPa RC	BracedTube	40 MPa RC	[7, 7]	4.8	7.2
957	FEM957	70	50 MPa RC	BracedTube	50 MPa RC	[7, 7]	4.8	7.2
958	FEM958	70	32 MPa RC	BracedTube	32 MPa RC	[7, 7]	7.2	7.2
959	FEM959	70	40 MPa RC	BracedTube	40 MPa RC	[7, 7]	7.2	7.2
960	FEM960	70	50 MPa RC	BracedTube	50 MPa RC	[7, 7]	7.2	7.2

.

Appendix D. Results of regression analyses and predictive modelling of embodied environmental flows

The computed regression coefficients and basic descriptive statistics for the prediction models of the embodied greenhouse gas emissions of 12 unique structural systems are presented in Table D.1

Table D1
Regression coefficients and basic descriptive statistics for the prediction models of structural systems

Structural system typology	Structural material	β_0	β_1	β_2	β_3	β_4	β_5	β_6	β_7	β_8	R^2
Shear Wall	32 MPa RC	85.72	0.06	-2.51	1.66	1.08	-6.76	-6.59	6.84	22.95	0.87
	40 MPa RC	89.42	0.05	-2.68	1.57	1.03	-6.14	-6.49	6.63	22.98	0.86
	50 MPa RC	92.15	0.05	-2.59	1.47	0.97	-5.68	-5.90	5.68	23.38	0.84
	300Plus Steel	120.51	0.26	-4.94	1.54	0.59	-2.05	-8.15	36.71	20.37	0.90
Outrigger and Belt	32 MPa RC	108.09	0.02	1.07	1.29	0.69	-7.68	-8.86	33.40	-8.10	0.90
	40 MPa RC	114.74	0.02	0.66	1.22	0.64	-7.25	-8.53	30.84	-5.77	0.89
	50 MPa RC	119.30	0.02	0.36	1.16	0.62	-6.97	-8.18	29.65	-3.83	0.87
	300Plus Steel	114.18	0.04	3.73	1.50	0.48	-6.02	-11.74	70.70	-13.52	0.90
Braced Tube	32 MPa RC	170.40	0.00	1.77	1.49	0.77	-10.58	-12.60	23.93	2.32	0.96
	40 MPa RC	179.36	0.01	1.55	1.30	0.67	-10.12	-12.04	22.70	1.96	0.96
	50 MPa RC	185.29	0.01	1.47	1.14	0.55	-9.03	-11.87	23.66	1.82	0.97
	300Plus Steel	264.09	0.66	-14.50	1.68	0.92	-2.91	-15.00	24.39	52.62	0.90

.

References

[1] IPCC. *Climate Change 2022: Mitigation of Climate Change. Contribution of Working Group III to the Sixth Assessment Report of the Intergovernmental Panel on Climate Change*. Retrieved from Cambridge, UK and New York, NY, USA: (2022).

[2] UNEP. *2022 Global Status Report for Buildings and Construction: Towards a Zero-emission, Efficient and Resilient Buildings and Construction Sector*. Retrieved from Nairobi, Kenya. (2022).

[3] J. Giesekam, J.R. Barrett, P. Taylor, Construction sector views on low carbon building materials, Build. Res. Inf. 44 (4) (2016) 423–444, https://doi.org/10.1080/09613218.2016.1086872.

[4] T. Ibn-Mohammed, R. Greenough, S. Taylor, L. Ozawa-Meida, A. Acquaye, Operational vs. embodied emissions in buildings—A review of current trends, Energ. Buildings 66 (2013) 232–245, https://doi.org/10.1016/j.enbuild.2013.07.026.

[5] A. Stephan, *Towards a comprehensive energy assessment of residential buildings : a multi-scale life cycle energy analysis framework.* (Doctor of Philosophy Bibliographies Theses Non-fiction), Université Libre de Bruxelles, Brussels, Belgium. (2013). Retrieved from https://ezp.lib.unimelb.edu.au/login?url=https://search.ebscohost.com/login.aspx?direct=true&db=cat00006a&AN=melb.b5152972&site=eds-live&scope=site.

[6] R.H. Crawford, G. Treloar, Validation of the use of Australian input-output data for building embodied energy simulation. Paper Presented at the IBPSA 2003: Proceedings of the Eighth International Building Performance Simulation Association Conference on Building Simulation: For better Building Design, 2003.

[7] M.K. Dixit, J.L. Fernández-Solís, S. Lavy, C.H. Culp, Identification of parameters for embodied energy measurement: A literature review, Energ. Build. 42 (8) (2010) 1238–1247, https://doi.org/10.1016/j.enbuild.2010.02.016.

[8] N. Huberman, D. Pearlmutter, A life-cycle energy analysis of building materials in the Negev desert, Energ. Buildings 40 (5) (2008) 837–848, https://doi.org/10.1016/j.enbuild.2007.06.002.

[9] I. Sartori, A.G. Hestnes, Energy use in the life cycle of conventional and low-energy buildings: A review article, Energ. Buildings 39 (3) (2007) 249–257, https://doi.org/10.1016/j.enbuild.2006.07.001.

[10] A. Stephan, L. Stephan, Reducing the total life cycle energy demand of recent residential buildings in Lebanon, Energy 74 (2014) 618–637, https://doi.org/10.1016/j.energy.2014.07.028.

[11] Y.G. Yohanis, B. Norton, Life-cycle operational and embodied energy for a generic single-storey office building in the UK, Energy 27 (1) (2002) 77–92, https://doi.org/10.1016/S0360-5442(01)00061-5.

[12] N. Huberman, D. Pearlmutter, E. Gal, I.A. Meir, Optimizing structural roof form for life-cycle energy efficiency, Energ. Buildings 104 (2015) 336–349, https://doi.org/10.1016/j.enbuild.2015.07.008.

[13] M.C. McManus, M. Bowick, J. Meil, *Life Cycle Impacts in the Building Industry: a Temporal GHG Perspective*. (2017).

[14] A. Säynäjoki, J. Heinonen, S. Junnila, A scenario analysis of the life cycle greenhouse gas emissions of a new residential area, Environ. Res. Lett. 7 (3) (2012), 034037.

[15] CTBUH, The Skyscraper Center, Retrieved from, https://www.skyscrapercenter.com/, 2021.

[16] P. Du, A. Wood, B. Stephens, X. Song, Life-cycle energy implications of downtown high-rise vs. suburban low-rise living: An overview and quantitative case study for Chicago, Buildings 5 (3) (2015) 1003–1024, https://doi.org/10.3390/buildings5031003.

[17] G.J. Treloar, R. Fay, B. Ilozor, P.E.D. Love, An analysis of the embodied energy of office buildings by height, Facilities 19 (5/6) (2001) 204, https://doi.org/10.1108/02632770110387797.

[18] F.R. Khan, *Optimization of Building Structures.* Paper presented at the Proceedings of the Structural Engineering Conference held at University of Illinois. (1966).

[19] B. Stafford Smith, A. Coull, *Tall building structures: analysis and design*: Wiley-Interscience. (1991).

[20] Emporis Standards, High-rise Building (ESN 18727), Retrieved from, https://www.emporis.com/building/standard/3/high-rise-building, 2018.

[21] M. Gunel, H. Ilgin, A proposal for the classification of structural systems of tall buildings, Build. Environ. 42 (7) (2007) 2667–2675, https://doi.org/10.1016/j.buildenv.2006.07.007.

[22] K.S. Moon, J.J. Connor, J.E. Fernandez, Diagrid structural systems for tall buildings: characteristics and methodology for preliminary design, Struct. Design Tall Spec. Build. 16 (2) (2007) 205–230.

[23] R.H. Crawford, Life Cycle Assessment in the Built Environment, Spon Press, London, United Kingdom, 2011.

[24] ISO. *ISO 14040:2006 Environmental management – Life cycle assessment – Principles and framework*. Brussels, Belgium: European Committee for Standardization.. (2006).

[25] S. Tae, C. Baek, S. Shin, Life cycle CO_2 evaluation on reinforced concrete structures with high-strength concrete, Environ. Impact Assess. Rev. 31 (3) (2011) 253–260, https://doi.org/10.1016/j.eiar.2010.07.002.

[26] Y.S. Cho, J.H. Kim, S.U. Hong, Y. Kim, LCA application in the optimum design of high rise steel structures, Renew. Sustain. Energy Rev. 16 (5) (2012) 3146–3153, https://doi.org/10.1016/j.rser.2012.01.076.

[27] P. Foraboschi, M. Mercanzin, D. Trabucco, Sustainable structural design of tall buildings based on embodied energy, Energy Build. 68(Part A) (2014), 254–269. doi:https://doi.org/10.1016/j.enbuild.2013.09.003.

[28] X. Zhao, M.A. Haojia, Structural system embodied carbon analysis for super tall buildings, Procedia Eng. 118 (2015) 215–222, https://doi.org/10.1016/j.proeng.2015.08.420.

[29] Z.S. Moussavi Nadoushani, A. Akbarnezhad, Effects of structural system on the life cycle carbon footprint of buildings, Energ. Buildings 102 (2015) 337–346, https://doi.org/10.1016/j.enbuild.2015.05.044.

[30] D. Trabucco, A. Wood, O. Vassart, N. Popa, D. Davies, Life Cycle Assessment of Tall Building Structural Systems, CTBUH, Chicago, Illinois, 2015.

[31] D. Mavrokapnidis, C.C. Mitropoulou, N.D. Lagaros, Environmental assessment of cost optimized structural systems in tall buildings, J. Build. Eng. 24 (2019), 100730, https://doi.org/10.1016/j.jobe.2019.100730.

[32] J. Helal, A. Stephan, R.H. Crawford, The influence of life cycle inventory approaches on the choice of structural systems to reduce the embodied greenhouse gas emissions of tall buildings, IOP Conference Series: Earth and Environmental Science 588 (3) (2020) 032028.

[33] J. Helal, A. Stephan, R.H. Crawford, The influence of structural design methods on the embodied greenhouse gas emissions of structural systems for tall buildings, Structures 24 (2020) 650–665, https://doi.org/10.1016/j.istruc.2020.01.026.

[34] J. Helal, A. Mehdipanah, A. Stephan, E. Lumantarna, R.H. Crawford, *Embodied greenhouse gas emissions of structural systems for tall buildings: is there a premium for plan irregularity?*, in: Paper presented at the Architectural Science and User

Experience: How can Design Enhance the Quality of Life, 55th International Conference of the Architectural Science Association 2022, Curtin University, Perth, Australia (2022). https://www.asaconference2022.com/_files/ugd/456bf3_b43dc55b5ad34ae2b91f35a321b9a1e0.pdf.
[35] J. Helal, Towards a Comprehensive Framework for Integrating Embodied Environmental Flow Assessment into the Structural Design of Tall Buildings, Doctor of Philosophy, University of Melbourne, Melbourne, Australia, 2022.
[36] R.H. Crawford, P.-A. Bontinck, A. Stephan, Establishing a comprehensive database of construction material environmental flow coefficients for Australia. Paper Presented at the Engaging Architectural Science: Meeting the Challenges of Higher Density: 52nd International Conference of the Architectural Science Association 2018, 2018.
[37] P. Mendis, T. Ngo, N. Haritos, A. Hira, B. Samali, J. Cheung, Wind loading on tall buildings, Electron. J. Struct. Eng. 7 (1) (2007) 41–54.
[38] A. Stephan, R.H. Crawford, P.-A. Bontinck, A model for streamlining and automating path exchange hybrid life cycle assessment, Int. J. Life Cycle Assess. 24 (2) (2019) 237–252.
[39] C.K. Chau, T.M. Leung, W.Y. Ng, A review on life cycle assessment, life cycle energy assessment and life cycle carbon emissions assessment on buildings, Appl. Energy 143 (2015) 395–413, https://doi.org/10.1016/j.apenergy.2015.01.023.
[40] H.L. Gauch, W. Hawkins, T. Ibell, J.M. Allwood, C.F. Dunant, Carbon vs. cost option mapping: A tool for improving early-stage design decisions, Autom. Constr. 136 (2022), 104178, https://doi.org/10.1016/j.autcon.2022.104178.
[41] C.F. Dunant, M.P. Drewniok, J.J. Orr, J.M. Allwood, Good early stage design decisions can halve embodied CO2 and lower structural frames' cost, Structures 33 (2021) 343–354, https://doi.org/10.1016/j.istruc.2021.04.033.
[42] J. Hart, B. D'Amico, F. Pomponi, Whole-life embodied carbon in multistory buildings: Steel, concrete and timber structures, 25 (2) (2021) 403–418.
[43] M. Lenzen, R.H. Crawford, The path exchange method for hybrid LCA, Environ. Sci. Tech. 43 (21) (2009) 8251–8256, https://doi.org/10.1021/es902090z.
[44] B.S. Taranath, Tall Building Design, CRC Press, Boca Raton, 2017.
[45] M. Ali, K. Moon, Advances in structural systems for tall buildings: Emerging developments for contemporary urban giants, Buildings 8 (2018) 104.
[46] C.C. Pouangare, J.J. Connor, New structural systems for tall buildings: The space-truss concept, Struct. Des. Tall Buil. 4 (2) (1995) 155–168.
[47] CTBUH, CTBUH Year in Review: Tall Trends of 2017, Retrieved from Chicago, Illinois: http://www.skyscrapercenter.com/year-in-review/2017, 2017.
[48] Standards Australia. *AS/NZS 2890 (Set):2009 - Parking Facilities Set*: Sydney: Standards Australia International; Wellington : Standards New Zealand, 2009. (2009).
[49] CTBUH, CTBUH Height Criteria for Measuring & Defining Tall Buildings, Retrieved from Chicago, USA: http://www.ctbuh.org/LinkClick.aspx?fileticket=KdtWFbXpBQc%3d&tabid=7456&language=en-US, 2017.
[50] K. Allacker, Sustainable building: the development of an evaluation method. In (2010) (Vol. 71).
[51] X. Oregi, P. Hernandez, C. Gazulla, M. Isasa, Integrating Simplified and Full Life Cycle Approaches in Decision Making for Building Energy Refurbishment: Benefits and Barriers, Buildings 5 (2) (2015) 354–380, https://doi.org/10.3390/buildings5020354.
[52] M. Robati, P. Oldfield, A.A. Nezhad, D.G. Carmichael, A. Kuru, Carbon value engineering: A framework for integrating embodied carbon and cost reduction strategies in building design, Build. Environ. 192 (2021), 107620, https://doi.org/10.1016/j.buildenv.2021.107620.
[53] X. Zhang, F. Wang, Analysis of embodied carbon in the building life cycle considering the temporal perspectives of emissions: A case study in China, Energ. Buildings 155 (2017) 404–413, https://doi.org/10.1016/j.enbuild.2017.09.049.
[54] P. Winistorfer, Z. Chen, B. Lippke, N. Stevens, Energy consumption and greenhouse gas emissions related to the use, maintenance, and disposal of a residential structure, Wood Fiber Sci. 37 (2007) 128–139.
[55] European Committee for Standardization. *EN 15978:2011 Sustainability of construction works. Assessment of environmental performance of buildings. Calculation method*: BSI Standards Limited. (2011).
[56] A. Abdelrazaq, Validating the Structural Behavior and Response of Burj Khalifa, *CTBUH J.* 6 (2011).
[57] Computers and Structures Inc. ETABS. Retrieved from https://www.csiamerica.com/products/etabs/releases#17-17.0.0. (2018).
[58] G. Finnveden, M.Z. Hauschild, T. Ekvall, J. Guinée, R. Heijungs, S. Hellweg, A. Koehler, D. Pennington, S. Suh, Recent developments in Life Cycle Assessment, J. Environ. Manage. 91 (1) (2009) 1–21.
[59] R.H. Crawford, Validation of a hybrid life-cycle inventory analysis method, J. Environ. Manage. 88 (3) (2008) 496–506, https://doi.org/10.1016/j.jenvman.2007.03.024.
[60] M. Lenzen, Errors in conventional and input-output-based life-cycle inventories, J. Ind. Ecol. 4 (4) (2000) 127–148, https://doi.org/10.1162/10881980052541981.
[61] G. Majeau-Bettez, A.H. Strømman, E.G. Hertwich, Evaluation of process- and input–output-based life cycle inventory data with regard to truncation and aggregation issues, Environ. Sci. Tech. 45 (23) (2011) 10170–10177, https://doi.org/10.1021/es201308x.
[62] R.E. Miller, P.D. Blair, Input-Output Analysis: Foundations And Extensions, Cambridge University Press, Cambridge, United Kingdom, 2009.
[63] G.J. Treloar, Extracting embodied energy paths from input-output tables: towards an input–output-based hybrid energy analysis method, Econ. Syst. Res. 9 (4) (1997) 375–391, https://doi.org/10.1080/09535319700000032.
[64] R.H. Crawford, A. Stephan, F. Prideaux, Environmental Performance in Construction (EPiC) Database, The University of Melbourne, Melbourne, 2019.
[65] B. D'Amico, F. Pomponi, On mass quantities of gravity frames in building structures, J. Build. Eng. 31 (2020) 101426, https://doi.org/10.1016/j.jobe.2020.101426.
[66] W. McKinney, *Data structures for statistical computing in python.* Paper presented at the Proceedings of the Ninth Python in Science Conference. (2010).
[67] C.R. Harris, K.J. Millman, S.J. van der Walt, R. Gommers, P. Virtanen, D. Cournapeau, E. Wieser, J. Taylor, S. Berg, N.J. Smith, R. Kern, M. Picus, S. Hoyer, M.H. van Kerkwijk, M. Brett, A. Haldane, J.F. del Río, M. Wiebe, P. Peterson, P. Gérard-Marchant, K. Sheppard, T. Reddy, W. Weckesser, H. Abbasi, C. Gohlke, T.E. Oliphant, Array programming with NumPy, Nature 585 (7825) (2020) 357–362.
[68] P. Virtanen, R. Gommers, T.E. Oliphant, M. Haberland, T. Reddy, D. Cournapeau, E. Burovski, P. Peterson, W. Weckesser, J. Bright, S.J. van der Walt, M. Brett, J. Wilson, K.J. Millman, N. Mayorov, A.R.J. Nelson, E. Jones, R. Kern, E. Larson, C. J. Carey, İ. Polat, Y.u. Feng, E.W. Moore, J. VanderPlas, D. Laxalde, J. Perktold, R. Cimrman, I. Henriksen, E.A. Quintero, C.R. Harris, A.M. Archibald, A.H. Ribeiro, F. Pedregosa, P. van Mulbregt, A. Vijaykumar, A.P. Bardelli, A. Rothberg, A. Hilboll, A. Kloeckner, A. Scopatz, A. Lee, A. Rokem, C.N. Woods, C. Fulton, C. Masson, C. Häggström, C. Fitzgerald, D.A. Nicholson, D.R. Hagen, D. V. Pasechnik, E. Olivetti, E. Martin, E. Wieser, F. Silva, F. Lenders, F. Wilhelm, G. Young, G.A. Price, G.-L. Ingold, G.E. Allen, G.R. Lee, H. Audren, I. Probst, J. P. Dietrich, J. Silterra, J.T. Webber, J. Slavič, J. Nothman, J. Buchner, J. Kulick, J. L. Schönberger, J.V. de Miranda Cardoso, J. Reimer, J. Harrington, J.L. C. Rodríguez, J. Nunez-Iglesias, J. Kuczynski, K. Tritz, M. Thoma, M. Newville, M. Kümmerer, M. Bolingbroke, M. Tartre, M. Pak, N.J. Smith, N. Nowaczyk, N. Shebanov, O. Pavlyk, P.A. Brodtkorb, P. Lee, R.T. McGibbon, R. Feldbauer, S. Lewis, S. Tygier, S. Sievert, S. Vigna, S. Peterson, S. More, T. Pudlik, T. Oshima, T.J. Pingel, T.P. Robitaille, T. Spura, T.R. Jones, T. Cera, T. Leslie, T. Zito, T. Krauss, U. Upadhyay, Y.O. Halchenko, Y. Vázquez-Baeza, SciPy 1.0: fundamental algorithms for scientific computing in Python, Nat. Methods 17 (3) (2020) 261–272.
[69] J.D. Hunter, Matplotlib: A 2D graphics environment, Comput. Sci. Eng. 9 (3) (2007) 90–95, https://doi.org/10.1109/MCSE.2007.55.
[70] Plotly Technologies Inc, Collaborative Data Science, Plotly Technologies Inc., Montréal, QC, 2015. Retrieved from https://plot.ly.
[71] S. Kim, Y.H. Lee, A. Scanlon, Comparative study of structural material quantities of high-rise residential buildings, Struct. Design Tall Spec. Build. 17 (1) (2008) 217–229, https://doi.org/10.1002/tal.348.
[72] S. Kang, B. Kim, S. Bae, H. Lee, M.J.E.S. Kim, Earthquake-induced ground deformations in the low-seismicity region: A case of the 2017 M5. 4 Pohang, South Korea, earthquake. 35 (3) (2019) 1235–1260.
[73] Standards Australia. *AS/NZS 1170.4:2007 - Structural design actions : earthquake actions in Australi*: Sydney : Standards Australia International ; Wellington : Standards New Zealand, 2002. (2007).
[74] S. Kim, Seismic performance evaluation of high-rise steel buildings dependent on wind exposures Seismic performance evaluation of high-rise steel buildings dependent on wind exposures. 11 (3) (2019) doi:https://doi.org/10.1177/1687814019835111.
[75] P. Du, A. Wood, B. Stephens, Empirical operational energy analysis of downtown high-rise vs. suburban low-rise lifestyles: A Chicago case study, *Energies* 9 (6) (2016) 445.
[76] A.K. Chopra, Dynamics of Structures: Theory and Applications to Earthquake Engineering, 4th ed., Prentice Hall, Upper Saddle River, N.J., 2012.
[77] K.S. Moon, Comparative efficiency of structural systems for steel tall buildings, Int. J. Sustain. Build. Technol. Urban Dev. 5 (3) (2014) 230–237, https://doi.org/10.1080/2093761X.2014.948099.
[78] R.J. Cole, Energy and greenhouse gas emissions associated with the construction of alternative structural systems, Build. Environ. 34 (3) (1998) 335–348, https://doi.org/10.1016/S0360-1323(98)00020-1.

Glossary

API: Application program interface
AR: Aspect ratio
AS: Australian standard
ASCE: American Society of Civil Engineers
C40: Case study building used for software validation with a 40-storey structural system composed of a shear wall and frame made of 40 MPa reinforced concrete
C60: Case study building used for software validation with a 60-storey structural system composed of an outrigger and belt, shear wall and frame made of 50 MPa reinforced concrete
C80: Case study building used for software validation with an 80-storey structural system composed of an outrigger and belt, shear wall and frame made of 50 MPa reinforced concrete
EE: Embodied energy
EEIO: Environmentally-extended input–output
EGHGE: Embodied greenhouse gas emissions
EPD: Environmental product declaration
EPiC: Environmental performance in construction
GHG: Greenhouse gas
GWP: Global warming potential
ICE: Inventory of carbon and energy
IPCC: Intergovernmental Panel on Climate Change
ISO: International Organization for Standardization
LCA: Life cycle assessment
LCEA: Life cycle energy assessment
LCGHGEA: Life cycle greenhouse gas emissions assessment
LCI: Life cycle inventory
NFA: Net floor area
OOP: Object-oriented programming
R^2: Coefficient of determination
RC: Reinforced concrete
SE2050: Structural engineers 2050 commitment program
SR: Slenderness ratio